TESIS DE LA UNIVERSIDAD DE ZARAGOZA

2014

80

Alessandro Santagata

Coulomb Phases: from Graphene to Quark Confinement

Departamento
Física Teórica

Director/es
Asorey Carballeira, Manuel

ISSN 2254-7606

Prensas de la Universidad
Universidad Zaragoza

Universidad Zaragoza
1542

Tesis Doctoral

COULOMB PHASES: FROM GRAPHENE TO QUARK CONFINEMENT

Autor

Alessandro Santagata

Director/es

Asorey Carballeira, Manuel

UNIVERSIDAD DE ZARAGOZA

Física Teórica

2014

Universidad de Zaragoza
Facultad de Ciencias
Departamento de Física Teórica

COULOMB PHASES: FROM GRAPHENE TO QUARK CONFINEMENT

Ph. D. Thesis

Alessandro Santagata

Director: Manuel Asorey

Junio 2014

COULOMB PHASES: FROM GRAPHENE TO QUARK CONFINEMENT

Ph. D. Thesis

Alessandro Santagata

Agradecimientos

En primer lugar quería agradecer a Manolo, para haberme dado la posibilidad de realizar uno de mis sueños, aportar contribuciones personales originales al campo de la física teórica. Seguramente trabajar contigo es algo muy particular: lo que siempre me ha sorprendido ha sido tu entusiasmo, que sólo se puede encontrar en las personas que de verdad aman lo que están haciendo, en el lanzarse en los problemas de la física. Lo que más he apreciado y que seguramente me acompañará por mucho tiempo ha sido tu capacidad de no contentarse nunca con el primer resultado, intentando de ver siempre más allá, explorando todas las posible consecuencias para sacar siempre el máximo partido, con gran fuerza y optimismo. Esto, seguramente, es una guía y un ejemplo que intentaré seguir en todo lo que haga.

Gracias a todos los miembros del departamento de Física Teórica, con los cuales he pasado 5 años estupendos. Siempre habéis estado muy disponibles y he apreciado mucho el clima casi familiar del departamento. En particular, gracias a José Maria, que ha sido muy importante para el comienzo de este trabajo, y a Matteo, Cesar, Amilcar, David, Pulak y Leo por la paciencia que habéis tenido en contestar a mis preguntas.

Agradezco el apoyo económico que recibí con la beca asociada al proyecto "Grupo de Excelencia: 2009. Grupo Teórico de Altas Energías" la beca doctoral de la DGA y el contracto de Investigador Novel de la Universidad de Zaragoza, en el proyecto "FPA2012-35453. Física del modelo estándar

y sus posible extensiones", que me han permitido de realizar este trabajo.

Grazie a tutti quelli che hanno condiviso in qualche modo Zaragoza. In particolare a Silvia per "a chill pelat u sacc", a Ola per "mi globo", a Daniele per il torcicollo in aula lectura, a tutti quelli del viaggio in Andalucia (Camilla, Alberto, Angelo, Adriano, Zagni, Coty, Elisabetta, Carlo), a Diana per "ci beviamo na cosa?", a Robertina per ridere sempre, alla Lella per non rispondere mai, a Ross per condividere la sopportazione delle ultime tre galline, al conte Ugolini per la panza piena tutte le sere, a tutti quelli del viaggio al Norte e degli aperitivi a Milano quando torno (Claudia, Andrea, Daniele, Chiara, Emilio, Marti, Leo, Vale, Michela), a Carol per avermi fatto da infermiera, a Betty Brown, Eri, Iuso, Giò che hanno assistito, consenzienti, a Daniela spalmarmi la cioccolata in testa, a Gennaro per i tre scudetti visti insieme, a Gabriele per la diretta gol la domenica pomeriggio, a Valeria per il cammino dell'amarezza, a Monica per le tonnellate di pasta, a Marianna e Livia per "-todo bien? -si! pasa! pasa!", a Margherita per aver reso infinita la mia pazienza, a Marzia per "Café y comida". Grazie anche ad Alex, Laura e Andres per tutte le feste. Y a todos los compañeros de piso de estos años.

Grazie a tutti i Gugnis, alle loro tifose, fidanzate, mogli e figli. Soprattutto per "Quando sei tornato? sei arrivato a Bergamo? Quando riparti? Riparti sempre da Bergamo? quanto ti fermi? come va con lo spagnolo? quanto ti manca? qual è la tua giornata tipo?" Grazie per avermi fatto sempre le stesse domande, tutti e 20/25, in fila, uno dopo l'altro. Ogni volta. Maledetti. E comunque no, una volta per tutte, dalla mia ricerca non si può trovare la pesca senza nocciolo e non mi metto il camicie bianco in ufficio. Ma la domanda è: ringraziandovi, ho voluto essere gentile solo per gentilezza? No, questa volta l'ho fatto davvero con gentilezza (non ne usciremo mai). In rappresentanza, per dimostrarvi che al quinto anno ho imparato queste due nuove parole, "agradezco con humildad" Gogo per aver sfangato insieme molte giornate e aver condiviso il peso, altrimenti insostenibile, di tutte le amarezze fantacalcistiche, i due passi circolari di Alex Maro e l'Alberta per "mi hai caricato la puntata?". E grazie alla Vale

Cucca perché la lontananza non ha influito nel rendermi partecipe di un evento importante.

Grazie alla mia famiglia, in particolare a mio fratello per avermi tartassato di messaggi per 5 anni. E alle mie nonne, Luisa e Carla, che solo mi hanno visto partire.

Contents

Resumen

La demostración analítica del confinamiento en QCD es unos de los problemas abiertos más destacado de la física teórica. Con la motivación de aportar contribuciones significativas en la comprensión de este fenómeno, el objetivo principal de este trabajo de tesis ha sido dar resultados analíticos, a partir de primeros principios de QCD, sobre la interpolación contínua entre el régimen de libertad asintótica y el de confinamiento, demostrando que ambos son compatibles para valores intermedios de energías. La importancia de investigar el régimen intermedio de energías está en el hecho que una demostración analítica de la ausencia de transiciones de fase correspondería a demostrar el confinamiento.

Nuestro trabajo ha sido inspirado principalmente para la imagen del confinamiento de Gribov. La motivación inicial de Gribov ha sido la inestabilidad de los átomos hidrogenoides para carga del núcleo más grande de $Z_c = 137$, a partir de la cual, el vacío decae a un par de electrón y positrón. Con esta analogía, Gribov sugirió que un fenómeno similar, debido a la inestabilidad de fase de Coulomb en QCD, pudiese ser la causa del confinamiento. Él encontró una valor crítico de la constante de acoplo, $\alpha_s \cong 0.43$, a partir de la cual el vacío de QCD es inestable y decae en pares de quarks y antiquarks. Desafortunadamente, debido a su muerte, no pudo acabar la demostración.

Recientemente, el aislamiento de capas bidimensionales del grafeno ha permitido la verificación experimental de muchas predicciones teóricas en QED, incluso la motivacion principal del mecanismo de confinamiento de

Gribov. Por un lado, las evidencias experimentales de que en presencia de impurezas con cargas supercrítica en el grafeno una descripción cuantomecánica es posible, nos ha motivado a un estudio desde el punto de vista matemático de la transición desde el régimen subcrítico al supercrítico. Hemos propuesto una descripción global de las fases de Coulomb para todos los valores de carga de la impureza. Hemos definido rigurosamente el Hamiltoniano de Dirac con potencial de Coulomb en dos dimensiones, como operador autoadjunto en términos de las condiciones del contorno cerca de la singularidad. En la renormalización de la singularidad juegan un papel fundamental los cero modos asintóticos (véase el apéndice para una disertación similar para el caso del potencial conforme en mecánica cuántica). El análisis muestra que existen una infinidad de extensiónes autoadjuntas para $\alpha > 0$, paramatrizadas por un ángulo θ, que define un flujo espectral con propiedades físicas observables (Capítulo 2).

Por otro lado, este tipo de análisis se puede extender al caso tridimensional para la QED, mostrando que la motivación inicial de Gribov basada en la pérdida de la unitariedad del vacío para cargas supercrítica no es completamente correcta. De todas formas, sus argumentos todavía son muy atractivos. El objetivo principal de la tesis ha sido obtener una imagen del confinamiento similar a la de Gribov pero desde una nueva perspectiva, de primeros principios , analizando la función de partición Euclídea definida por el Lagrangiano de QCD.

En primer lugar hemos considerado el caso de un quark pesado estático. Hemos analizado la estabilidad de la fase de Coulomb en la aproximación de punto silla. En la disertación, hemos aprovechado el análisis desarrollado para el grafeno, para definir las extensiones autoadjuntas del operador de segunda variaciones bosonica en terminos de las condiciónes al contorno. Hemos encontrado que para constantes de acoplo $\alpha > \sqrt{5}/2$ la fase de Coulomb se vuelve inestable debido a la aparición de modos negativos para las fluctuaciones bosónicas. La aparición de estos modos negativos está estrictamente relacionada con la ruptura de la simetría conforme, debido a una escala de energía introducida con las condiciones al contorno. El resultado es que para constantes de acoplos pequeñas la libertad asintótica está preservada, mientras que a cargas grandes la inestabilidad de la fase

de Coulomb abre la posibilidad de comportamientos confinantes (Capítulo 3).

En segundo lugar, para obtener una imagen mas próxima del confinamiento, hemos considerado el caso de un par quark-antiquark pesada estática neutra de color, que reproduce un mesón. La novedad principal es la introducción de una nueva escala en la teoría, la separación entre los quarks. Antes de atacar el problema en tres dimensiones, hemos estudiado el caso quark-antiquark en una dimensión. Esto ha permitido obtener resultados analíticos que han sido fundamentales para la comprensión del caso tridimensional. En particular, para un intervalo intermedio de cargas, hemos encontrado la existencia de una distancia crítica entre el par tal que para separaciones menores el sistema es estable e inestable para separaciones mayores. El fenómeno de la distancia critica es una consecuencia directa de la introducción de las condiciones de contorno autoadjuntas para ambas singularidades de los quarks (Capítulo 4).

Hemos extendido los resultados al caso tridimensional. Debido a su mayor complejidad, el análisis ha sido realizado principalmente a través de métodos numéricos. Como es esperado, hemos encontrado un régimen intermedio de constante de acoplo $\sqrt{2} < \alpha < 3/2$ donde, debido a las fluctuaciones gluónicas, la fase de Coulomb es estable para pequeñas separaciones entre los quarks e inestable para grandes separaciones. Este resultado muestra que la libertad asíntotica y el confinamiento son compatibles para un régimen intermedio de constantes de acoplo, abriendo una nueva perspectiva en el enfoque analítico al confinamiento (Capítulo 5).

Gribov asigna un papel fundamental a los quarks ligeros en el mecanismo de confinamiento. Para verificar esta afirmación, hemos estudiado las posibles inestabilidades de la fase de Coulomb debidas a las fluctuaciones fermiónicas. En este caso, las inestabilidades están marcadas por la existencia de modos cero del operador de Dirac en el trasfondo de Coulomb. El análisis muestra la aparición de este nuevo tipo de inestabilidad, asociado a la creación de pares quark-antiquark, a partir de la constante crítica $\alpha = \sqrt{3}$. El mecanismo que las genera es el flujo espectral inducido para las condiciones al contorno en la singularidades, similar al caso del grafeno. Las inestabilidades aparecen a una constante de acoplo mayor respecto a la del

caso gluónico, mostrando que el mecanismo de confinamiento está dirigido principalmente por los gluones respecto a quarks ligeros, en contradicción con la afirmación de Gribov (Capítulo 6).

1

Introduction

1.1. Quark Confinement in Quantum Chromodynamics

The goal of this thesis is to develop a new approach to the more striking feature of Quantum Chromodynamics, quark confinement. Let us start with historical review of the role of Quantum Chromodynamcs in the description of strong interactions.

The first theory of strong interaction is due to Yukawa and was formulated in 1934. The need of such an interaction is a consequence of the multiproton nuclei stability. The only way of compensate the electric repulsion of protons is to postulate the existence of a very strong attractive interaction. The strong interaction in the Yukawa model is mediated by the exchange of a new massive particle. The particle responsible for the interaction, the pion, was later discovered by Powell in 1947. The mass of the pion signals the short range scope of the strong interaction.

The pion was one of the first of the saga of elementary particles which soon became a zoo. A very successful classification scheme, known as Eight-

fold Way, was introduced by Gell-Mann in 1961. Gell-Mann's way consist in organizing the families of strongly interacting particles according to irreducible representations of a new kind of internal symmetry associated to a unitary group $SU(3)$.

The success of the $SU(3)$ model lead to Gell-Mann and Zweig to raise in 1964 the conjecture that all the hadrons are composed of more elementary constituents, the *quarks*. The problem generated by discovery of the Ω particle made of three identical quarks, apparently in contradiction with Pauli principle, lead to Gell-Mann to propose the existence of new quantum number, the color, associated to a new internal $SU(3)$ symmetry. The strange property of the color quantum number is that only particles which are neutral of color are stable. This means that the quarks themselves cannot be isolated as independent particles. They can only live in combination with other quarks in a color neutral hadron. This is the first manifestation of quark confinement.

However, the existence of quarks can be made manifest by scattering experiments. The study of the inner hadronic structure can be made through high energy electron scattering with large momentum transfers. The results obtained at the end of the sixties in the experiments of deep inelastic electron-proton scattering, which were reminiscent of Rutherford's experiments, confirmed the existence of three almost-free point-like constituents inside the proton, which were called *partons* by Feynman and identified with the quarks.

The search for a quark dynamics started right after the foundation of the quark model. The dynamics governing the quark system should have the property that the strong interaction between the quarks becomes weaker at shorter distances as observed in the deep inelastic electron-nucleon scattering experiments. The quantum field theories of relativistic interactions known at that moment had the opposite properties. For example, in Quantum Electrodynamics (QED), the quantum field theory describing the electromagnetic interaction, the strength of the interaction is increasing at short distances.

The strength of an interaction are in general parameterized by coupling constant. Due to quantum corrections the value of this coupling changes

with the distance. In the presence of an electric charge vacuum fluctuations include virtual pair creation which means that the quantum vacuum is a polarizable medium where electric charge gets screened. The dependence of the screening with the distance to the external charge can be derived from its dependence on the momentum transfer q^2 carried by the mediating photon (large q^2 correspond to small distance). In perturbation theory QED predicts that the electromagnetic coupling constant is running as

$$\alpha(q^2) = \frac{\alpha(m)}{1 - \dfrac{\alpha(m)}{3\pi} \ln(q^2/m^2)}, \tag{1.1}$$

valid for values of the four momentum $q^2 \gg m^2$ much larger than the the electron mass m. This shows that the effective coupling $\alpha(q^2)$ tends to increase at large q^2. This screening of the effective charge associated with the vacuum polarization disappears at the Compton wavelength of the electron $1/m$.

Until 1973 it was believed that all the quantum field theories behaves in a similar manner, with the coupling constant increasing logarithmic with Q^2. But in that year Gross, Wilczek and Politzer showed that the non-Abelian gauge field theories, introduced by Yang and Mills in 1954, satisfy the desired property for the coupling to decrease with the energy. This property was called *asymptotic freedom*. The quantization of Yang Mills theory was already achieved including its renormalization by 't Hooft and Veltman in 1971.

This confirmed that the strong interaction of quarks is driven by non-Abelian gauge theories. These theories differ from QED by the fact that are the internal symmetry group is non-Abelian. It is just the SU(3) symmetry group associated to the internal color quantum number. The theory of quark dynamics based on that mechanism is the celebrated quantum chromodynamics (QCD).

The particle mediating the strong interaction, the gluon, plays a similar role that the photon plays in electromagnetic interactions. There are some differences photons have no electric charge but gluons carry color charge; photons do not interact between then at tree level, whereas gluons interact

with each other even in the absence of the quarks. This property of gluons is an essential ingredient for understanding the behaviour of QCD at short distances. In particular, to understand why the quarks inside an hadron at very short distances do have light interactions, i.e. they are almost asymtotically free.

As in QED the production of virtual quark and antiquark tends to screen the color charge of the quark, but now in QCD we have to consider also the auto-interaction of the gluons. The net effect of the production of virtual gluons in the vacuum is not to screen the color charge but its anti-screening. Getting closer to a quark diminishes the anti-screening effect of the surrounding virtual gluons, weakening the effective charge which decreases as we approach the quark core. Since the virtual quarks and the virtual gluons contribute opposite effects, which effect wins out depends on the number of different flavors of quark. For standard QCD with three colors and six flavors the anti-screening prevails. This is described by the running of the strong coupling constant formula, obtained in perturbation theory:

$$\alpha_s(q^2) = \frac{\alpha_s(\mu^2)}{1 + \dfrac{33 - 2F}{12\pi}\alpha_s(\mu^2)\ln(q^2/\mu^2)}, \tag{1.2}$$

where and F is the number of quark flavors. Notice that if $F = 6$ the sign of the logarithmic term is positive and not negative as in QED (1.1) which implies that $\alpha_s(q^2) \to 0$ as $q^2 \to \infty$. Notice the presence in the formula (1.2) of a new parameter μ with dimensions of mass. In QED the similar parameter was the electron mas, but in QCD quarks are not physical particles, then, there is not an apriori natural scale. The QCD scale μ has to be fixed by scattering experiments. From a theoretical viewpoint the emergence of this scale in a conformal invariant theory (in absence of quarks) is due to a conformal anomaly which not only generates a new scale, but also a induces a dimensional transmutation of some physical observables.

The discovery of asymptotic freedom promoted the QCD as the theory of strong interactions and permitted to Gross, Wilczek and Politzer to win the Nobel Prize in 2004. With the birth of QCD the interaction between

two hadrons, for example two protons in a nucleus, which Yukawa though to be a fundamental process, must be regarded as a complicated interaction of six quarks.

The high energy experiments provided the evidence that there are quarks inside the hadrons but they also confirmed the fact that no isolated quark have been ever observed. The situation is quite different respect QED: even though bound states arise also in QED, the constituent electrons and nuclei are themselves frequently observed, as processes like ionization, in which constituents are released from their bound states when a sufficiently large transfer of energy is attained. The analogs of these processes have never been seen for strongly interacting particles, even though the bound states have been exposed to collision energies that are many times the rest energy of the bound particles themselves. Quarks are absolutely confined inside baryons and mesons. *Quark confinement* is also a physical characteristic of strong interactions. Whether QCD can account for that behavior of the theory or not was the next question addressed by the high energy physics community in the late seventies.

In opposition to asymptotic freedom, confinement has not been understood in QCD in analytic terms. Confinement is a genuine non-perturbative phenomenon. It cannot be seen at any finite order of weak-coupling perturbation theory. It requires new non-perturbative analytic tools to deal with. One technical difficulty is that the standard QED regularization techniques necessary to control the UV divergences are not gauge invariant in non-abelian gauge theories. A new kind of regularization technique, dimensional regularization, was introduced to prove the renormalizability of the theory and the emergence of asymptotic freedom in perturbation theory. However, the dimensional regularization method does not work beyond perturbation theory.

The first step in the analysis of confinement was the introduction by K. Wilson of a new type of regularization method based on a space-time lattice. In lattice gauge theory the continuum space-time is replaced by a four dimensional Euclidean discretized space-time, the quarks are situated at the points of this lattice and the gauge fields on the links between the lattice points.

Once the theory is regularized it is possible to calculate the strength of the force between quarks. This can be done in absence of dynamical quarks by computing the expectation value of a gauge invariant observable known as Wilson loop. In the strong coupling limit $g_s \gg 1$ one obtains by a simple analytical calculation that

$$< W > \cong \ \mathrm{e}^{-\sigma TL}$$

in the large loop approximation, where T and L are, respectively, the Euclidean time and space span of the the square loop. This behavior implies that the potential between a $q - \bar{q}$ pair of heavy static quark-antiquarks grows linearly with the distance L between then, i.e. $V = -\sigma L$, which implies the need of linearly increasing amount of energy to separate these quarks a large distance L. This linear behavior is radically different of the expected Coulombian behaviour $V = a/L$ of the perturbative approach ($L \ll 1$).

In summary, the analytic approach to QCD is successful in two opposite regimes: in the limit of weak coupling, the quarks interact with a Coulomb like potential, which leads to asymptotic freedom, while on the other hand, the limit of strong coupling shows the existence of a linear potential that confines the quarks. However this is not a proof confinement, it is necesary to show that both behaviors arise in the same theory. This means to prove that the coupling constant flows from small value at high energy to large value at small energy without any phase transition, otherwise we should see just one of the two regimes. The formula (1.2) indicates that a_s increases as the energy becomes smaller and smaller but it stop to be valid at a scale of energy beyond $\Lambda_{QCD} \simeq 200$Mev as the perturbative calculus is no more valid. The QED for example also shows confinement for strong coupling, but we know that in the continuum limit electrons and photons are free. The consistency of the lattice theory with the continuum limit requires the existence a phase transition separating the strong coupling phase to the weak coupling phase. Such a transition has been clearly seen in numerical simulations when going from strong coupling to weak coupling.

The proof that no phase transition occurs for intermediate value of the coupling constant in QCD would be equivalent to a proof of confinement.

Although the numerical simulations on the lattice do not show any trace of such a transition in the intermediate phase, the analytic proof of this fact has remained elusive for decades and still is one of the challenging theoretical questions in QCD. It must be shown that the same theory that confines on the lattice for strong coupling has a continuum limit for weak coupling that is consistent with the asymptotically free behavior at short distances of QCD.

On the other hand the intermediate regime of the coupling constant is very rich of interesting phenomena, like for example the existence of a plethora of Quarkonia, that are bound states of heavy quarks. The relevant energies in a quark bound state are in most cases of the order the scale of 1 fm, the average hadron size, that correspond to the scale of energy of Λ_{QCD}, where it is supposed to happen the crossover between the perturbative regime of asymptotic regime and non perturbative regime of confinement. So the theoretical comprehension of these phenomena is directly connected to the physics of confinement. In case of heavy quarks, like *bottom* and *charm*, the velocities of the quarks are non relativistic and the time scale associated with the binding of the gluons is smaller than the time scale associated with the quark motion: the gluon interaction between heavy quarks can be considered instantaneous. Therefore, the non relativistic quarkonium bound state can be modeled with a potential and the energy can be obtained solving the corresponding non-relativistic Schrödinger equation.

The effective potential that can be obtained in perturbation theory from one gluon exchange, as mentioned above, has a Coulomb like form. It cannot be the final answer since it does not confine quarks and gives a spectrum incompatible with the data, but adding a linear potential, motivated by the strong coupling limit, we can form a phenomenological potential (Cornell potential)

$$V_c(r) = -\frac{4}{3}\frac{\alpha_s}{r} + \sigma\, r,$$

where α_s and σ are parameters to be fitted with the data. The Schrödinger equation with this potential and $\alpha_s = 0.38$ and $\sigma = 0.18\text{GeV}^{-2}$ gives a quite satisfactory agreement with the data.

1.2. The Gribov picture of confinement

To show the absence of phase transition in the intermediate regime of QCD, we need an inspiration to guess how from pure QCD dynamics a confining color string can be created out of the vacuum by the presence of a quark-antiquark pair. Some very appealing pictures have been proposed in the past, but none was completely successful.

The oldest one is based on the dual superconductor scenario. In a normal superconductor the phenomenon of superconductivity is due to the condensation, below the critical temperature, of Cooper electron pairs. A related aspect is the Meissner effect: an external magnetic field permeating the superconductor is expelled from the bulk material as the temperature drops below the critical value. This implies that one magnetic monopole cannot exists in the superconductor. The amount of magnetic flux that comes out from the monopole inside the superconductor cannot be completely expelled out. Because of the Meissner effect in the presence of a monopole-antimonopole pair, the magnetic flux coming out from the monopole into the antimonopole can be expelled from a type II superconductor by forming a thin flux tube connecting both magnetic sources and inducing a potential between them growing linearly with the size of the pair. This implies that it cost more and more energy to pull the monopoles apart. This phenomenon is reminiscent of the Wilson area law, and the confinement of monopoles induced by Meissner effect suggests a possible mechanism for quarks confinement. If the QCD vacuum behaves like a dual superconductor generated by the condensation of magnetic monopoles the chromo-electric flux will be expelled from the vacuum by the dual Meissner effect. Thus, the immersion of a quark-antiquark pair in such a magnetic superconducting vacuum will generate a concentration of the chromo-electric flux along the line connecting the two particles. The flux tube behaves like a string, inducing an effective quark-antiquark potential growing linearly with the distance, i.e. we will get quark confinement. The dual superconductor picture illuminated many approaches to the confinement problem but none of then achieved a analytic formulation leading to a proof quark confinement.

A complementary picture came from the AdS/CFT correspondence. The main point of this correspondence is that strongly coupled gauge theories are dual to perturbative string theories. This connection created a bridge between two fields of physics. Problems that are unaccessible in gauge theory can be in principle translated in the language of string theory and viceversa. This connection inspired the search of a string theory dual to QCD in order to make progress in the analytic comprehension of non perturbative effects of strong interactions. In particular one promising duality was represented by IIB string theory in a background of five-dimensional anti-de Sitter space times a five-sphere and the large N limit of $\mathcal{N} = 4$ supersymmetric Yang-Mills theory in four dimensions. However, the resulting dual gauge theory is conformally invariant and is not confining.

Both pictures can help in the understand how the mechanism should work, but they are not connected with real QCD. There is an alternative picture, proposed by Gribov, that was inspired by real QCD, which is based on Coulomb phase instability. Gribov was motivated by the instability of the relativistic hydrogenoid atoms, pointed out by complex values of the energies

$$E = mc^2 \left[1 + \left(\frac{Z\alpha}{n - (j + \frac{1}{2}) + \sqrt{(j + \frac{1}{2})^2 - (Z\alpha)^2}} \right)^2 \right]^{-\frac{1}{2}} \tag{1.3}$$

when $Z\alpha > 1$ for $j = \frac{1}{2}$, for example. This means that there is a critical value for the atomic number $Z_c = 137$, beyond which the vacuum becomes unstable and generates electron-positron pairs: the electrons, with negative energy, fall into the heavy nucleus reducing its charge Z and the positrons are left free. If the new atom is still unstable the process repeats until the charge of the nucleus becomes sufficiently small. This phenomenon is possible only due to the existence of light fermion. Based in this analogy, Gribov suggested that a similar phenomenon could be re root of the confinement of quarks in QCD. The existence of very light quarks, can drastically change the vacuum structure. He claimed that understanding the physics of light quarks was directly connected with the solution of the confinement

problem. He pointed out that in QCD already the color charge of a single quark could be supercritical, in contrast to QED where a very large charge $Z_c = 137$ is required. In QCD the role of the supercritical charge is in fact played by the strong coupling constant which becomes large at low momentum scales because of the anti-screening phenomena (1.2).

The confinement of heavy quarks in Gribov's scenario is very similar to the supercritical binding in QED. In the presence of a single quark, due to its supercritical effective charge, the vacuum becomes unstable and decays into quark-antiquark pairs. In this sense the quark exists only as a resonance and cannot be observed as a free particle. To provide a quantitative support to the picture, Gribov analyzed the Green function of light quarks, to get a full dynamical physical picture of the supercritical charge regime. He derived the Green function from the corresponding Dyson-Schwinger equation and he found a critical coupling

$$\alpha_c = \frac{2\pi N}{N^2 - 1}(1 - \sqrt{\frac{2}{3}}),$$

for any $SU(N)$ gauge theory. In particular, $\alpha_c \simeq 0.43$ for real QCD ($N = 3$). For couplings bigger that α_c the Green function changes its behavior pointing out a chiral symmetry breaking.

Although the light quark Green function did not correspond to confined quarks, Gribov argued that taking into account the effects of pions which arise as Goldstone bosons of the symmetry broken, the modified effective Green function would display an the analytic structure of confined quarks. Unfortunately, in 1997 Gribov died right after claiming to have a full proof of confinement, but before concluding the papers ([38], [39]).

1.3. Coulomb impurities in graphene

The source of vacuum instability in the Gribov approach requires further clarification. The fact that the Hydrogenoid spectrum of the Coulomb potential becomes complex for $Z_c > 137$ does not mean that unitarity is lost. Even for such large charges the relativistic Dirac Hamiltonian remains hermitian. The energy spectrum is real, and the complex values obtained by the analytic continuation of (1.3) only suggest the appearance of resonances in the scattering matrix of the one-particle relativistic system. This cast some doubts on the naive interpretation of phenomenon. In QED the phenomenon can be interpreted as follows. What happens for $Z \sim 137$ (forgetting about the finite size corrections of the atomic nucleus which shifts Z_c to 170) is that there is a lower bound state which sinks into the lower negative continuum spectrum $E = -m$. Then, a spontaneous electron-positron pair production becomes possible. Pictorially in the Dirac sea language the phenomenon can be understood in the following terms: if the bound state is empty an electron from the Dirac sea can fill this additional state, leaving an hole in the sea which can be interpreted as a positron escaping to infinity. The electron remains near the charged nuclei, it is said to fall into the center, forming a supercritical bound state. In this process, the neutral vacuum becomes unstable, decaying into a charged vacuum. The new vacuum is stable due to the Pauli principle. However, in full quantum field theory this one particle scenario is not correct due to the production of electron-positron pairs.

In spite of the difficulties of synthesizing nuclei with such large electric charges, in heavy ion collisions of lead-lead and gold-lead an excess of positrons has been detected. The number of positrons is increasing with the total number of protons involved in the collision. The experiments claim that the excess of positrons fits the expectations of the Coulomb vacuum instability for supercritical charges of the nuclei resulting of the fusion of the colliding nuclei.

However, very recently a new testing ground of the Coulomb instability has arisen with the discovery of graphene. The analysis of the consistency of the Dirac equation with supercritical Coulomb potential can be translated

from the complicated world of nuclear physics the simplest one of charged impurities in graphene.

Graphene is a two dimensional layer of carbon atoms arranged on a honeycomb lattice of hexagons. Graphite was known from centuries, but graphene has been isolated for the first time only in 2004 by Geim and Novoselov. The electronic properties of graphene are well described by an effective theory of massless two dimensional Dirac fermions. Graphene is sensitive to material disorder that break the lattice symmetry. Disorder in graphene can have remarkable consequences, e.g. it can induce a gap generating a mass term for the fermion in the effective relativistic theory. Moreover, the presence of a charge impurity with strong Coulomb interactions generate remarkable effects in the spectroscopic and transport properties. The physics of the effective theory mimics the studies of the relativistic atomic phenomena which were performed few decades earlier. In any case they revived the interest on the theoretical and experimental studies on the Coulomb potential supercritical instabilities. The main difference with respect to the 3D analogue, Hydrogen-like atom, is that the value of the supercritical charge is much smaller $Z\alpha = \frac{1}{2}$, where

$$\alpha = \frac{e_*^2}{v_F}, \quad e_*^2 = \frac{2e^2}{\epsilon + 1},$$

Z being the impurity valence, ϵ the dielectric constant of the substrate where graphene is grown and v_F is the Fermi velocity of the electrons in graphene which is about 300 times smaller than the light speed. For example in the vacuum $\alpha \simeq 2$, while for SiO_2 $\alpha \simeq 1$. Thus, already for Coulomb impurities with $Z = 1$ the system in the supercritical regime: graphene is intrinsically strongly coupled. The physics of the Coulomb impurities in graphene correspond to the supercritical relativistic heavy atoms and it can provide the first experimental tests of many elusive predictions from strong-coupling QED, included the main motivation of Gribov mechanism of quark confinement.

The physics of graphene points out that a quantum mechanical description of a strongly coupled system is possible and that the single particle Coulomb problem constitutes the first step in addressing nontrivial features

of the full, many-body interacting problem. This is also the road map of the Gribov approach to quark confinement. For such a reason we will address both problems from the same perspective.

In the graphene case, the first step is to understand the meaning of the apparent complex character of the Hydrogen-like spectrum for supercritical coupling. In particular, to address the correct definition of the Hamiltonian as self adjoint operator. The result will be valid not only for graphene but also for the 3D real QED case. From a mathematical viewpoint, the only problem in that one has to fix the boundary conditions that define the selfadjoint extension of Dirac Hamiltonian for any value of the coupling constant. The non uniqueness of the self adjoint extension of the Dirac Hamiltonian, arise in graphene for any value of the impurity charge $Z\alpha > 0$, where as only for very large values in $Z\alpha > \frac{\sqrt{3}}{2}$ in the 3D QED case. The ambiguities are associated to the many possible choices of boundary conditions which introduces an anomalous breaking of conformal symmetry.

Although the instabilities that motivated the Gribov approach are not so dramatic, nevertheless, there is a significative change in the behavior of the system. We will see that this fact requires a change in the Gribov approach to confinement.

1.4. Objectives and outline

The main goal of this thesis is to develop an approach to the proof of quark confinement which is inspired by the Gribov approach to confinement.

The confirmation in graphene physics that many of the insights of the Gribov picture work in the similar effective models of condensed matter boosted the interest in this study in both directions. In one direction the analysis of the stability of Coulomb backgrounds is interesting to understand the effects of charge impurities in graphene, and in the other direction, the analysis of the physical effects in graphene physics which mimic the pair creation associated to the vacuum instability in QCD might shed some light in the confinement mechanism.

In graphene theory there is not a global description of Coulomb phases

for all the values of impurities charges. One aim of this work is perform such a study in a comprehensive way to better analyze the transition between the subcritical and the supercritical regime in a rigourous way. We address the coherent description of the self-adjoint Hamiltonian in all the regime of the charge in Chapter 2. The global analysis also allowed us to address a new non-trivial spectral flow of bound states along the space of boundary conditions.

Even if the analysis of the Coulomb point charges that motivated the Gribov picture of confinement has revealed to be incomplete, his arguments still remain very appealing. Our main goal in this work is to obtain a similar picture from a new perspective, directly based on first principles, i.e. the Euclidean partition function defined by the QCD Lagrangian. First we analyze the case of one heavy static quark (Chapter 3) and, later, in a more realistic neutral heavy static quark-antiquark pair background (Chapters 4 and 5).

In the analysis of the Coulomb phase in one single quark background, we use the analysis of the self adjoint extensions of the relevant operators in terms of boundary conditions developed for the graphene case. The classification of the self adjoint extensions is done in terms of boundary conditions and the renormalization of the singularity is performed in terms of asymptotic zero modes. The scale introduced by the boundary conditions in the critical regimes of the coupling constant arises from the regularization of the ultraviolet (UV) divergences associated to the static quarks. However, it can be connected with scale which governs the perturbative phenomena of asymptotic freedom and dimensional transmutation. A more general perspective of this connection for singular potentials is analyzed in appendix A.

The case of a heavy quark-antiquark presents many interesting features. First, since the system can be globally colorless it is physically consistent with Gauss law. Second, the new scale of theory that the separation between the two quarks introduces. We shall show that it will play a crucial role in the description of the confinement mechanism (Chapter 5). First, we analyze a simpler case, the same pair but in one-dimension (Chapter 4). This simplifies very much the analysis and it is possible to get analytic

results which provide hints for the behavior of the 3D meson system. We observe, for some regime of coupling constants, that depending on the separation between the two quarks we have stability or not of the vacuum in the presence of the external quark-anti-quark pair of heavy sources.

We extend this analysis to QCD in Chapter 5 and obtain similar results for the intermediate coupling regime, i.e. the expected behavior of a theory which is asymptotically free at short distances, whereas it confines at large distances. In any case the instability of the Coulomb regime at large distances is induced by gluonic instabilities, i.e. the Coulomb saddle point becomes unstable as the distance of the two quarks is larger than a critical distance,

Gribov's picture assigns a leading role to lighter dynamical quarks in the confinement mechanism. In section 6 we check whether this claim is still valid or if the gluonic fluctuations drive the full mechanism (see appendix B for a more complete analysis of gluonic instabilities). The results is not in agreement with Gribov expectations. The main source of instability of Coulomb phases is driven by gluonic fluctuation rather that ferminonic fluctuations usually associated with $q - \bar{q}$ pair creation.

The main result is that we have derived from first principles a novel approach to the Gribov picture of quark confinement, and have not found any signal of a phase transition for intermediate regimes which might prevent the connection of the two asymptotic regimes of QCD, i.e. both regimes are compatible with QCD in the same theory. Asymptotic freedom at short distances and infrared slavery at large distances are not separated by a phase transition. The analysis provides the first analytic glimpse of confinement in QCD and opens a new method of addressing the phenomelogy of QCD at intermediate scales.

2

Coulomb impurities in graphene

The main motivation of Gribov picture of confinement was based on the instability of Coulomb phase in QED. However, this instability requires $Z > 137$ and is very difficult to obtain nuclei with such a large electric charge. Although they can be created by heavy nuclei collisions and an associated positron abundance has been observed, the nuclear instabilities do now allow us to get a clean picture of the physical phenomena. However, very recently with the discovery of graphene a similar phenomenon occurs in the presence of charged impurities, but with a much lower critical charge $Z_c = 1$. In this case the instability yields to screening of the charge impurity which in pure QED cannot occur. The phenomenon has been very recently experimentally observed. Motivated by this new physical phenomenon the analysis of the instability has been deeply analyzed shedding some new light in the Gribov approach. The novel viewpoint shows that unitarity is never lost by the introduction of charge impurities. In fact the formal transmutation of the bounded spectrum of the Hydrogen-like atom analysis into complex values does not means the lost of hermiticity of the corresponding

effective Hamiltonian. It only shows the existence of non-trivial spectral densities in the continuum spectrum which correspond to the existence of resonances in the scattering approach. To clarify the possible application to the Gribov picture we analyze in this chapter the transition between from subcritical regime to a supercritical in the graphene impurities problem. In particular we address a rigorous definition of the Dirac Hamiltonian in the presence o charged impurities potential as self adjoint operator. The problem requires a renormalization the singularity due the Coulomb potential which is more severe for relativistic interactions. Finally the problem is reduced to setting the right boundary conditions near the singularity. This will show us how to proceed in the analysis of the confinement problem from a Coulomb regime in QCD. A similar discussion for conformal potential in Quantum Mechanics is provided in Appendix A.

2.1. 2D Dirac Hamiltonian in a Coulomb background

The electron states in the graphene in presence of a charge impurity are described by two dimensional Dirac Hamiltonian with Coulomb potential:

$$H = -i(\sigma_1\partial_x + \sigma_2\partial_y) + m\sigma_3 - \frac{\alpha}{r}, \tag{2.1}$$

where σ_i, i=1,2,3, are the Pauli matrices, α the charge of the impurity, m the mass and $r = \sqrt{x^2+y^2}$. We assume that the speed of light is normalized to 1.

The singularity at the origin requires some renormalization mechanism. First we introduce a space a cut-off $r_0 > 0$ and then a boundary condition at the cut-off which defines a self adjoint Hamiltonian H. Then, we introduce a renormalization prescription and remove the cut-off. The final result will lead to a selfadjoint Hamiltonian defined over $\mathbb{R}^2\backslash\{\mathbf{0}\}$. In the cut-off domain $r \geq r_0$ shielding the impurity, the domain of the self adjoint extension of the hamiltonian can be defined by imposing the following boundary conditions

$$(1 + \not{\hat{n}})\psi(r_0) = U(r_0)\sigma_3(1 - \not{\hat{n}})\psi(r_0), \tag{2.2}$$

where $U(\,r_\epsilon)$ is an unitary operator defined on the square integrable spinors defined over the circle of radius r_0. and $\hat{n}$ is its normal unit vector, i.e. $\hat{n} = \mathbf{r}/r$.

Using polar coordinates r and θ a general spinor ψ can be expanded, as

$$\psi(r,\theta) = \sum_{l=-\infty}^{\infty} (F_l(r)\Phi_l^+(\theta) + G_l(r)\Phi_l^-(\theta)),$$

with $l \in \mathbb{Z}$ in terms of the orthogonal eigenfunctions of the total angular momentum $J_z = L_z + S_z = -i\frac{\partial}{\partial\theta} + \frac{1}{2}\sigma_3$, with semi-integer eigenvalues $j = l + \frac{1}{2}$

$$\Phi_l^+ = \begin{pmatrix} e^{i\,l\,\theta} \\ 0 \end{pmatrix} \text{ and } \Phi_l^- = \begin{pmatrix} 0 \\ i\,e^{i\,(l+1)\,\theta} \end{pmatrix}.$$

The space of spinors can be then decomposed as orthogonal sum of subspaces with fixed total angular momentum j, $\mathcal{H} = \oplus\mathcal{H}_j$, i.e. general spinor can be written as $\psi = \sum_j \psi_j$, where ψ_j will denote the spinor component in the subspace of total angular momentum j,

$$\psi_j(r,\theta) = \begin{pmatrix} F^j(r)e^{i\,(j-\frac{1}{2})\,\theta} \\ iG^j(r)e^{i\,(j+\frac{1}{2})\,\theta} \end{pmatrix}. \tag{2.3}$$

If the boundary condition defined by U preserves rotational symmetry, U reduces, on each subspace of fixed angular momentum j, to a $U(1)$ phase, i.e. the boundary condition (2.2) becomes

$$(1 + \hat{\not{n}})\psi_j(r_0) = e^{i\,\beta_0^j}\sigma_3(1 - \hat{\not{n}})\psi_j(r_0). \tag{2.4}$$

Explicitly, F and G satisfy on the boundary:

$$e^{i\,\beta_0^j} = \frac{F^j(r_0) + iG^j(r_0)}{F^j(r_0) - iG^j(r_0)}, \tag{2.5}$$

where $F(r_0)/G(r_0)$ are real functions.

Renormalization of the UV divergences and boundary conditions

Let us now introduce now a fundamental ingredient in our discussion, *asymptotic zero modes* near the origin. They will play a fundamental role in the renomalization of the singularity introduced by the singularity. We can by means of these zero-modes define the self adjoint extension of the Hamiltonian as a limit when the cut-off goes to zero in terms of appropriate the boundary conditions. The form of the zero modes is strongly dependent on the value of the charge. To find the zero modes near the singularity of the Hamiltonian (2.1) we have to keep only the leading terms of of the asymptotic expansion around the impurity. Using the expansion (2.3) is easy to show that they have to satisfy the following coupled equations

$$\frac{dF_0^j}{dr} - \frac{j-\frac{1}{2}}{r}F_0^j + \frac{\alpha}{r}G_0^j = 0, \tag{2.6}$$

$$\frac{dG_0^j}{dr} + \frac{j+\frac{1}{2}}{r}G_0^j - \frac{\alpha}{r}F_0^j = 0. \tag{2.7}$$

We search a solution of (2.6) and (2.7) of the form

$$\begin{aligned} F_0^j(r) &= r^s \\ G_0^j(r) &= C\, r^s \end{aligned}$$

This requires that

$$s = -\frac{1}{2} + \nu, \quad C_+ = \frac{j-\nu}{\alpha},$$

or

$$s = -\frac{1}{2} - \nu, \quad C_- = \frac{j+\nu}{\alpha},$$

where $\nu = \sqrt{\alpha^2 - j^2}$. These solutions are only valid for $\alpha^2 \neq j^2$. For $\alpha^2 = j^2$ the two solutions are instead are given by

$$\begin{aligned} F_0^j(r) &= r^{-\frac{1}{2}} \\ G_0^j(r) &= C\, r^{-\frac{1}{2}} \end{aligned}$$

and

$$\begin{aligned} F_0^j(r) &= r^{-\frac{1}{2}} \log(\Lambda\, r)) \\ G_0^j(r) &= \frac{j}{|j|}\, r^{-\frac{1}{2}} (\log(\Lambda\, r)) - \frac{1}{j}), \end{aligned}$$

where ϵ is an arbitrary parameter with dimension $[L]^{-1}$.

Notice that for $\alpha^2 < j^2$ the parameter ν is real, while for $\alpha^2 > j^2$ it is purely imaginary. Taking also into account the local L^2 normalizability at the origin, there are four different types of regimes depending on the strength of the charge impurity.

i) For $\alpha^2 \leq j^2 - \frac{1}{4}$ the solution with $s = -\frac{1}{2} - \nu$ is not locally normalizable at the origin, so it must be excluded. The general zero mode is in this case of the form

$$\begin{aligned} F_0^j(r) &= r^{-\frac{1}{2}+\nu} \\ G_0^j(r) &= C_+ r^{-\frac{1}{2}+\nu}. \end{aligned} \tag{2.8}$$

For $\alpha^2 > j^2 - \frac{1}{4}$ both the solutions are normalizable so the most general zero mode is a linear combination of the two behaviors. The only constraint is the ratio F/G have to be a real functions. The structure strongly depend on the value of the charge. We will parametrize the different linear combinations (up to a normalization constant N) in terms of an angle $\theta \in [0, \pi)$ and the scale parameter Λ.

ii) $j^2 - \frac{1}{4} < \alpha^2 < j^2$:

$$\begin{aligned} F_0^j(r) &= N\, r^{-\frac{1}{2}} \big(\cos\theta\, (\Lambda\, r))^{\nu} - \sin\theta\, (\Lambda\, r))^{-\nu} \big) \\ G_0^j(r) &= N\, r^{-\frac{1}{2}} \big(\cos\theta\, C_+ (\Lambda\, r))^{\nu} - \sin\theta\, C_- (\Lambda\, r))^{-\nu} \big), \end{aligned} \tag{2.9}$$

iii) $\alpha^2 = j^2$:

$$\begin{aligned} F_0^j(r) &= N\, r^{-\frac{1}{2}} \big(\cos\theta + \sin\theta\, \log(\Lambda\, r)) \big) \\ G_0^j(r) &= N\, C\, r^{-\frac{1}{2}} \Big(\cos\theta + \sin\theta\, \big(\log(\Lambda\, r)) - \frac{1}{j} \big) \Big), \end{aligned} \tag{2.10}$$

iv) $\alpha^2 > j^2$:

$$\begin{aligned} F_0^j(r) &= N\, r^{-\frac{1}{2}} \big(\exp(-i\,\theta)\,(\Lambda r)^{\nu} + \exp(i\,\theta)\,(\Lambda r)^{-\nu} \big) \\ G_0^j(r) &= N\, r^{-\frac{1}{2}} \big(\exp(-i\,\theta)\, C_+ (\Lambda r)^{\nu} + \exp(i\,\theta)\, C_- (\Lambda r)^{-\nu} \big), \end{aligned} \quad (2.11)$$

In the UV limit the cut-off $r_0 \to 0$ and any eigenfunction of H satisfying the boundary condition (2.5) must also become an asymptotic zero mode. Thus, we can associate to each boundary condition in the four regimes an asymptotic zero mode and reciprocally each zero mode defines one class of boundary conditions:

$$\frac{F_0^j(r_0) + iG_0^j(r_0)}{F_0^j(r_0) - iG_0^j(r_0)} := e^{i\,\beta_0^j}. \quad (2.12)$$

In other terms, once the cut-off is fixed r_0, we can associate to each boundary condition parametrized by β_0^j, a particular asymptotic zero mode (F_0^j, G_0^j) satisfying (2.12). Again, the relation depends on the regime of the coupling constant.

i) For $\alpha^2 \leq j^2 - \frac{1}{4}$ since we have only one asymptotic zero mode means that there is only a selfadjoint extension. In fact the constraint (2.12) completely fixes β_0^j, independently from r_0:

$$\beta_0^j = \arccos \sqrt{j^2 - \alpha^2}.$$

This means that we have only one self adjoint extension on H.

For $\alpha^2 > j^2 - \frac{1}{4}$ there is a family of asymptotic zero modes which can be parametrized by the phase β_0^j at the boundary cut-off r_0. For simplicity we define $\zeta = \tan\theta$ and $y = \tan(\beta_0^j/2)$.

ii) For $j^2 - \frac{1}{4} < \alpha^2 < j^2$, for each $\beta_0^j \in [0, 2\pi)$ we can associate a zero mode by the relation:

$$\zeta = \frac{(j-\nu) - \alpha\, y}{(j+\nu) - \alpha\, y} (\Lambda\, r_0)^{2\nu}. \quad (2.13)$$

iii) For $\alpha^2 = j^2$, fixed r_0, to each $\beta_0^j \in [0, 2\pi)$ we can assign a zero mode by

$$\zeta = \frac{j - |j|\, y}{1 - (j - |j|\, y)\log(\Lambda\, r_0)}. \tag{2.14}$$

iv) For $\alpha^2 > j^2$, if we define $\xi = -\tan\left(|\nu| \log(\Lambda\, r_0)\right)$, we can associate to each $\beta_0^j \in [0, 2\pi)$ a zero mode by the relation:

$$\zeta = \frac{j - \xi|\nu| - \alpha\, y}{j\,\xi + |\nu| - \alpha\,\xi\, y}. \tag{2.15}$$

In summary, we have defined the boundary condition on the cut off r_0 by means of an unitary operator, which for each angular momentum is given by a phase which is in one-to one correspondence with a locally normalizable asymptotic zero mode.

The next step is to remove the cut-off, sending r_0 to zero. For any other cut-off $r_\epsilon < r_0$ the boundary condition can be determined by a running phase β_ϵ^j that can be defined in terms of the initial one β_0^j which converges to a well defined boundary condition when the cut-off is removed, which gives a well defined Hamiltonian for the dynamics of electrons in presence of the impurity in the graphene sheet. The running phase β_ϵ^j at different r_ϵ is renormalized according to

$$e^{i\,\beta_\epsilon^j(\,r_\epsilon)} = \frac{F_0^j(\,r_\epsilon) + iG_0^j(\,r_\epsilon)}{F_0^j(\,r_\epsilon) - iG_0^j(\,r_\epsilon)}, \tag{2.16}$$

in terms of the zero mode (F_0^j, G_0^j) associated to the initial phase β_0^j at r_0 by the relations (2.13), (2.14) or (2.15), That is, the initial phase β_0^j defines a zero mode (F_0^j, G_0^j), and the boundary phase β_ϵ^j runs with the cut-off while keeping fixed the zero mode. Once more the explicit form of the renormalization function for β^j depends by the value and regime of the charge.

ii) **Case** $j^2 - \frac{1}{4} < \alpha^2 < j^2$

$$\tan\frac{\beta_\epsilon^j}{2} = -\frac{j+\nu}{\alpha}\left(1 + \frac{2\tan\theta}{(\Lambda\, r_\epsilon)^{2\nu} - \tan\theta}\right),$$

iii) **Case** $\alpha^2 = j^2$

$$\tan\frac{\beta^j}{2} = \frac{j - \tan\theta + j\,\tan\theta\,\log(\Lambda\, r_\epsilon)}{|j|\,(1 + \tan\theta\,\log(\Lambda\, r_\epsilon))},$$

iv) **Case** $\alpha^2 > j^2$

$$\tan\frac{\beta^j_\epsilon}{2} = \frac{1}{\alpha}\left(j + |\nu|\frac{\tan\theta + \tan\left(|\nu|\log(\Lambda\, r_\epsilon)\right)}{\tan\theta\,\tan\left(|\nu|\log(\Lambda\, r_\epsilon)\right) + 1}\right);$$

Finally we can define the selfadjoint extensions of the Hamiltonian on $\mathbb{R}^2\setminus\{\mathbf{0}\}$ in the limit $r_\epsilon \to 0$. Once we impose the boundary condition (2.5) on the cut off r_0, we impose that

$$e^{i\,\beta^j_\epsilon(\,r_\epsilon)} = \frac{F^j(\,r_\epsilon) + iG^j(\,r_\epsilon)}{F^j(\,r_\epsilon) - iG^j(\,r_\epsilon)},$$

with $\beta(\,r_\epsilon)$ running according (2.16). Explicitly, if we remove the cut-off $r_\epsilon \to 0$ the boundary condition in terms of the zero mode is given by

$$\lim_{r\to 0}\Big(F^j(r)G^j_0(r) - G^j(r)F^j_0(r)\Big) = 0. \tag{2.17}$$

Any selfadjoint extension of H on $\mathbb{R}^2\setminus\{\mathbf{0}\}$ is then defined by boundary conditions in terms of a zero mode, and the family of self adjoint extensions for $\alpha^2 > j^2 - \frac{1}{4}$ is parameterized by the zero-mode phase θ. The explicit forms of (2.17) depends again on the regime of the charge α:

i) **Case** $\alpha^2 \le j^2 - \frac{1}{4}$

$$\lim_{r\to 0}\big((-j+\nu)F^j(r) + \alpha G^j(r)\big) = 0; \tag{2.18}$$

ii)Case $j^2 - \frac{1}{4} < \alpha^2 < j^2$

$$\lim_{r\to 0}\Big((\Lambda r)^{2\nu}\big((-j+\nu)F^j(r)+\alpha G^j(r)\big)+\tan\theta\big((j+\nu)F^j(r)-\alpha G^j(r)\big)\Big)=0; \tag{2.19}$$

iii)Case $\alpha^2 = j^2$

$$\lim_{r\to 0}\Big(j\,G(r)\Big(1+\log(\Lambda r)\tan\theta\Big)-F(r)\Big(|j|+\big(-1+j\,\log(\Lambda r)\big)\tan\theta\Big)\Big)=0. \tag{2.20}$$

iv)Case $\alpha^2 > j^2$

$$\lim_{r\to 0}\Big((\Lambda r)^{2\nu}\big((-j+\nu)F^j(r)+\alpha G^j(r)\big)-\exp(2i\theta)\big((j+\nu)F^j(r)-\alpha G^j(r)\big)\Big)=0. \tag{2.21}$$

2.2. Bound states spectral problem

Once the boundary conditions give rise to a self adjoint Hamiltonian, we can find the bound states in the spectrum,

$$H\psi = E\psi. \tag{2.22}$$

Using the ansatz (2.3), in each subspace of fixed j, the eigenvalue problem reduce to the following coupled differential equation:

$$\frac{dF^j}{dr} - \frac{j-\frac{1}{2}}{r}F^j + (E+m+\frac{\alpha}{r})G^j = 0, \tag{2.23}$$

$$\frac{dG^j}{dr} + \frac{j+\frac{1}{2}}{r}G^j - (E-m+\frac{\alpha}{r})F^j = 0. \tag{2.24}$$

Replacing

$$F^j(r) = \frac{\sqrt{m+E}}{2\,r}\big(a(r)-b(r)\big), \qquad G^j(r) = \frac{\sqrt{m-E}}{2\,r}\big(a(r)+b(r)\big),$$

$$x = 2\epsilon\, r, \qquad \epsilon = \sqrt{m^2 - E^2}, \tag{2.25}$$

gives the following coupled equations for $a(x)$ and $b(x)$:

$$x\frac{d}{dx}a(x) + \Big(\frac{x}{2} - \frac{1}{2} - \frac{\alpha E}{\epsilon}\Big)a(x) + \Big(\frac{\alpha m}{\epsilon} + j\Big)b(x) = 0, \tag{2.26}$$

$$x\frac{d}{dx}b(x) - \Big(\frac{x}{2} + \frac{1}{2} - \frac{\alpha E}{\epsilon}\Big)b(x) + \Big(-\frac{\alpha m}{\epsilon} + j\Big)a(x) = 0. \tag{2.27}$$

It is now possible to decouple $a(x)$ and $b(x)$. From (2.26) one can get

$$b(x) = \frac{(2\alpha E + \epsilon - \epsilon\, x)a(x) - 2\epsilon\, x\, a'(x))}{2(\alpha m + j\epsilon)}, \tag{2.28}$$

and plugging it in (2.27), gives rise to an equation for $a(x)$

$$\frac{d^2a(x)}{d^2x} + \Big(-\frac{1}{4} + \frac{\frac{1}{2} + \alpha\frac{E}{\epsilon}}{x} + \frac{\frac{1}{4} - j^2 + \alpha^2}{x^2}\Big)a(x) = 0, \tag{2.29}$$

which can be solved in terms of Whittaker functions W and M

$$a(x) = A\, W(\frac{1}{2} + \frac{\alpha E}{\epsilon}, \nu, x) + B\, M(\frac{1}{2} + \frac{\alpha E}{\epsilon}, \nu, x), \tag{2.30}$$

where A and B are constants. Substituting (2.30) in (2.28), we have

$$b(x) = (j - \frac{\alpha m}{\epsilon})\, A\, W(-\frac{1}{2} + \frac{\alpha E}{\epsilon}, \nu, x) + \Big(\frac{\alpha m - j\epsilon}{\alpha E + \nu\epsilon}\Big)\, B\, M(-\frac{1}{2} + \frac{\alpha E}{\epsilon}, \nu, x). \tag{2.31}$$

Inserting these expressions into (2.25) we have that the general solution of

(2.23) and (2.24) is

$$
\begin{aligned}
F^j(r) &= \frac{\sqrt{m+E}}{2\,r}\Bigg(A\Big(W(\frac{1}{2}+\frac{\alpha E}{\epsilon},\nu,2\epsilon r)-(j-\frac{\alpha m}{\epsilon})W(-\frac{1}{2}+\frac{\alpha E}{\epsilon},\nu,2\epsilon r)\Big)\\
&\quad +B\Big(M(\frac{1}{2}+\frac{\alpha E}{\epsilon},\nu,2\epsilon r)-\Big(\frac{\alpha m-j\epsilon}{\alpha E+\nu\epsilon}\Big)M(-\frac{1}{2}+\frac{\alpha E}{\epsilon},\nu,2\epsilon r)\Big)\Bigg),\\
G^j(r) &= \frac{\sqrt{m-E}}{2\,r}\Bigg(A\Big(W(\frac{1}{2}+\frac{\alpha E}{\epsilon},\nu,2\epsilon r)+(j-\frac{\alpha m}{\epsilon})W(-\frac{1}{2}+\frac{\alpha E}{\epsilon},\nu,2\epsilon r)\Big)\\
&\quad +B\Big(M(\frac{1}{2}+\frac{\alpha E}{\epsilon},\nu,2\epsilon r)+\Big(\frac{\alpha m-j\epsilon}{\alpha E+\nu\epsilon}\Big)M(-\frac{1}{2}+\frac{\alpha E}{\epsilon},\nu,2\epsilon r)\Big)\Bigg).
\end{aligned}
\tag{2.32}
$$

Recalling the asymptotic expressions of M and W for $r << 1$

$$
\begin{aligned}
M(\pm\frac{1}{2}+\frac{\alpha E}{\epsilon},\nu,x) &\cong x^{\frac{1}{2}+\nu} \qquad (2.33)\\
W(\pm\frac{1}{2}+\frac{\alpha E}{\epsilon},\nu,x) &\cong x^{\frac{1}{2}}\Big(x^{\nu}\frac{\Gamma[2\,\nu]}{\Gamma[\frac{1}{2}\mp\frac{1}{2}-\nu-\frac{\alpha E}{\epsilon}]}+x^{-\nu}\frac{\Gamma[2\,\nu]}{\Gamma[\frac{1}{2}\mp\frac{1}{2}+\nu-\frac{\alpha E}{\epsilon}]}\Big),
\end{aligned}
$$

for $\alpha \neq j$, whereas that for $\alpha = j$ we have

$$
\begin{aligned}
M(\pm\frac{1}{2}+\frac{\alpha E}{\epsilon},\nu,x) &\cong x^{\frac{1}{2}}\\
W(\pm\frac{1}{2}+\frac{\alpha E}{\epsilon},\nu,x) &\cong -\frac{x^{\frac{1}{2}}}{\Gamma[\frac{1}{2}\mp\frac{1}{2}-\frac{jE}{\epsilon}]}\Big(\log x+\psi(\frac{1}{2}\mp\frac{1}{2}-\frac{jE}{\epsilon})+2\gamma\Big),
\end{aligned}
$$

where where ψ is the digamma function and γ is Euler's constant.

2.3. Bound states and the spectral flow

The spectrum of bound states generated by the impurity is different in the four regimes of the coupling introduced in the section in the previous section.

i) Case $\alpha^2 \leq j^2 - \frac{1}{4}$

The boundary conditions (2.18) imply that A must be fixed to $A = 0$ in the general solution (2.32). The solution must also decay at infinity, that is, keeping only the leading terms of (2.23) and (2.24), it must behave like $F^j(r) \cong \exp[-\epsilon r], G^j(r) \cong \exp[-\epsilon r]$ for $r >> 1$. Thus the solution should be of the form

$$F^j(r) = r^{-\frac{1}{2}+\nu} \exp[-\epsilon r] f(r), \;\; G^j(r) = r^{-\frac{1}{2}+\nu} \exp[-\epsilon r] g(r),$$

with functions $f(r)$ and $g(r)$ polynomially bounded at infinity. Then, it easy to show that this occurs when the expressions

$$r^{-\frac{1}{2}-\nu} \exp[\epsilon r] M(\frac{1}{2} + \frac{\alpha E}{\epsilon}, \nu, 2\epsilon r), \tag{2.34}$$

$$r^{-\frac{1}{2}-\nu} \exp[\epsilon r] M(-\frac{1}{2} + \frac{\alpha E}{\epsilon}, \nu, 2\epsilon r) \tag{2.35}$$

reduce both to polynomials, or when only (2.34) is polynomial and $\alpha m - j\epsilon = 0$. Expanding (2.34) and (2.35) it is possible one finds that his happens when $-\alpha E/\epsilon + \nu = -n$, with $n = 0, 1, 2, ..$ if $j > 0$ and $n = 1, 2, ..$ if $j < 0$. More explicitly

$$E_n^H = \frac{m}{\sqrt{1 + \frac{\alpha^2}{(n+\sqrt{j^2-\alpha^2})^2}}}, \qquad \begin{cases} n = 0, 1, 2, .. \text{ for } j > 0 \\ n = 1, 2, .. \text{ for } j < 0 \end{cases}. \tag{2.36}$$

This is the well known Hydrogenoid atom bound states spectrum.

The spectrum of bound states is different when $\alpha^2 > j^2 - \frac{1}{4}$ because in that case there is an extra parameter θ in the boundary conditions (2.19),

(2.20) and (2.21). Let us assume that $\theta \neq 0, \theta \neq \frac{\pi}{2}$ in the case (2.19) and $\theta \neq 0$ in the case (2.20)(we will analyze these cases later, separately), and an arbitrary value of θ in the case (2.21). In this cases the boundary conditions can be matched setting $B = 0$ in the general solution (2.32), i. e. keeping only the terms involving the Whittaker function W, which automatically decays exponentially at infinity.
Then, it is possible to find the spectrum of bound states that satisfy the boundary conditions (2.19) for $\theta \neq 0$ and $\theta \neq \frac{\pi}{2}$, (2.20) for $\theta \neq 0$ and (2.21) for any value of θ.

ii) Case $j^2 - \frac{1}{4} < \alpha^2 < j^2$ $(\theta \neq 0, \theta \neq \frac{\pi}{2})$

The spectrum of bound states is given by a discrete series of values $E_n^{II}(\theta)$ which are solutions of the spectral equation

$$\frac{\big(\alpha(-E+m)+(-j+\nu)\epsilon\big)}{\big(\alpha(E-m)+(j+\nu)\epsilon\big)}\frac{\Gamma[2\,\nu]\Gamma\left[1-\nu-\frac{\alpha E}{\epsilon}\right]}{\Gamma[-2\,\nu]\Gamma\left[1+\nu-\frac{\alpha E}{\epsilon}\right]} = \tan\theta\Big(\frac{\Lambda}{2\,\epsilon}\Big)^{-2\,\nu}, \tag{2.37}$$

iii)Case $\alpha^2 = j^2$ $(\theta \neq 0, \theta \neq \pi)$
The spectrum of bound states is given by a discrete series of values $E_n^{III}(\theta)$ which are solutions of the spectral equation

$$\frac{R(\epsilon)}{R(\epsilon) - S(\epsilon)\,\log\epsilon} = \tan\theta \tag{2.38}$$

with

$$R(\epsilon) = \left(j - \frac{|j|\,m}{\epsilon}\right)\frac{2\gamma + \log(2\epsilon) + \psi\left(1 - \frac{|j|\,E}{\epsilon}\right)}{\Gamma\left[1 - \frac{|j|\,E}{\epsilon}\right]} - \frac{2\gamma + \log(2\epsilon) + \psi\left(-\frac{|j|\,E}{\epsilon}\right)}{\Gamma\left[-\frac{|j|\,E}{\epsilon}\right]},$$

$$S(\epsilon) = -\frac{j - \frac{|j|\,m}{\epsilon}}{\Gamma\left[1 - \frac{|j|\,E}{\epsilon}\right]} + \frac{1}{\Gamma\left[-\frac{|j|\,E}{\epsilon}\right]}$$

where ψ is the digamma function and γ the Euler Gamma,

iv) **Case** $\alpha^2 > j^2$ In this case the spectrum of bound states is given by a discrete series of values $E_n^{IV}(\theta)$ which are solutions of the spectral equation

$$\frac{\big(\alpha(-E+m)+(-j+\nu)\epsilon\big)}{\big(\alpha(E-m)+(j+\nu)\epsilon\big)}\frac{\Gamma[2\,\nu]\Gamma\left[1-\nu-\frac{\alpha E}{\epsilon}\right]}{\Gamma[-2\,\nu]\Gamma\left[1+\nu-\frac{\alpha E}{\epsilon}\right]} = -\exp(2\,i\,\theta)\Big(\frac{\Lambda}{2\,\epsilon}\Big)^{-2\,\nu}. \tag{2.39}$$

In the regime **ii**), $j^2-\frac{1}{4}<\alpha^2<j^2$, we have two special cases: for $\theta=0$ and $\theta=\frac{\pi}{2}$ where the zero mode that defines the boundary conditions is reduced to one of the two different asymptotic behaviors near the origin.

H) **Case** $j^2-\frac{1}{4}<\alpha^2<j^2$**,** $\theta=0$

The boundary conditions reduce in this case to (2.18) of the regime i) and then the spectrum is the same as in (2.36), i.e the bound states spectrum is the same as the Hydrogenoid atom E_n^H.

h) **Case** $j^2-\frac{1}{4}<\alpha^2<j^2$**,** $\theta=\frac{\pi}{2}$

It $\theta=\frac{\pi}{2}$ the boundary conditions are defined by the zero mode characterized by the exponent $s=-\frac{1}{2}-\nu$ and become

$$\lim_{r\to 0}\Big(-(j+\nu)F^j(r)+\alpha G^j(r)\Big)=0, \tag{2.40}$$

These boundary conditions can be satisfied by setting A=0 in the general solutions and making the replacement $\nu\to-\nu$. Using the same procedure of the case i), we obtain the spectrum analytically

$$\begin{cases} E_0^h = -\dfrac{m}{\sqrt{1+\frac{\alpha^2}{(\sqrt{j^2-\alpha^2})^2}}} \\ E_n^h = \dfrac{m}{\sqrt{1+\frac{\alpha^2}{(n-\sqrt{j^2-\alpha^2})^2}}} \end{cases} \quad \text{for } j>0, \tag{2.41}$$

$$E_n^h = \frac{m}{\sqrt{1+\frac{\alpha^2}{(n-\sqrt{j^2-\alpha^2})^2}}} \quad \text{for } j<0, \tag{2.42}$$

with $n = 1, 2, 3, ...$

For $\alpha^2 = j^2$, $j > 0$ again $E_0 = 0$ and the special case is $\theta = 0$. In the literature, the bound states of the spectrum obtained with these boundary conditions $\theta = 0$ are called *meta-Hydrogenoid* states [1].

H') Case $\alpha^2 = j^2$, $\theta = 0$ (or $\theta = \pi$)

For boundary conditions with $\theta = 0$ the Hydrogenoid and meta-Hydrogenoid spectra coincide and can be derived from the special case $\theta = 0$. They are defined by (2.36) with the only difference that for $\alpha^2 = j^2$ and $j > 0$, $E_0 = 0$, which is obtained taking $b(r) = 0$ in (2.25). The Hydrogenoid and meta-Hydrogenoid spectra are not defined for $\alpha^2 > j^2$.

The problem which inspired the Gribov approach to confinement is the fact that the energy of the bound states given by E_n^H become complex for $\alpha^2 > j^2$. To better understand what happens let us analyse the flow of the bound state spectrum as we increase the charge α of the impurity.

• Let us analyze first the range of charge $j^2 - 1/4 < \alpha^2 < j^2$, the *subcritical regime*. In this range, there is continuous flow of the spectrum as we change the parameter θ characterizing the boundary conditions. This can be shown in Figure 1, where we display the θ dependence of the lowest energy bound states in this regime. Notice that in the limits $\theta = 0, \theta = \pi/2, \theta = \pi$ we recover the Hydrogenoid and meta-Hydrogenoid spectrum, i.e.

[1] The meta-Hydrogenoid states first appeared in the literature as hydrino states. However, the misuse of its properties for claiming magic generation of energy requires the introduction of new clean name. Notice that in Hydrogen atom $Z = 1, D = 3$ is a subcritical regime where the Hamiltionian is essentially selfadjoint the there is a canonical boundary condition giving rise to the well know spectrum. There is no meta-Hydrogen spectrum. On the other hand it is a pity because if we had the possibility of more exotic boundary conditions we could explain the puzzle of proton radius in an elegant way.

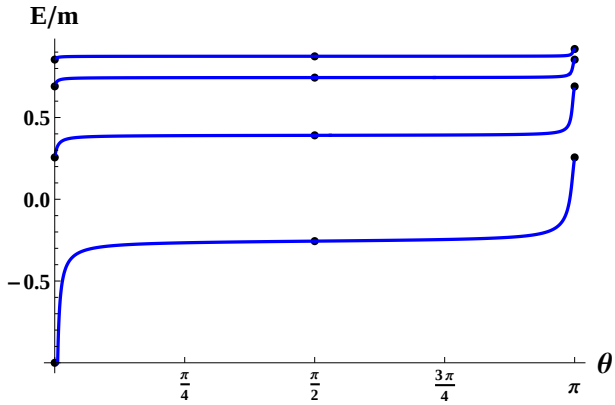

Figure 2.1: θ dependence of the energy E/m of the lowest bound states with angular momentum $j = 3/2$ for $\alpha = 1.45$ inside the subcritical regime $2 < \alpha^2 < \frac{9}{4}$ ($\Lambda = m/10$). The dots correspond to the Hydrogenoid and meta-Hydrogenoid energy levels at $\theta = 0$, $\theta = \frac{\pi}{2}$ and $\theta = \pi$.

$$\lim_{\theta\to 0} E_n^{II}(\theta) = E_n^H, \tag{2.43}$$

$$\lim_{\theta\to \frac{\pi}{2}} E_n^{II}(\theta) = E_n^h \tag{2.44}$$

$$\lim_{\theta\to \pi} E_n^{II}(\theta) = E_{n+1}^H \tag{2.45}$$

$$\tag{2.46}$$

The continuity should be obvious from the fact that the boundary conditions (2.19) reduce to the boundary conditions of the Hydrogenoid and meta-Hydrogenoid spectra in these limits. What is more surprising is the fact that the spectral flow is not periodic. The spectrum is periodic, i.e. it is the same at θ and $\theta + \pi$, but the flow shifts the energy levels by one unit each time that we increase θ by π. In general, for fixed angular momentum and charge we have

$$E_n^{II}(\theta + k\pi) = E_{n+k}^{II}(\theta), \tag{2.47}$$

for any integer $k \in \mathbb{Z}$. Another interesting property of the spectral flow has a monotonic character, i.e. $E^{II}(\theta) < E^{II}(\theta')$ if $\theta < \theta'$. In particular this implies the standard sandwich inequalities between the Hydrogenoid and meta-Hydrogenoid energy levels

$$-m < E_0^h < E_0^H < E_1^h < E_1^H < ... < E_{n-1}^h < E_{n-1}^H < E_n^h < E_n^H < ... < m \tag{2.48}$$

For negative angular momentum $j < 0$, we have the same behaviour as in the positive case $j > 0$. The only difference is the absence of zero levels (n=0) for the Hydrogenoid and meta-Hydrogenoid energy levels. Thus the sandwich inequalities become

$$-m < E_1^h < E_1^H < ... < E_{n-1}^h < E_{n-1}^H < E_n^h < E_n^H < ... < m. \tag{2.49}$$

Another interesting fact in the subcritical regime is that from (2.36) and (2.42) it follows that for $n > 0$ the spectra E_n^H and E_n^h with $j > 0$ and $j < 0$ are degenerate. The boundary condition (2.19) for $\theta \neq k\pi$ and $\theta \neq \frac{2k+1}{2}$ breaks this degeneracy and creates a gap between the energies corresponding to $j > 0$ and $j < 0$. The situation is described in figure 2.2 for $\alpha = 1.45$. For $\theta = 0$ we have the energy corresponding to $n = 1$ of the Hydrogen spectrum E_1^H that is degenerate for $j = \pm\frac{3}{2}$. As we increase the parameter θ a gap appears between the states $j = \pm\frac{3}{2}$. The energy of the state $j = -\frac{3}{2}$ becomes lower than the one corresponding to $j = \frac{3}{2}$. The gap becomes disappears again for $\theta = \frac{\pi}{2}$, where we have the degenerate energy level corresponding to $n = 2$ of the meta-Hydrogenoid spectrum E_2^h. Increasing more the parameter θ, a gap appears again. This time with the energy corresponding to $j = \frac{3}{2}$ lower than the one corresponding to $j = -\frac{3}{2}$. Finally, for $\theta = \pi$ the two energy levels become again degenerate at the level $n = 2$ of E_2^H.

• For $\alpha^2 = j^2$, as we anticipated before, the Hydrogenoid and meta-Hydrogenoid spectra coincide $E_n^{III}(0) = E_n^{III}(\frac{\pi}{2})$ and are given by (2.36) with the only difference that for $\alpha^2 = j^2$ and $j > 0$, $E_0 = 0$. Once more we can understand this in terms of the identification of boundary conditions. Analyzing how the spectrum $E_n^{III}(\theta)$ changes with θ, we find that the

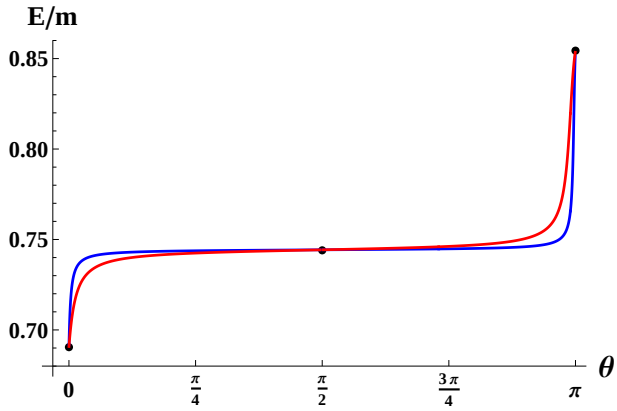

Figure 2.2: Gap between the energies corresponding to $j = 3/2$ (blue) and $j = -3/2$ (red) for $\alpha = 1.45$, $m = 10$ and $\Lambda = 1$ in the subcritical regime.

correspondence in this case is, for $j > 0$,

$$\lim_{\theta\to 0} E_n^{III}(\theta) = E_n^H, \tag{2.50}$$

$$\lim_{\theta\to \pi} E_n^{III}(\theta) = E_{n+1}^h \tag{2.51}$$

$$\tag{2.52}$$

The spectrum is also periodic in this case, i.e. it is the same at θ and $\theta + \pi$, but the flow shifts the energy levels by one unit each time that we increase θ by π. In general, for fixed angular momentum and charge we have

$$E_n^{III}(\theta + k\pi) = E_{n+k}^{III}(\theta), \tag{2.53}$$

for any integer $k \in \mathbb{Z}$. Also in this case the spectral flow has monotonic character, i.e. $E^{III}(\theta) < E^{III}(\theta')$ if $\theta < \theta'$. However, in this case inequalities between the Hydrogenoid and meta-Hydrogenoid energy levels (2.49) become the trivial inequality of the Hydrogenoid levels $E_n^H < E_{n+1}^H$.

• Let us now analyze the *supercritical regime* of charge $\alpha^2 > j^2$. As anticipated before, in this regime, the spectra E_n^H and E_n^h are not defined,

so we cannot establish any correspondence between the impurity spectrum and the Hydrogenoid or meta-Hydrogenoid spectrum for any particular value of θ. In fact for any value of θ $E_n^{IV}(\theta)$ contains an infinity number of bound states that accumulate near $E = m$. In figure (2.3) we plot the flow of some eigenvalues of the spectrum $E_n^{IV}(\theta)$ when parameter θ flows from 0 to π. In that figure we see how one eigenvalues pops up from the continuum $E < -m$ at a particular value of the parameter θ.

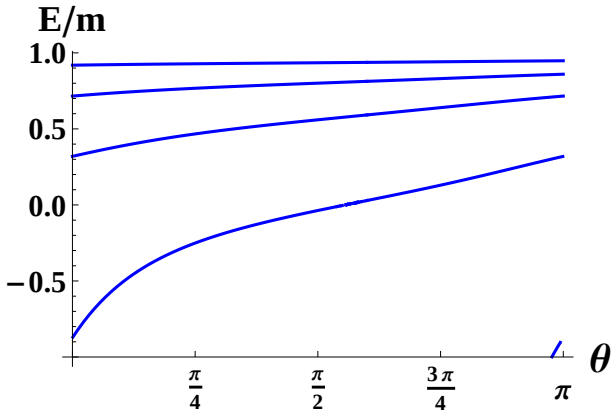

Figure 2.3: Spectral flow for $\alpha = 1.55$, $\Lambda = m/10$ and $j = 3/2$ in the supercritical regime. The lowest bound state energy level emerges from the continuum spectrum for θ close to $\theta = \pi$.

This is the only signal of the instabilities pointed out by the fact that the analytic expressions of Hydrogenoid or meta-Hydrogenoid energy levels become formally complex.

In order to analyze the transition from the subcritical regime to the supercritical regime we choose an appropriate parameter θ for $E_n^{II}(\theta)$, $E_n^{III}(\theta)$ and $E_n^{IV}(\theta)$. By changing α we can move each energy level of the subcritical region into one of the critical region by a continuous path. Notice that for each $\theta \neq$ and $\theta \neq$ there is a bound state in the subcritical regime that merge into the continuum at a particular value of $\alpha < j^2$ and in the supercritical regime a bound state emerges form the continuum for any $\theta \neq \pi$

For all other levels we the following relation:

$$\lim_{\alpha\to|j|_-} E_n^{II}(\theta) = E_n^{III}(0) = \lim_{\alpha\to|j|_+} E_n^{IV}(\theta'); \tag{2.54}$$

whenever $\theta \neq \frac{\pi}{4}$ and $\theta' \neq \frac{\pi}{2}$. This means that, fixed any values of $\theta \neq \frac{\pi}{4}$ and $\theta' \neq \frac{\pi}{2}$, $E_n^{II}(\theta)$ and $E_n^{IV}(\theta')$, converge to $E_n^{III}(0)$ as $\alpha \to \alpha = |j|$, pointing out the continuity of the flow of energy levels in the transition from the subcritical regime to the critical one (See figure 2.4). In the exceptional

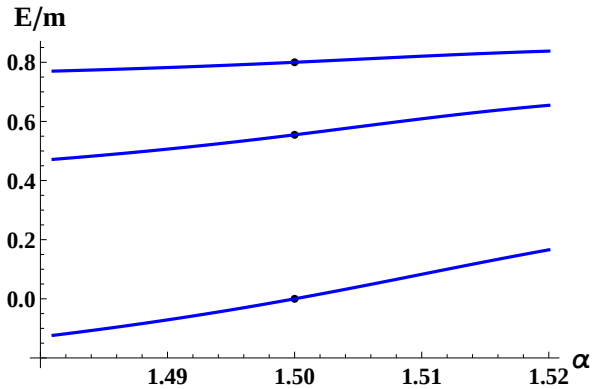

Figure 2.4: Energy level flow in charge impurity α for boundary conditions $\theta = \frac{3\pi}{4}$, and $\theta' = 0$, for $j = 3/2$ ($\Lambda = m/10$).

cases we also have continuity in the path crossing the transition border

$$\lim_{\alpha\to|j|_-} E_n^{II}(\tfrac{\pi}{4}) = E_n^{III}(\tfrac{\pi}{2}) = \lim_{\alpha\to|j|_+} E_n^{IV}(\tfrac{\pi}{2}), \tag{2.55}$$

provided we choose the suitable values for the parameter of the boundary condition in the different regimes.

In Figure (2.5) the α flow of energy levels of H is displayed for E_n^{II} and E_n^{IV} for different values of $\theta \in [0, 1)$ for $j = \frac{3}{2}$. The top and the bottom curves correspond to two consecutive levels $E_n^{II}(\frac{\pi}{4})$, $E_n^{IV}(\frac{\pi}{2})$ and $E_{n+1}^{II}(\frac{\pi}{4})$, $E_{n+1}^{IV}(\frac{\pi}{2})$. Notice that the flow is unstable around these *isolated*

lines. The energy levels converge at $\alpha^2 = j^2$ to energy levels of $E_n^{III}(\frac{\pi}{2})$ (red dots). The flows of all the other energy levels reach one of the energy levels of $E_n^{III}(0)$, which correspond to the Hydrogenoid and meta-Hydrogenoid atomic spectrum (black dots). This situation is similar for every energy level of $E_n^{III}(0)$. All bound state energy levels, except the *isolated* ones are attracted by the levels Hydrogenoid levels of $E_n^{III}(0)$. In figures (2.6)

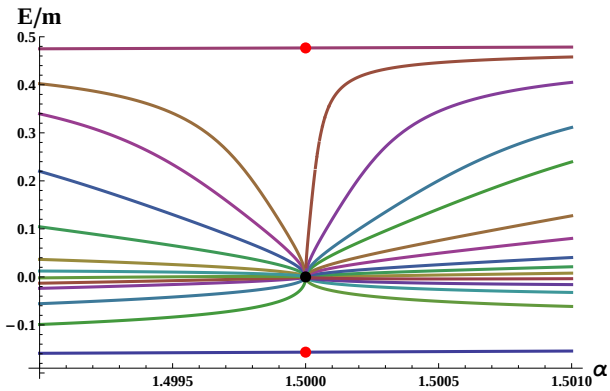

Figure 2.5: Flow of energy levels with angular momentum $j = 3/2$ ($\Lambda = m/10$) when the impurity charge crosses from subcritical regime to supercritical regime.

and (2.7) we show the instability of the *isolated* flow lines. The central flux lines correspond, respectively to $\theta = \frac{\pi}{4}$ and $\theta = \frac{\pi}{2}$, while the others correspond to small perturbations of these lines, respectively $\theta = \frac{\pi}{4} \pm 0.001$ and $\theta = \frac{\pi}{2} \pm 0.005$. We can see how, approaching to $\alpha^2 = j^2$, the perturbed curves follow the *isolated* lines flow but eventually they are attracted by two different eigenvalues of $E_n^{III}(0)$.

In summary, the above analysis in terms of boundary conditions shows that in graphene we have infinite set of self adjoint Dirac operator for any $\alpha > 0$ (for $j = \frac{1}{2}$) which are parameterized by an angle $\theta \in [0, \pi)$. Unitarity is guaranteed for any value of the charge impurity α. Even more, there is an extra parameter θ with observable consequences generated by

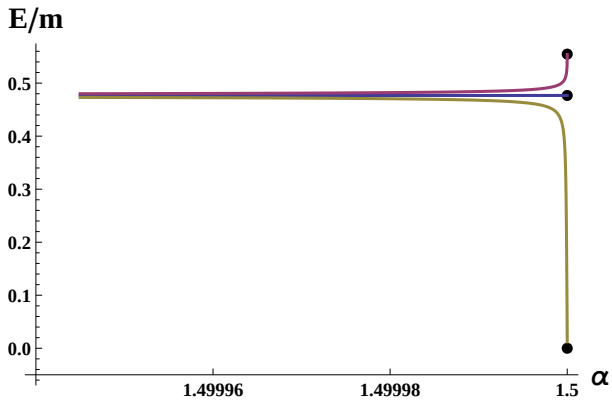

Figure 2.6: Instability properties of the flow of $E_n^{II}(\theta)$ for $\theta = \frac{\pi}{4}$ and $\theta_\pm = \frac{\pi}{4} \pm 0.001$ (up/down) and $j = 3/2$ ($\Lambda = m/10$).

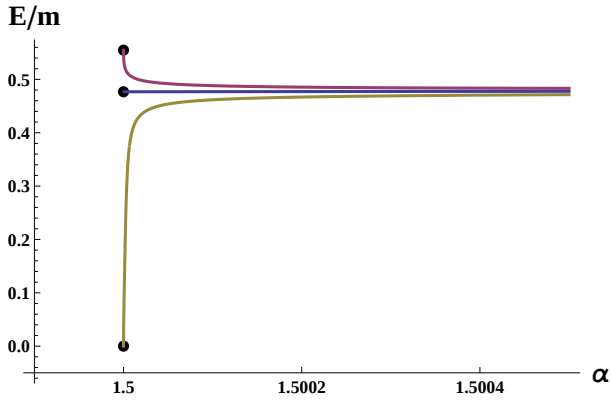

Figure 2.7: Instability properties of the flow of $E_n^{IV}(\theta)$ for $\theta = \frac{\pi}{2}$ and $\theta_\pm = \frac{\pi}{2} \pm 0.005$ (up/down) and $j = 3/2$ ($\Lambda = m/10$).

the renormalization of the singular UV of the impurity. The dependence on the choice of boundary conditions at the singularity defines a RG flow of energy levels. The analysis of the boundary flow points out interest-

ing physical properties. Changes of the θ parameter which characterizes the self adjoint extension we can bring each Hydrogenoid level in the next one after a recursive loop in the parameter space. All energy levels in the Hydrogenoid spectrum, except the fundamental one, are degenerate, but the introduction of the parameter θ breaks breaks down this degeneracy. Moreover, it is possible to move, varying α, the energy levels from the subcritical to the supercritical region in a continue way; This is a consequence of the interesting properties of the RG flow for the subcritical and supercritical region. Near the critical charge the energy levels are attracted by the points of the spectra of the Hamiltonian at the critical charge $\alpha^2 = j^2$ and the particular value of the boundary conditions $\theta = 0$. The attracting Hamiltonian corresponds to the Hydrogenoid atom spectrum at the critical charge. Only few levels remain isolated in a unstable way. This point out in particular that the critical charge $\alpha^2 = j^2$ of the Hydrogenoid case is not singular, the theory is well defined below and above this critical charge in the subcritical and supercritical regimes. The transition from the subcritical to the supercritical regime does not imply a change in the physical description of the system.

However, the apparent stability of the vacuum pointed out by the careful analysis of the boundary conditions of the Hamiltonian does not hide that the physical behaviour of graphene is quite special in the supercritical phase. The fact that Hydrogenoid energy levels become complex in the supercritical regime implies that the presence of resonances in the spectral density of the scattering matrix in the positron (hole) channel. These resonances are also the root of bound states levels which emerge from the continuum negative spectrum $E < -m$ (see Fig. (2.3)). In the supercritical regime there is an infinite number of quasi-bound states embedded in the lower continuum $E < -m$ which are visible in the spectral density. If they are not filled as we cross the supercritical value some normal electrons will jump into these empty levels generating particle/hole pairs. The positive charge will move to infinite and disappears whereas the negative sticks localized near the impurity giving rise to a screening of the impurity charge. We have assumed a positively charged impurity but due to the CP invariance of the theory a similar phenomenon occurs for negative charged

impurities.

In QED we expect the same phenomenon to occur. In a superheavy nucleus with high enough Z, the hydrogenoid bound levels can merge with the positron continuum. When that happens, the bound energy level becomes degenerate with the positron states and by the Schwinger mechanism an electron-positron pair can be created since there is no energy cost involved in creating an electron-positron pair. The electron occupies the bound level close to the nucleus, while the positron escapes to infinity. Since the positron continuum constitutes the vacuum of QED, the spontaneous creation of an electron in a level below $E = -m$ leads to a restructuration of the vacuum and an effective screening of Coulomb charge.

The main difference of the same phenomenon in graphene and QED is that the value of the critical charge in graphene is $\alpha = j$ whereas in QED is $Z = 137$ which is very hard to realize in Nature. The screening phenomenon due to supercritical pair creation has been recently observed in graphene and in QED a similar phenomenon has been observed in the lead-lead collisions. There is another remarkable difference with the QED case. Graphene for any value of $\alpha > 0$ is a subcritical regime which requires an extra parameter to fix the boundary condition at the origin. However, in QED for $Z < 118$, e.g. for the Hydrogen atom the Hamiltonian is essentially selfadjoint. Thus there is no need to fix the boundary condition at the origin. In particular a δ like perturbation has no effect in the spectrum. This means that the relativistic interpretation of the Lamb effect requires a full field theoretical analysis, unlike in the non-relativistic approach.

Thus, although the basics of the Gribov hypothesis is confirmed the emergence of quark confinement in QCD requires a stronger mechanism going beyond the simple (anti)screening of the color charge of the quarks.

3

Coulomb Instabilities in heavy quark backgrounds

In the previous chapter we analyzed the problem of supercritical charges in Coulomb backgrounds. In spite of the unitary time evolution governed by Dirac Hamiltonian we found some traces of instability when particle creation is permitted. This was just the hint that motivated Gribov to raise his conjecture about quark confinement. In this chapter we address the derivation of Gribov's confinement scenario from first principles, i.e. from Euclidean functional integral defined by the QCD Lagrangian. In particular we consider a heavy static quark background. The Coulomb potential is a saddle point configuration of the partition function and we analyze its stability properties under gauge field fluctuations.

3.1. Euclidean functional integral in one quark background

The basic dynamical fields of QCD are a $SU(3)$ gauge field and three dynamical quarks in the fundamental representation of $SU(3)$ fluctuating a Minkowski space-time with metric $g_{\mu\nu} = \text{diag}(+---)$. The $SU(N)$ Yang Mills action is given by

$$S^{YM} = \frac{1}{2g_s^2} \int d^4x \, Tr(F_{\mu\nu} F^{\mu\nu}), \tag{3.1}$$

where

$$F_{\mu\nu} = \partial_\mu A_\nu - \partial_\nu A_\mu + [A_\mu, A_\nu], \tag{3.2}$$

g_s is the coupling constant and $A_\mu(x)$ the gauge field with values on a traceless anti-hermitian $N \times N$ matrix. The theory is invariant under gauge transformations $U(x)$

$$A'_\mu(x) = U(x) A_\mu U^{-1}(x) - (\partial_\mu U(x)) U^{-1}(x), \tag{3.3}$$

with values on $SU(N)$. The transformation rule of the field streght $F_{\mu\nu}$ is covariant

$$F'_{\mu\nu} = U(x) F_{\mu\nu} U^\dagger(x),$$

which guarantees the gauge invariance of (3.1). It is convenient to use a basis of $N-1$ generators T^a of the Lie algebra $su(N)$ of $SU(N)$, i.e a basis of anti-hermitian, traceless matrices that satisfy the commutation relations

$$[T^a, T^b] = f^{abc} T^c, \tag{3.4}$$

with f^{abc} antisymmetric, and the normalization condition

$$Tr[T^a T^b] = -\frac{1}{2} \delta^{ab}. \tag{3.5}$$

In terms of these generators any gauge transformation $U(x)$ can be given as as

$$U = \exp[w^a T^a],$$

where $w^a(x)$ a family of real fields. In this basis the gauge fields

$$A_\mu(x) = A^a_\mu(x) T^a,$$

can be expanded in a series of real field components $A^a_\mu(x)$. The same expansion is valid for $F_{\mu\nu}$, so the action (3.1) becomes

$$S^{YM} = -\frac{1}{4g_s^2} \int d^4x \, F^a_{\mu\nu} F^{\mu\nu}_a. \tag{3.6}$$

The covariant derivative is defined as:

$$D_\mu = \partial_\mu + A_\mu, \tag{3.7}$$

and it transforms also in a covariant way

$$D'_\mu = U(x) D_\mu U^\dagger(x).$$

The coupling of the Yang-Mills lagrangian to any external current $J_\mu = J^a_\mu(x) T^a$ is given by a term of the form

$$S^I = -2 \int d^4x \, Tr \, (A^\mu J_\mu), \tag{3.8}$$

The dynamical quarks can be introduced in a similar way in terms of Dirac fermions in the fundamental $SU(N)$ representation:

$$S^F = \int dx^4 \, \overline{\Psi} \left(i \not{D} - m \right) \Psi, \tag{3.9}$$

where $\not{D} = D_\mu \gamma^\mu$, $D_\mu = \partial_\mu + A_\mu$ and γ^μ are the four dimensional Dirac gamma matrices, that satisfy

$$\{\gamma^\mu, \gamma^\nu\} = 2g^{\mu\nu}, \qquad (\gamma^0)^\dagger = \gamma^0, \qquad (\gamma^i)^\dagger = -\gamma^i,$$

and can be chosen in the Dirac representation:

$$\gamma^0 = \begin{pmatrix} I & 0 \\ 0 & -I \end{pmatrix}, \qquad \gamma^i = \begin{pmatrix} o & \sigma^i \\ -\sigma^i & 0 \end{pmatrix}.$$

In summary , the total action of the theory is:

$$S = S^{YM} + S^F + S^I.$$

Let us for simplicity consider the $SU(2)$ gauge group, although the results are easily generalized for any gauge group $SU(N)$. The generators of the Lie algebra can written as

$$T^a = \frac{1}{2i}\sigma^a, \quad a = 1, 2, 3,$$

in terms of the Pauli σ^a matrices. In this case the structure constant $f^{abc} = \epsilon^{abc}$, reduce to the completely anti-symmetric Levi-Civita symbol. It is useful to choose a Cartan basis for the $su(2)$ Lie algebra

$$T^{\pm} = \frac{1}{\sqrt{2}}(T^1 \pm iT^2), \quad T^3. \tag{3.10}$$

The gauge fields can be then expressed in terms of the $su(2)$ Cartan components

$$A_\mu = A_\mu^+ T^+ + A_\mu^- T^- + A_\mu^3 T^3, \tag{3.11}$$

and a similar expression exists for the field stregth $F_{\mu\nu}$. The fields components A_μ^a (with a=1,2,3) of the gauge field are real, i.e.

$$(A_\mu^+)^* = A_\mu^-, \qquad (A_\mu^-)^* = A_\mu^+, \qquad (A_\mu^3)^* = A_\mu^3 \tag{3.12}$$

The external source corresponding to heavy static quark sitting at the origin, is given by a fixed color Dirac delta distribution

$$J^0 = \delta^3(\vec{x})\, T^3, \qquad J^i = 0, \;\; i = 1, 2, 3. \tag{3.13}$$

To have a connection with the Wilson loop approach, the current (3.13) is substituted into (3.8):

$$S^I = \int dx^0\, A_0^3, \tag{3.14}$$

which can be considered as the abelian projection of a Wilson line extending in the time direction, describing the interaction with one static heavy quark.

The quantum theory is encoded in the partition function,

$$Z = \int DA\, D\overline{\Psi}\, D\Psi\, \exp\left[i\left(S^{YM}(A) + S^{F}(\overline{\Psi},\Psi) + S^{I}(A)\right)\right], \qquad (3.15)$$

In Minkowski space-time the integrand is oscillating: in order to have a well defined functional integral we have to perform a Wick rotation from real time to Euclidean time. The procedure consist in replacing the time coordinate and the time component of the gauge potentials in the following way

$$t \to x^4 = it, \qquad A^0 \to A^4 = -iA^0,$$
$$J^0 \to J^4 = -iJ^0, \qquad \gamma^0 \to \gamma^4 = -i\gamma^0.$$

For simplicity x^4, A^4, J^4 and γ^4 will be denoted as x^0, A^0, J^0 and γ^0, respectively, and we will use Greek letters to denote covariant euclidean indices. Consequently the Euclidean functional integral of QCD in a heavy quark background is

$$\begin{aligned} Z &= \int DA\, D\overline{\Psi}\, D\Psi\, \exp[-S_E(A)] \\ &= \int DA\, D\overline{\Psi}\, D\Psi\, \exp[-(S_E^{YM}(A) + S_E^{F}(\overline{\Psi},\Psi) + S_E^{I}(A))], \end{aligned} \qquad (3.16)$$

where

$$S_E^{YM}(A) = -\frac{1}{2g_s^2}\int d^4x\, Tr(F^{\mu\nu}F_{\mu\nu}) = \frac{1}{4g_s^2}\int d^4x\, F^{\mu\nu}F_{\mu\nu}, \qquad (3.17)$$

$$S_E^{F}(\overline{\Psi},\Psi) = \int d^4x\, \overline{\Psi}\left(i\not{D} + m\right)\Psi \qquad (3.18)$$

with $\not{D} = \gamma_\mu(\partial_\mu + iA_\mu)$, and

$$S_E^{I}(A) = -\int d^4x\, Tr(A_\mu J^\mu). \qquad (3.19)$$

The metric is now the identity $\delta^{\mu\nu}$, while the euclidean gamma matrices satisfy:

$$\{\gamma^\mu,\gamma^\nu\} = -2\delta^{\mu\nu}, \qquad (\gamma^\mu)^\dagger = -\gamma^\mu.$$

The external current has to be Wick rotated as well, and becomes

$$J^0 = -i\,\delta^3(\vec{x})\,T^3, \qquad J^i = 0, \;\; i = 1,2,3.$$

The functional integral (3.16) is now converging and real because of the symmetry is $A(x) \to -A(-x)$). Performing the functional integration over quark fluctuations it becomes

$$Z = \int DA\, \exp[-S_E^{YM}(A) - S_E^I(A)] \det\left(i\not{D} + m\right).$$

3.1.1. Coulomb saddle point

To evaluate our functional integral we shall use the saddle point method. First we have to find the stationary configurations, i.e. we have to find solutions of the Euclidean Yang-Mills equations. They are obtained from the vanishing condition of the first variation of the action. First, the variation of the Yang-Mills terms is

$$\delta S_E^{YM} = -\frac{1}{g_s^2}\int d^4x\, Tr(F_{\mu\nu}\delta F^{\mu\nu}),$$

with

$$\delta F^{\mu\nu} = \partial^\mu \delta A^\nu + \delta A^\mu A^{nu} + A^\mu \delta A^{nu} - (\mu \leftrightarrow \nu).$$

Let us forget for a while the dynamical quarks contributions, Using the antisymmetry of $F^{\mu\nu}$, integration by parts and the cyclic properties of the trace the action variation can be rewritten as

$$\delta S_E^{YM} = \frac{2}{g_s^2}\int d^4x\, Tr[(\partial^\mu F_{\mu\nu} + [A^\mu, F_{\mu\nu}])\delta A^\nu] = \frac{2}{g_s^2}\int d^4x\, Tr[(D^\mu F_{\mu\nu})\delta A^\nu], \tag{3.20}$$

where the last equality follows by the fact that $F_{\mu\nu}$ transforms according the adjoint representation. The variation of S_E^I is simply

$$\delta S_E^I = -2\int d^4x\, Tr\,(J_\mu \delta A^\mu). \tag{3.21}$$

Combining (3.20) and (3.21) we get the Euclidean equation of motion

$$D^{\mu}F_{\mu\nu} = g_s^2 J_{\nu}. \tag{3.22}$$

which after inserting the explicit form of the external current reduces to

$$\begin{aligned} \nu = 0 \qquad & \partial^i F^+_{i0}T^+ + \partial^i F^-_{i0}T^- + \partial^i F^3_{i0}T^3 + [A^i, F_{i0}] = -i\, g_s^2 \delta^{(3)}(x) T^3 \\ \nu = j \qquad & \partial^0 F_{0j} + \partial^i F_{ij} + [A^0, F_{0j}] + [A^i, F_{ij}] = 0, \quad i \neq j. \end{aligned} \tag{3.23}$$

To analyze the stability of the quantum vacuum in heavy quark backgrounds let us consider only static configurations. A solution of the Euclidean Yang Mills equations with only temporal component $A^3_{\mu} = (A^3_0, 0, 0)$ of the gauge fields

$$\partial^i \partial_i (A^0)^3 = -i\, g_s^2 \delta^{(3)}(x),$$

is the following (imaginary) Coulomb potential

$$A^0(\mathbf{x}) = i\Phi T^3, \quad \vec{A} = 0, \quad \text{with } \Phi = \frac{\alpha}{|\mathbf{x}|}, \quad \alpha = \frac{g_s^2}{4\pi}. \tag{3.24}$$

Notice that this saddle point solution is also a saddle point in the presence of dynamical quarks when we consider when $\Psi = 0$.

3.2. Gluonic instabilities of the Coulomb phase

According to the saddle point method, the next leading order corrections to the Coulomb background are given by the quadratic fluctuations. The one loop corrections to the partition function are

$$\begin{aligned} Z^{(1)} &= \exp[-S_c] \det\left(i\not{D}_c + m\right) \int D\tau \exp[-\tau\, \delta^{(2)} S^{YM}_{E,c}\, \tau] \\ &= \exp[-S_c] \det{}^{-\frac{1}{2}} \left(\delta^{(2)} S^{YM}_{E,c}\right) \det\left(i\not{D}_c + m\right), \end{aligned}$$

where S_c, $\delta^{(2)} S^{YM}_{E,c}$ and $\left(i\not{D}_c + m\right)$ are respectively the action, the second order variation of the Yang Mills action and the Dirac operator calculated at the saddle point, the imaginary Coulomb potential .

There are two possible sources of instability of the Coulomb phase. The first one is due to real gluonic fluctuations that give rise to negative second order variations of the Yang Mills action. In this case, according to the steepest descent method, the contour of integration in the space of complex gauge field configurations has to be restricted to pure imaginary flutuations of the Coulomb saddle point when their real partner modes give rise to negative quadratic terms in order to get positive second order variations. But in that case the partition function might become a complex expression. Due to the phase $e^{i\frac{\pi}{2}} = i$ in (**??**) of the change of variable, it picks up a facto i for each negative mode. Physical consistency requires that the partition function, thus , in this case the effect simply means that the Coulomb saddle point becomes an irrelevant contribution the the Euclidean functional integral. The second possible source of instability can arise from the contribution of the fermionic determinant $\left(i\not{D}_c + m\right)$ when there exist fermionic fluctuations which are zero modes of the $i\not{D}_c + m$ operator. In that case the fermionic determinant vanishes which means an infinite contribution to the vacuum energy of the system. In absence of these instabilities, the Coulomb potential will dominate the partition function. The instabilities does not means that the path integral is not well defined. The pathologies only means that the Coulomb saddle point is gives an irrelevant contribution , opening the window to other possible configurations that generate a confining behavior.

To search possible instabilities due to gluonic fluctuations, let us analyze the structure of the quadratic term of quantum fluctuations of Yang Mills action. The variations in the fields around a background configuration are

$$A'_\mu = A_\mu + \tau_\mu,$$

where τ_μ verifies the conditions

$$(\tau_\mu^+)^* = \tau_\mu^-, \qquad (\tau_\mu^-)* = \tau_\mu^+, \qquad (\tau_\mu^3)* = \tau_\mu^3 \tag{3.25}$$

It is easy to show that

$$F_{\mu\nu} \mapsto F'_{\mu\nu} = F_{\mu\nu} + D_\mu\tau_\nu - D_\nu\tau_\mu + [\tau_\mu, \tau_\nu],$$

where $D_\mu\tau_\nu = \partial_\mu\tau_\nu + [A_\mu, \tau_\nu]$. Keeping only second order terms in the variation of the Lagrangian

$$\begin{aligned} Tr(F'_{\mu\nu}F'_{\mu\nu}) &= Tr(F_{\mu\nu}F_{\mu\nu}) + 2Tr(F_{\mu\nu}(D_\mu\tau_\nu - D_\nu\tau_\mu)) \\ &\quad +2Tr(F_{\mu\nu}[\tau_\mu,\tau_\nu]) + Tr((D_\mu\tau_\nu - D_\nu\tau_\mu)^2). \end{aligned}$$

we get for the action

$$\delta^{(2)}S_E = -\frac{1}{2}\int d^4x\, Tr\big((D_\mu\tau_\nu - D_\nu\tau_\mu)^2 + 2F_{\mu\nu}[\tau_\mu,\tau_\nu]\big).$$

By integrating by parts and using the cyclic property of the trace $Tr(F_{\mu\nu}[\tau_\mu,\tau_\nu]) = (\tau_\nu[F_{\mu\nu},\tau_\mu])$, it can be rewritten as

$$\delta^{(2)}S_E = -\int d^4x\, Tr\big(\tau_\mu(-\delta_{\mu\nu}D^2 + D_\mu D_\nu - 2ad_{F_{\mu\nu}})\tau_\nu\big), \qquad (3.26)$$

where $ad_{F_{\mu\nu}}$ mean $[F_{\mu\nu},\,\cdot\,]$.

Let us now considerthe imaginary Coulomb background (3.2):

$$\begin{aligned} D^2 &= \big((\partial_0 + [A_0,\cdot])(\partial_0 + [A_0,\cdot]) + (\partial_i + [A_i,\cdot])(\partial_i + [A_i,\cdot])\big) \\ &= \big(\partial_0^2 + [\partial_0 A_0,\cdot] + 2[A_0,\partial_0\cdot] + [A_0,[A_0,\cdot]] + \\ &\quad \partial_i^2 + [\partial_i A_i,\cdot] + 2[A_i,\partial_i\cdot] + [A_i,[A_i,\cdot]]\big) \\ &= \big(\partial_0^2 - \Phi^2 ad_{T^3}^2 + 2i\Phi\, ad_{T^3}\,\partial_0 + \triangle\,\big), \end{aligned}$$

where $\triangle = \sum_{i=1}^3 \partial^i\partial_i$,

$$\begin{aligned} D_\mu D_\nu &= (\partial_\mu + [A_\mu,\cdot])(\partial_\nu + [A_\nu,\cdot]) \\ &= \partial_\mu\partial_\nu + [\partial_\mu A_\nu,\cdot] + [A_\nu,\partial_\mu\cdot] + [\partial_\nu A_\mu,\cdot] + [A_\mu,[A_\nu,\cdot]] \\ &= \partial_\mu\partial_\nu + i(\delta_{\nu0}\partial_\mu\Phi + \delta_{\nu0}\Phi\,\partial_\mu + \delta_{\mu0}\Phi\,\partial_\nu)ad_{T^3} - \delta_{\mu0}\delta_{\nu0}\Phi^2 ad_{T^3}^2, \end{aligned}$$

$$F^a_{\mu\nu} = \delta^{a3}i(\delta_{\nu0}\partial_\mu\Phi - \delta_{\mu0}\partial_\nu\Phi)$$

and

$$\Rightarrow \quad ad_{F_{\mu\nu}} = i(\delta_{\nu0}\partial_\mu\Phi - \delta_{\mu0}\partial_\nu\Phi)ad_{T^3}.$$

Finally, we obtain

$$\begin{aligned}\delta^{(2)}S_E &= -\int dx^4\, Tr\big[\tau_\mu[-\delta_{\mu\nu}(\partial_0^2+\triangle)+\partial_\mu\partial_\nu+\delta_{\mu j}\delta_{\nu j}\Phi^2\, ad_{T^3}^2 \\ &\quad +i(-2\delta_{\mu\nu}\Phi\,\partial_0+2\delta_{\nu 0}\,\partial_\mu\Phi+\Phi\,\delta_{\nu 0}\,\partial_\mu+\Phi\,\delta_{\mu 0}\,\partial_\nu-\delta_{\mu 0}\,\partial_\nu\Phi)ad_{T^3}]\tau_\nu\big]\end{aligned} \tag{3.27}$$

The existence of possible negative quadratic contributions generating instabilities of the Coulomb potential background, is reduced to the existence of negative eigenvalues of the second order variations operator

$$\begin{aligned}&[-\delta_{\mu\nu}(\partial_0^2+\triangle)+\partial_\mu\partial_\nu+\delta_{\mu j}\delta_{\nu j}\Phi^2\, ad_{T^3}^2 \\ &+i(-2\delta_{\mu\nu}\Phi\,\partial_0+2\delta_{\nu 0}\,\partial_\mu\Phi+\Phi\,\delta_{\nu 0}\,\partial_\mu+\Phi\,\delta_{\mu 0}\,\partial_\nu-\delta_{\mu 0}\,\partial_\nu\Phi)ad_{T^3}]\end{aligned} \tag{3.28}$$

In presence of negative eigenvalues the saddle point method contribution in the Gaussian approximation might lead to a complex contribution to the partition function.

Using the expansion in Cartan components (3.11) for the variations and remembering the relations (**??**), the eigenvalue equations of $\tau^\pm$ read

$$\begin{aligned}&\big(\partial_\mu\partial_\nu-\delta_{\mu\nu}(\partial_0^2+\triangle)\big)\tau_\nu^\pm-\delta_{\mu j}\delta_{\nu j}\Phi^2\tau_\nu^\pm \\ &\pm(-2\delta_{\mu\nu}\Phi\,\partial_0+2\delta_{\nu 0}\,\partial_\mu\Phi+\Phi\,\delta_{\nu 0}\,\partial_\mu+\Phi\,\delta_{\mu 0}\,\partial_\nu-\delta_{\mu 0}\,\partial_\nu\Phi)\tau_\nu^\pm=-\lambda^2\tau_\mu^\pm.\end{aligned} \tag{3.29}$$

Now using the facts

$$\partial_0\Phi=0,\quad \text{and}\quad \boldsymbol{\nabla}\Phi=-\frac{\alpha}{r^3}\mathbf{r},$$

and restricting ourselves to static fluctuations ($\partial_0\tau_\mu=0$), we get

$$\begin{aligned}-\triangle\,\tau_0^\pm\pm\tfrac{\alpha}{r}[\boldsymbol{\nabla}\cdot\boldsymbol{\tau}^\pm+\tfrac{1}{r^2}\boldsymbol{\tau}^\pm\cdot\mathbf{r}]&=-\lambda^2\tau_0^\pm, \\ \boldsymbol{\nabla}(\boldsymbol{\nabla}\cdot\boldsymbol{\tau}^\pm)-\triangle\,\boldsymbol{\tau}^\pm-\tfrac{\alpha}{r^2}\boldsymbol{\tau}^\pm\pm\tfrac{\alpha}{r}[-\tfrac{2}{r^2}\tau_0^\pm\,\mathbf{r}+\boldsymbol{\nabla}\tau_0^\pm]&=-\lambda^2\boldsymbol{\tau}^\pm.\end{aligned} \tag{3.30}$$

3.2.1. Critical coupling constant

Considering only pure magnetic perturbations [1]

$$\boldsymbol{\tau}^{\pm} = \frac{\mathbf{x}\times\hat{\mathbf{n}}}{|\mathbf{x}|^2}\,\phi^{\pm}(|\mathbf{x}|), \quad \tau_0^{\pm} = 0, \tag{3.31}$$

where $\hat{\mathbf{n}}$ is a unit vector, instabilities are defined the following eigenvalues equation, in spherical coordinates:

$$\Big[-\frac{d^2}{d\,r^2} + \frac{2-\alpha^2}{r^2}\Big]\phi^{\pm}(r) = -\lambda^2\phi^{\pm}(r), \tag{3.32}$$

where $r = |\mathbf{x}|$. $\phi^{\pm}$ satisfy the same equation. In order to restrict the fluctuation to real gauge fields we have to impose the condition $(\phi^{+})^{*} = \phi^{-}$ (3.12). The index $\pm$ will omitted from now on to simplify the notation.

The singularity introduced by the Coulomb potential has a very special behavior. The corresponding operator within the bracket in eq. is symmetric acting on functions vanishing at the origin but it is not self-adjoint. In order to have real eigenvalues, it must be a self adjoint operator. This situation is well known and it has been reviewed in Appendix A, where we introduce an novel way of renormalizing the singularity. The results are the following. In general, the self adjoint extensions are defined in terms of boundary conditions at the singularity. There are four regimes, depending on the value of the coupling constant.

i) For $\alpha^2 \leq \frac{5}{4}$ the operator is essentially self-adjoint and has a unique self-adjoint extension with boundary Dirichlet conditions at the singularity. In this case the spectrum is continuum and positive. The absence of negative eigenvalues means that in this region of the coupling constant the Coulomb potential is stable.

For $\alpha > \frac{5}{4}$ there is a one parameter family of boundary conditions which give rise selfadjoint extensions. This parameter $\Lambda \in [0,\infty)$ has dimension

[1] In Appendix B we consider the general solution

of mass $[L]^{-1}$.

ii) For $\frac{5}{4} < \alpha^2 < \frac{9}{4}$ there is a one parameter family of selfadjoint extensions given by the boundary conditions

$$\lim_{r\to 0}\left(2r\phi'(r) - (1 + 2\nu\coth[\nu\log(\Lambda r)])\phi(r)\right) = 0,$$

where $\nu = \sqrt{\frac{9}{4} - \alpha^2}$. Apart from the positive continuum spectrum, in this case there is also one negative eigenvalue

$$-\lambda^2 = -4\Lambda^2\left(\frac{\Gamma[1+\nu]}{\Gamma[1-\nu]}\right)^{\frac{1}{\nu}},$$

corresponding to the eigenstate

$$\phi(r) = r^{\frac{1}{2}}K_\nu(\lambda r).$$

iii) For $\alpha^2 = \frac{9}{4}$ the self adjoint boundary boundary conditions are

$$\lim_{r\to 0}\left(2r(\log(\Lambda r) - 1)\phi'(r) - (\log(\Lambda r) + 1)\phi(r)\right) = 0,$$

Also in this case there is one negative eigenvalue

$$-\lambda^2 = -4\Lambda^2 e^{-2-2\gamma},$$

corresponding to the eigenstate

$$\phi(r) = r^{\frac{1}{2}}K_0(\lambda r).$$

For $\frac{5}{4} < \alpha^2 \leq \frac{9}{4}$ the arbitrary parameter Λ, introduced by the boundary conditions in order to guarantee the Hermiticity of the second-order variations operator, breaks conformal invariance which is crucial for having negative eigenvalues. This region characterizes a regime of weakly instability for the Coulomb background potential.

For $\frac{5}{4} < \alpha^2 < 2$ the unstable mode diverges at the singularity, for $\alpha^2 = 2$ it approaches to a constant, while $2 < \alpha^2 \leq \frac{9}{4}$ it goes to zero.

iv) Finally for $\alpha^2 > \frac{9}{4}$ the family of self adjoint extension with boundary boundary conditions

$$\lim_{r\to 0}\left(2r\phi'(r) - (1+2|\nu|\cot[|\nu|\log(\Lambda r)])\phi(r)\right) = 0.$$

give rise to operators with an infinity negative eigenvalues.

$$-\lambda_n^2 = -4\Lambda^2 \exp\left(\frac{2i\pi n}{\nu} + \frac{1}{\nu}\log\frac{\Gamma[1+\nu]}{\Gamma[1-\nu]}\right),$$

corresponding to the eigenstates

$$\phi_n(r) = r^{\frac{1}{2}} K_\nu(\lambda_n r).$$

with $n = 0, \pm 1, \pm 2 \ldots$. Thus, in this case we have a strong instability of the Coulomb potential for the heavy quark background and again the parameter Λ introduced by the boundary condition breaks conformal invariance, but not completely since a discrete conformal symmetry is preserved. The boundary conditions and the spectrum are invariant under the discrete rescaling $\Lambda \to \Lambda\, e^{\frac{2\pi i}{\nu}}$. The unstable modes in this region oscillate approaching the singularity. In figure 3.1 the unstable modes of the different regimes of the coupling constant are displayed.

The picture emerging from this analysis is that for small α the Coulomb potential is the leading contribution to the partition function. In that regime the Coulomb background is a good approximation for the system, but when we reach a critical value of the coupling constant $\alpha = \sqrt{\frac{5}{4}}$, six degenerate unstable modes appear: one for each axis and each color different of the quark color. The partition function calculated by the steepest descent method acquires a factor $i^6 = -1$. As consequence the free energy, being the logarithm of the partition function, becomes complex: this can be seen as the smoking gun of the instability of the Coulomb phase. In other words the for large values of the coupling constant, the Coulomb solution is no more a relevant configuration for the system, opening the window to confinement.

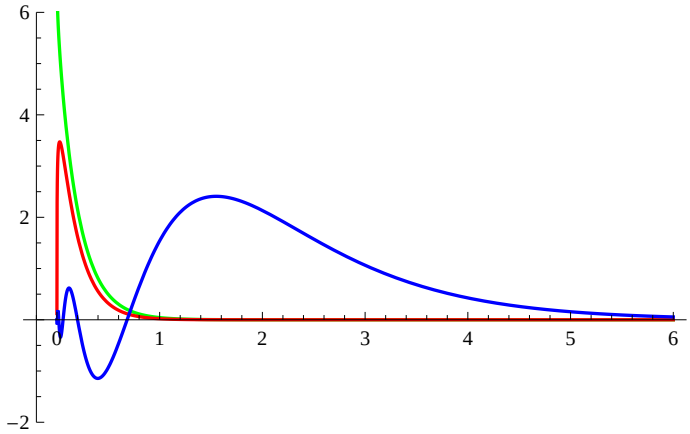

Figure 3.1: Unstable modes for $\alpha = 1.4$ (green), $\alpha = 1.49$ (red) and $\alpha = 3$ (blue) for $\Lambda = 5$

The instability of the Coulomb phase is intrinsically associated to the breaking of conformal symmetry. In perturbation theory this emerges from the renormalization of the coupling constant α. In this picture it arises from the need of fixing the boundary conditions of the singularity of quark potentials. The novelty is that in this case it implies the instability of the Coulomb vacuum background for large enough coupling constant. A similar critical coupling, precisely $\alpha = \frac{3}{2}$, was founded from previous analysis of the stability of the Coulomb solution in classical Yang Mills field theory in presence of external source. That critical coupling coincides with our value marking the transition from the weakly to the strong instability regime of the Coulomb potential.

However, the connection of the picture with real confinement is not yet clear because one quark background alone does not match the neutrality of color. For this reason in the next chapters will be analyzed what happen in presence of a quark-antiquark pair.

4

Two quarks in one dimension

Until now we have analyzed the instability of the Coulomb potential generated by a single point charge. However, a single quark background does not correspond to a consistent physical system since it does not match the color neutrality condition. For this reason it is convenient to introduce an antiquark, in order to get a neutral system with the same quantum numbers than a meson. An important novelty of the introduction of an antiquark will be the presence of a new parameter in the theory, the distance between the $q - \bar{q}$ pair.

Before dealing with this problem in three dimensions, we will analuze a simpler system: a pair $q - \bar{q}$ in one space dimension, expecting to shed light and understand how the distance between the quarks can affect the stability of the system. The relevance of the analysis of this simplified model stands in the fact that it can be solved analytically and many of its properties can hold in the generalization to three dimensions.

In order to analyze the situation with neutral quark-antiquark pair, we consider the equation (3.2.1) in the presence of two external sources

of opposite charge located at $x = L$ and $x = -L$. What we are going to study is then the bound states of the following one dimensional Schrödinger equation

$$\left[-\frac{d^2}{d\,x^2} - \alpha^2\left(\frac{1}{|x-L|} - \frac{1}{|x+L|}\right)^2\right]\phi(x) = -\lambda^2\phi(x). \tag{4.1}$$

The aim is to analyze the dependence of the bound states spectrum on the separation $2L$ between the $q-\bar{q}$ pair.

Due to the singularities of the quarks sitting at $x = \pm L$, we have to fix proper boundary conditions at $x = \pm L$ to have a well defined self adjoint operator. They can be given in terms of asymptotic zero modes near the singularities. The equations of these zero modes near $x = \pm L$, are

$$\left[-\frac{d^2}{d\,x^2} - \alpha^2\left(\frac{1}{|x-L|^2} - \frac{1}{L\,|x+L|}\right)^2\right]\phi_0(x) = 0.$$

The solutions are

$$\phi^{\pm}_{0>}(x) = \sqrt{|x-L|}I_{\pm 2\nu}\Big(\frac{2\alpha}{\sqrt{L}}\sqrt{|x-L|}\Big),$$

for $x = L$ and

$$\phi^{\pm}_{0<}(x) = \sqrt{|x+L|}I_{\pm 2\nu}\Big(\frac{2\alpha}{\sqrt{L}}\sqrt{|x+L|}\Big),$$

for $x = -L$, where $\nu = \sqrt{\frac{1}{4} - \alpha^2}$. We recall the expansion of the Bessel I function near $x \pm L$:

$$I_{\pm 2\nu}\Big(\frac{2\alpha}{\sqrt{L}}\sqrt{|x \mp L|}\Big) \simeq \Big(\frac{\alpha^2}{L}|x \mp L|\Big)^{\pm\nu}\Big(\frac{1}{\Gamma[1 \pm 2\nu]} + \frac{\alpha^2 x}{L\,\Gamma[2 \pm 2\nu]} + \dots\Big). \tag{4.2}$$

In the vicinity of each singularity, both $\pm\nu$ solutions are normalizable at the origin for $\alpha > 0$. Since the term $x^{\frac{3}{2}-\nu}$ and its derivative go to zero as

$x \to 0$ for $\alpha \geq 0$, only the first term is relevant. The most general boundary conditions which leads to a self adjoint Hamiltonian is given by (A.11):

$$\begin{aligned} \lim_{x\to L} \left(\phi'(x)\phi_{\Lambda>}(x) - \phi(x)\phi'_{\Lambda>}(x)\right) = 0, \\ \lim_{x\to -L} \left(\phi'(x)\phi_{\Lambda<}(x) - \phi(x)\phi'_{\Lambda<}(x)\right) = 0, \end{aligned} \tag{4.3}$$

where

$$\begin{aligned} \phi_{\Lambda>}(x) &= \sqrt{|x-L|}\left((\Lambda|x-L|)^{\nu} - (\Lambda|x-L|)^{-\nu}\right), \\ \phi_{\Lambda<}(x) &= \sqrt{|x+L|}\left((\Lambda|x+L|)^{\nu} - (\Lambda|x+L|)^{-\nu}\right) \end{aligned} \tag{4.4}$$

for $0 < \alpha^2 \neq \frac{1}{4}$, and

$$\begin{aligned} \phi_{\Lambda>}(x) &= \sqrt{|x-L|}\left(1 - \log\left(\Lambda|x-L|\right)\right), \\ \phi_{\Lambda<}(x) &= \sqrt{|x+L|}\left(1 - \log\left(\Lambda|x+L|\right)\right) \end{aligned} \tag{4.5}$$

for $\alpha^2 = \frac{1}{4}$. Notice that in principle it is possible to choose different parameters approaching to the left or to the right at each singularity. For symmetry reasons, it has been chosen the same for the four cases.

4.1. Critical size of $q-\bar{q}$ pairs

The singularities introduced by the $q-\bar{q}$ pair at the points $x = \pm L$ act like infinite barriers between the left and right domains. For this reason, the complete problem in $x \in (-\infty, +\infty)$ can be split into three different problems defined in the subdomains: $x < -L$, $-L < x < L$ and $x > L$. These three problems can be analyzed separately: the spectrum of the complete problem will be the union of the spectra of these three regions. First we analyze the region $x > L$. Due to parity symmetry, the results obtained in this region can be translated immediately to the region $x < -L$. It is convenient to introduce a change of variable, $x \to x + L$, such that the equation becomes:

$$\left[-\frac{d^2}{d\,x^2} - \alpha^2\left(\frac{1}{x} - \frac{1}{x+2L}\right)^2\right]\phi(x) = -\lambda^2\phi(x), \tag{4.6}$$

defined for $x > 0$. The boundary conditions (4.3) reduce to:

$$\lim_{x\to 0^+} \left(\phi'(x)\phi_\Lambda(x) - \phi(x)\phi'_\Lambda(x)\right) = 0, \tag{4.7}$$

where

$$\phi_\Lambda(x) = x^{\frac{1}{2}} \left((\Lambda x)^\nu - (\Lambda x)^{-\nu}\right). \tag{4.8}$$

for $\alpha^2 \neq \frac{1}{4}$, and

$$\phi_\Lambda(x) = x^{\frac{1}{2}} \left(1 - \log(\Lambda x)\right). \tag{4.9}$$

The situation gets very much simplified in the limit $L \to \infty$ where equation (4.6) reduces to the case of a single quark. This is natural, if we move one of the quarks to infinity there is only one quark left in the space. The spectral equation then becomes

$$\Big[-\frac{d^2}{d\,x^2} - \frac{\alpha^2}{x^2}\Big]\phi(x) = -\lambda^2\phi(x), \tag{4.10}$$

As it is expected this correspond to the situation already analyzed of one quark (3.2.1), with the only replacement of $\alpha^2 \to \alpha^2 + 2$. For $0 < \alpha < \frac{1}{2}$ and $\alpha = \frac{1}{2}$ there is one bound state with energy respectively

$$-\lambda^2 = -4\Lambda^2 \left(\frac{\Gamma[1+\nu]}{\Gamma[1-\nu]}\right)^{\frac{1}{\nu}}, \tag{4.11}$$

and

$$-\lambda^2 = -4\Lambda^2 e^{-2-2\gamma}, \tag{4.12}$$

while for $\alpha > \frac{1}{2}$ there are infinite bound states, characterized by the energies

$$-\lambda_n^2 = -4\Lambda^2 \exp\left(\frac{2i\pi n}{\nu} + \frac{1}{\nu}\log\frac{\Gamma[1+\nu]}{\Gamma[1-\nu]}\right). \tag{4.13}$$

with $\nu = \sqrt{\frac{1}{4} - \alpha^2}$.

Another limit where we can obtain analytic results is in the analysis of zero modes ($\lambda = 0$), i.e. solutions of (4.6) with $\lambda^2 = 0$,

$$\Big[-\frac{d^2}{d\,x^2} - \alpha^2\Big(\frac{1}{x} - \frac{1}{x+2L}\Big)^2\Big]\phi(x) = 0, \tag{4.14}$$

satisfying the boundary conditions (4.7). A solution of (4.14) is

$$\phi(x) = x^{\frac{1}{2}+\nu}(x+2L)^{\frac{1}{2}-\nu} - x^{\frac{1}{2}-\nu}(x+2L)^{\frac{1}{2}+\nu}. \tag{4.15}$$

plotted in figure 4.1. Let us analyze first the case $\alpha^2 < \frac{1}{4}$, where, for

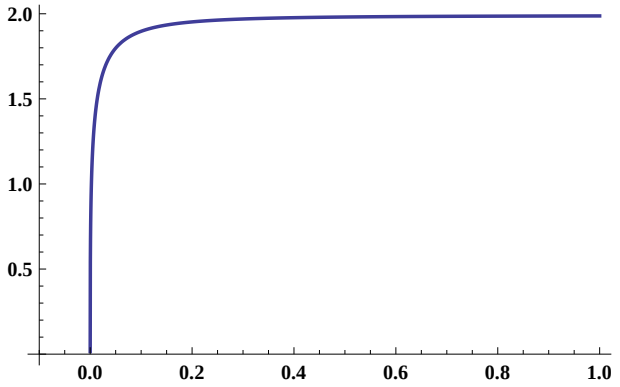

Figure 4.1: Zero mode for $\alpha = 0.4$

$L \to \infty$ there is just one bound state. To see if this solution can satisfy the boundary conditions (4.7), we expand the solution (4.15) around $x = 0$, keeping only the terms with power less then one,

$$\phi(x) \simeq \sqrt{2Lx}\left(\left(\frac{x}{2L}\right)^{\nu} - \left(\frac{x}{2L}\right)^{-\nu}\right),$$

It easy to show that the boundary conditions (4.7) are satisfied if and only if

$$L^c = \frac{1}{2\Lambda}. \tag{4.16}$$

This means that there is a zero mode exact solution of the spectral equation satisfying the boundary conditions only for a particular value of $2L$ the distance between the two quarks. [1]

[1] This should not be confused with with the asymptotic zero modes used to define the boundary conditions.

The emerging picture can be summarized in the following terms. If the two quarks are very far apart, there is one bound state with negative energy. The value of this energy tends to the energy of the bound state which exists in the presence of one single quark for that subcritical regime of the coupling constant. As far as the separation between the sources is reduced, the negative eigenvalue starts to increase, until it reaches zero value at a particular finite distance, defined by (4.16). This particular value defines a *critical distance*, where the right negative mode disappears from the spectrum.
More important than the explicit way that this energy increases with decreasing the distance between the quarks, is the fact that at some moment it will reach a null value and disappears. If the separation is less than the critical distance there are no bound state, while, if it is bigger there is one bound state. In other words, the variation of the separation between the sources affects the appearance or disappearance of bound states. This suggests us that a similar phenomenon can occur in three-dimensional system in the presence of quark-antiquark pair: the variation of the separation between the quarks could cause the appareance/disappearance of the negative eigenvalues of the second order variations operator, and affect to the stability of the Coulomb phase.

Let us now analyze the region $\alpha^2 > \frac{1}{4}$, where there is an infinite number of eigenvalues $-\lambda_n^2$, $n = 0, \pm 1, \pm 1, \ldots$ for $L = \infty$. In this case the boundary conditions are satisfied for infinite values of the distance:

$$L_n^c = \frac{\exp[-i\frac{\pi}{\nu}(\frac{1}{2} + n)]}{2\Lambda},$$

with $n = 0, \pm 1, \pm 1, \ldots$. This means that when we reduce the distance between the two quarks, each negative energy $-\lambda_n^2$ starts to increase until it will reach the zero value at a particular distance L_n^c. Now, even if every bound state disappears at some critical distance, there always remain, for each $q - \bar{q}$ distance, an infinite number of negative energy bound states. Moreover, the result anticipates somehow what happen in the presence of a quark-antiquark pair in three-dimensional QCD. In the supercritical regime of the coupling constant the Coulomb potential is always unstable,

no matter what is the distance between the two quarks, and there is not a transition between stability and instability changing the distance.

A remarkabe property is that the ratio of two consequtive values of the energies when $L = \infty$ is

$$\frac{\lambda_{n+1}^2}{\lambda_n^2} = \exp\left[\frac{2\pi}{\nu} i\right],$$

then the quotient between the corresponding critical distance is

$$\frac{L_{n+1}^c}{L_n^c} = \exp\left[-\frac{\pi}{\nu} i\right],$$

Both are consequence of the existence of remaining discrete conformal invariance in the supercritical regime. Even if the choice of boundary condition introduces a scale Λ in the theory reponsable for the anomalous breaking of conformal invariance, the domain of the corresponding selfadjoint extension is the same for Λ and $\Lambda e^{-\frac{\pi}{\nu} i}$. This means that the spectrum is the same for both boundary conditions. However, the flow induced by the adiabatic change of λ generates a non-trivial flow of energy levels mapping the level λ_n into λ_{n+1} when Λ flows to $\Lambda e^{-\frac{\pi}{\nu} i}$ in an adiabatic way.

4.2. Spectrum of bound states

To solve the equation (4.6) for any distance L, we use numerical approach. In this way we can follow the variation of the eigenvalues with the separation between the $q - \bar{q}$ pair. The technique we use is the balistic method which can be implemented for any type of boundary condition of the two quarks. This technique can be easily extended to the more complex case of 3-dimensional quark-antiquark backgrounds.

One advantage of the method we introduce to define the boundary conditions by means of a renormalization group flow following the asymptotic zero mode solutions, is that is very easy to implement in the ballistic numerical approach. Let be more specific with an explicit example. Let us

consider a charge value $\alpha = 0.4$ in the subcritical regime, and a unit distance between the quarks, i.e. $L = 0.5$. Once a boundary condition is selected ($\Lambda = 5$ and $\theta = \frac{\pi}{2}$) we introduce a cut-off near the quark source at $x = 0$, in our case we started with $x_0 = 10^{(-5)}$ At this point $x_0\Lambda \ll 1$ and it is reasonable to assume that the negative eigenvalues have practically reached their physical values in the physical limit $x_0 \to 0$. However, the stability of the spectrum in this approximation can always be tested and this is done in the simulations. The fast convergence is due to our procedure to define the self adjoint extensions. The renormalization of the singularity was done using the asymptotic zero modes. This procedure assures that reducing the cut off the domain and the eigenvalues vary slowly, reaching a well defined limit at $x_0 = 0$. In all cases the numerical tests of how the eigenvalues change with the cut off in the $\frac{1}{x^2}$ potential case are very explicity and confirm the validity of our method.
In our ballistic method we normalize the value of the function at x_0 by $\phi(x_0) = 1$ and from the relation (4.7) evaluated at x_0, we derive the value of the derivative of $\phi(x)$ imposed by the boundary condition. After refining the convergence we get the following resuls In that regime we have only one negative energy bound state with $\lambda^2 = 18.2164$. The shape of the solution is displayed in Figure 4.2. It is also possible to change the distance between the two quarks and see how this energy level changes with the separation of the two quarks. The result is displayed in Figure 4.3, where the dots represent the eigenvalues founded fine tuning the numerical solution, while the continue curve represent a fit of these points with the function

$$-\lambda^2(L) = c_1\big(1 + c_2 \arctan(c_3\, L)\big), \tag{4.17}$$

where $c_1 = -29.272$, $c_2 = -0.877$ and $c_3 = 4.24$. From this fitted curve $-\lambda^2(L \to \infty) = c_1$ and $\lambda^2(L_c) = 0$ with $L_c = 0.108$, in perfect agreement respectively with the analytic value of eigenvalue in the case of one quark $-\lambda^2 = -29.225$ and the analytic value of the critical distance $L_c = 0.1$ obtained from (4.16).

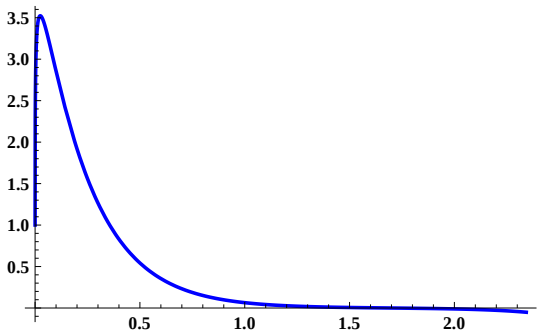

Figure 4.2: Bound states with negative energy $-\lambda^2 = -18.2164$. The bound state is attached to the right quark of the pair. There is a similar state attached to left quark.

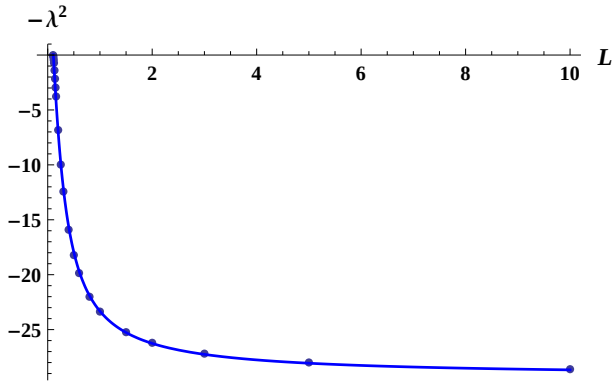

Figure 4.3: Variation of the negative energy of the bound state in the subcritical regime with the distance $2L$ between the two quarks of the $q-\bar{q}$ pair (blue dots). The continuous curve is phenomenological fit given by the expression (4.17)

4.3. Symmetric and antisymmetric bound states

Once analyzed the external region of the singularity, let us focus on the central region of the equation (4.1) between the two singularities, $-L < x <$

L. In that case there are two negative energy levels due to the existence of symmetric and antisymmetric bound state. The equation becomes:

$$\Big[-\frac{d^2}{d\,x^2} - \alpha^2 \Big(\frac{1}{L-x} - \frac{1}{x+L} \Big)^2 \Big] \phi(x) = -\lambda^2 \phi(x). \tag{4.18}$$

Since the potential terms is symmetric under reflection symmetry $x \to -x$, the solutions will be symmetric or antisymmetric respect to the point $x = 0$. When the separation L between the two sources goes to infinity, the symmetric and the antisymmetric modes are degenerate, they have the same eigenvalue defined by (4.11), (4.12) and (4.13). This can be understood for the following reason: because of the symmetry of the equation, it is possible to reduce the problem on half interval, for example, $0 \leq x < L$. In this interval, besides the boundary conditions in L the wave function vanish at $x = 0$ for the antisymmetric solution, whereas its derivative vanish for the symmetric solution. Then, in the limit where $q - \bar{q}$ distance is infinite, the problem reduces to the case (4.10) where the wave function already decayed exponentially fast to zero before reaching the origin. In that case at the origin both the function and his derivative is zero. Concluding, the symmetric and the antisymmetric mode coincide on $0 \leq x < L = +\infty$ and they have the same energy, i.e. they are degenerated. But only in that extreme limit.

It is also possible to find a solution of the equation with zero eigenvalue:

$$\Big[-\frac{d^2}{d\,x^2} - \alpha^2 \Big(\frac{1}{L-x} - \frac{1}{x+L} \Big)^2 \Big] \phi(x) = 0.$$

Let us concentrate on the values of the coupling constant $\alpha < \frac{1}{4}$. In this case the symmetric solution and the antisymmetric solutions of the previous equation are respectively

$$\phi_s(x) = \sqrt{L^2 - x^2} \left(L_{-\frac{1}{2}+\mu,2\nu}\Big(\frac{x}{L}\Big) + L_{-\frac{1}{2}+\mu,2\nu}\Big(-\frac{x}{L}\Big) \right) \tag{4.19}$$

and

$$\phi_a(x) = \sqrt{L^2 - x^2} \left(L_{-\frac{1}{2}+\mu,2\nu}\Big(\frac{x}{L}\Big) - L_{-\frac{1}{2}+\mu,2\nu}\Big(-\frac{x}{L}\Big) \right) \tag{4.20}$$

with $\mu = \sqrt{\frac{1}{4} - 4\alpha^2}$ and $\nu = \sqrt{\frac{1}{4} - \alpha^2}$, where $L_{\eta,\lambda}(x)$ are the associated Legendre functions of the first kind. In figure 4.4 these solutions are plotted for $\alpha = 0.4$. Expanding near the singularities and keeping only the diver-

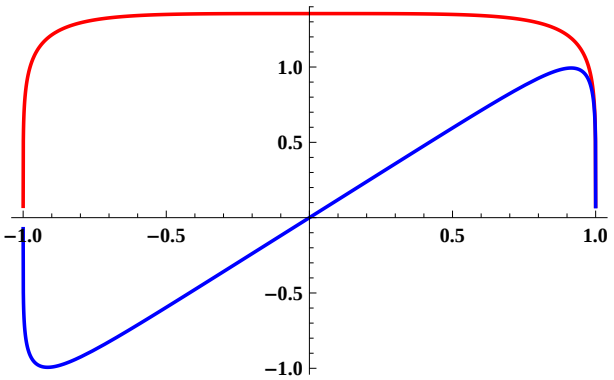

Figure 4.4: Symmetric (Red) and antisymmetric (blue) zero mode for $\alpha = 0.4$

gent terms, it is possible to see that the boundary conditions are satisfied if

$$L_s^c = \frac{1}{2\Lambda}\left(\frac{\Gamma(2\nu+1)\Gamma\left(\frac{1}{2}-\mu-2\nu\right)\Gamma\left(\frac{1}{2}+\mu-2\nu\right)\left(\cos(\pi\mu)+\sin(2\pi\nu)\right)}{\pi\Gamma(1-2\nu)}\right)^{-\frac{1}{2\nu}} \tag{4.21}$$

for the symmetric solution and

$$L_a^c = \frac{1}{2\Lambda}\left(\frac{\Gamma(2\nu+1)\Gamma\left(\frac{1}{2}-\mu-2\nu\right)\Gamma\left(\frac{1}{2}+\mu-2\nu\right)\left(\cos(\pi\mu)-\sin(2\pi\nu)\right)}{\pi\Gamma(1-2\nu)}\right)^{-\frac{1}{2\nu}} \tag{4.22}$$

for the antisymmetric one. L_s^c and L_a^c represent respectively the critical distance where the symmetric and antisymmetric bound states disappear. The dependence of these two critical distances on the coupling constant α is displayed in Figure 4.5. We remark that the antisymmetric one is always

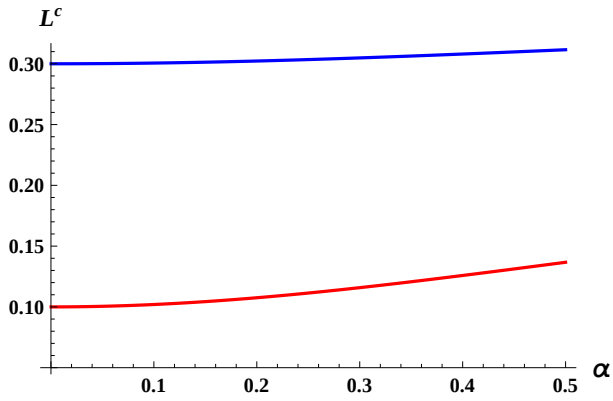

Figure 4.5: Red and blue lines represent the dependence of the critical distances on α for $\alpha^2 < \frac{1}{4}$ and $\Lambda = 5$ for the symmetric and antisymmetric bound states on the domain between the two quarks

bigger than the symmetric one. If we begin at large separations between the two quarks and start to decrease L, the antisymmetric bound state will disappear before the symmetric one does it. On the other hand if we begin with short distances between the quarks and star to move them appart the symmetric bound state will appear before the antisymmetric one .
This suggests that the energies of the symmetric bound state are always less negative respect the energies of the antisymmetric one. In Figure 4.6 we display the values of both energy levels for $\alpha = 0.4$ and $\Lambda = 5$ Even if in this case it does not work a fit of the type $-\lambda^2(L) = c_1\big(1+c_2\arctan(c_3\,L)\big)$, from the numerics results that the eigenvalue at $L = 10^3$ is $-\lambda^2 = -29.219$ in agreement with the analytic value for infinite separation 29.225, while for $L = 0.126$ and $L = 0.309$ respectively the symmetric and the antisymmetric eigenvalues are very close to zero (-0.058 and -0.09) in agreement with the analytic critical distance $L_s = 0.126$ and $L_a = 0.308$.

In the region $\alpha^2 > \frac{1}{4}$ there are instead an infinity of symmetric $-\lambda^2_{s,n}$ and antisymmetric $-\lambda^2_{a,n}$ bound states, labeled by an integer n. For large L these states become degenerate, $-\lambda^2_{s,n} = -\lambda^2_{a,n} = -\lambda^2_n$, and the quotient

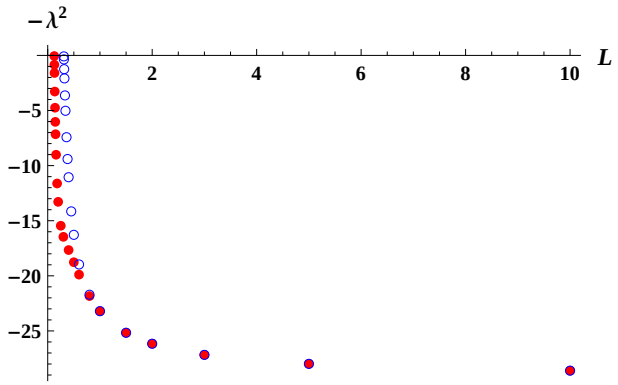

Figure 4.6: Negative energy of symmetric (red dots) and antysymmetric (blue dots) bound states locate in the domain between the $q-\bar{q}$ pair for $\alpha = 0.4$ and $\Lambda = 5$

between two successive is $\lambda_{n+1}/\lambda_n = \exp[\frac{2\pi}{\nu}i]$ is constant. Decreasing the separation between the quarks increases the gap between the eigenvalues, which never cross each other until both reach their zero values at two different critical distances. The analytic formulas for the symmetric $L^c_{s,n}$ and $L^c_{a,n}$ critical distances can be obtained in the same way as before and the results are plotted in figure 4.7. In the region $\alpha^2 < \frac{1}{4}$, for each couple of symmetric and antisymmetric degenerate bound states, the corresponding symmetric critical distance is always lower than the antisymmetric critical distance ($L_{s,n} < L_{a,n}$, for each n). Again it is possible to deduce the same analytic properties between the critical distances of different eigenvalues:

$$\frac{L^c_{s,n}}{L^c_{s,n-1}} = \frac{L^c_{a,n}}{L^c_{a,n-1}} = \exp\left[-i\frac{\pi}{\nu}\right]$$

$$\frac{L^c_{s,n} - L^c_{a,n}}{L^c_{s,n-1} - L^c_{a,n-1}} = \exp\left[-i\frac{\pi}{\nu}\right]$$

$$\frac{L^c_{s,n}}{L^c_{a,n}} = \left(\frac{2}{\sin(2\pi\nu)\sec(\pi\mu)+1} - 1\right)^{\frac{1}{2\nu}}.$$

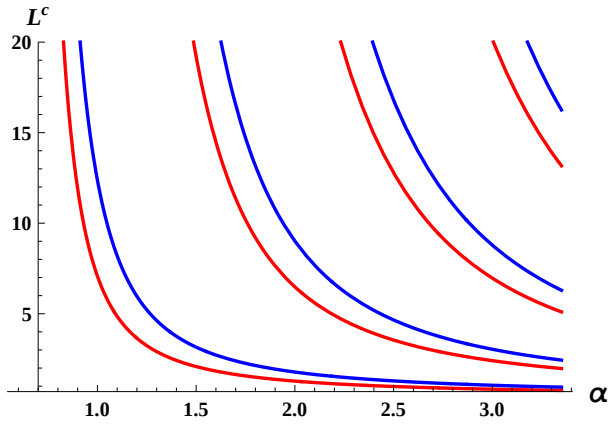

Figure 4.7: Critical distance dependence on the coupling constant for symmetric (red lines) and antysymmetric (blue lines) bound states locate in the domain between the $q - \bar{q}$ pair in the supercritical regime $\alpha^2 > \frac{1}{4}$ ($\Lambda = 5$.

In summary we have analysys of the problem of a $q-\bar{q}$ pair in one-dimension show us that is the introduction of a new parameter, the separation between the sources, affects the structure of the spectrum in a very interesting way. The fact that the problem is one-dimensional allow us to split it into three subdomains: the external regions respect the singularities and the central region between the two quarks. In the exterior regions, when the two sources are separated by infinite distance the spectrum coincides with the case of one source, studied in the previous chapter, with one bound state for small ($\alpha^2 < 1/4$) coupling constant or infinite bound states for large ($\alpha^2 > 1/4$) coupling constant. Reducing the separation between the two quarks all energy levels start to increase until at a particular distance, called critical distance, when they cross the zero. This is the principal novelty: the existence of a distance where the bound states disappear. This critical distance can be found analytically. The regime of small coupling is the

more interesting: for small separation there are not bound states, for large distance there is four bound states in the spectrum, two symmetric and two antisymmetric. For large coupling constant, even if some bound states disappears, at each distance there are always infinite number of bound states.

The importance of this model stands in the fact that it is quite similar to the dynamics of gluonic fluctuations in a $q-\bar{q}$ background which points out to a similarity between the negative energy bound states of this problem and unstable modes of the second order variation operator around the Coulomb saddle point. The above results suggest that similar phenomena could occur in the behavior of the Coulomb phase in the quark antiquark system.

5

Gluonic Instabilities in a Coulomb Heavy Quark-Antiquark background

The analysis of the effects of a $q-\bar{q}$ pair in a simple but very interesting one a dimensional model raise the question of whether similar effects can occur or not in three-dimensional real QCD. A colorless $q-\bar{q}$ pair having the same quantum numbers than a meson can be described by the current

$$J^0 = i\left(\delta^3(\mathbf{x}+\mathbf{L})\,T^3 - \delta^3(\mathbf{x}-\mathbf{L})\right)\,T^3, \qquad J^i = 0,\;\; i = 1,2,3. \tag{5.1}$$

The two quarks are located along the z axis: $\mathbf{L} = (0,0,L)$. The current induced by the heavy pair can be seen as the abelian projection of two Wilson lines extending in the time direction at a distance 2L. Inserting the current into the equations of motion (3.22)

$$D^\mu F_{\mu\nu} = \, g_s^2 J_\nu,$$

it easy to show the existence of a Coulomb like solution

$$A^0(\mathbf{x}) = i\Phi T^3, \quad \mathbf{A} = 0,$$

with

$$\Phi = \alpha\left(\frac{1}{|\mathbf{x}+\mathbf{L}|} - \frac{1}{|\mathbf{x}-\mathbf{L}|}\right), \quad \alpha = \frac{g_s^2}{4\pi}, \tag{5.2}$$

corresponding to an imaginary chromo-electric dipole potential. This is the classical background where the Euclidean action has be expanded.

5.1. Gluonic instabilities

The search of instabilities lead to the study of the real fluctuations on this background. Negative contributions coming from second order variations can give rise to instabilities. The separation between the quarks introduce a new scale in the theory. We have already studied the appearance of instabilities of the Coulomb regime in the case of single external heavy quark. By continuity, these instabilities should persist for large separations, but it is not clear if they hold at all the distances. The technical drawback is that the dipole structure of the $q-\bar{q}$ pair breaks the spherical symmetry and cylindrical symmetry is not enough to have analytical solutions.

Gluonic instabilities require the existence of negative eigenvalues of the second order operator which governs the quadratic terms in equation (3.29)

$$\begin{aligned}&\big(\partial_\mu\partial_\nu - \delta_{\mu\nu}(\partial_0^2 + \triangle)\big)\tau_\nu^\pm - \delta_{\mu j}\delta_{\nu j}\Phi^2\tau_\nu^\pm \\ &\pm(-2\delta_{\mu\nu}\Phi\,\partial_0 + 2\delta_{\nu 0}\,\partial_\mu\Phi + \Phi\,\delta_{\nu 0}\,\partial_\mu + \Phi\,\delta_{\mu 0}\,\partial_\nu - \delta_{\mu 0}\,\partial_\nu\Phi)\tau_\nu^\pm = -\lambda^2\tau_\mu^\pm,\end{aligned}$$

which split as

$$\begin{aligned}-\triangle\,\tau_0^\pm \pm [\Phi\boldsymbol{\nabla}\cdot\boldsymbol{\tau}^\pm - \boldsymbol{\tau}^\pm\cdot\boldsymbol{\nabla}\Phi] &= -\lambda^2\tau_0^\pm, \\ \boldsymbol{\nabla}(\boldsymbol{\nabla}\cdot\boldsymbol{\tau}^\pm) - \triangle\,\boldsymbol{\tau}^\pm - \Phi^2\boldsymbol{\tau}^\pm \pm [2\tau_0^\pm\,\boldsymbol{\nabla}\Phi + \Phi\boldsymbol{\nabla}\tau_0^\pm] &= -\lambda^2\boldsymbol{\tau}^\pm,\end{aligned} \tag{5.3}$$

In cylindrical coordinates,

$$\boldsymbol{\nabla}\Phi = \Phi'_\rho\hat{u}_\rho + \Phi'_z\hat{u}_z,$$

with

$$\begin{aligned}\Phi'_\rho &= -\alpha\left(\frac{\rho}{(\rho^2+(z-L)^2)^{\frac{3}{2}}}-\frac{\rho}{(\rho^2+(z+L)^2)^{\frac{3}{2}}}\right),\\ \Phi'_z &= -\alpha\left(\frac{(z-L)}{(\rho^2+(z-L)^2)^{\frac{3}{2}}}-\frac{(z+L)}{(\rho^2+(z+L)^2)^{\frac{3}{2}}}\right)\end{aligned}$$

Eventually, possible instabilities can arise from static magnetic modes

$$\boldsymbol{\tau}^{\pm}=\frac{\mathbf{x}\times\hat{\mathbf{e}}_z}{\rho^{\frac{3}{2}}}\,\phi^{\pm}(\rho,z),\quad \tau_0^{\pm}=0, \tag{5.4}$$

where $\hat{\mathbf{e}}_z$ is a unit vector in the direction of the axis connecting the two quarks. We postpone to appendix B the discussion of more general roots of instability. The functions $\phi^{\pm}(\rho,z)$ satisfy the following eigenvalues equation, in cylindrical coordinates:

$$\Big[-\frac{\partial^2}{\partial\,\rho^2}-\frac{\partial^2}{\partial\,z^2}+\frac{3}{4\rho^2}-V(\rho,z)\Big]\phi^{\pm}(\rho,z)=-\lambda^2\phi^{\pm}(\rho,z), \tag{5.5}$$

where

$$V(\rho,z)=\alpha^2\left(\frac{1}{\sqrt{\rho^2+(z+L)^2}}-\frac{1}{\sqrt{\rho^2+(z-L)^2}}\right)^2.$$

Again, to have real gauge fields(3.12), we must require that $(\phi^+)^*=\phi^-$. The equation (5.5) is invariant under the replacement $z\to -z$: for this reason, eventual solutions will be either symmetric or antisymmetric with respect reflections with respect to the plane $z=0$. The form of the unstable modes (5.4) induce a field lying on the plane perpendicular to the axis connecting the quarks and it has non-vanishing component only in the direction perpendicular to the radial direction of this plane. For simplicity we omit from now on the indices $\pm$ on the function ϕ.

The potential in (5.5) presents two singularities, situated at the positions of the quarks, and in order to have a self adjoint operator, both must be renormalized by the choice of proper boundary conditions. As usual,

the self adjoint boundary conditions are given in terms of the zero modes around the singularities $\rho \approx 0$ and $z \approx \pm L$. The equations that define the asymptotic zero modes are:

$$\Big[\frac{\partial^2}{\partial\,\rho^2} + \frac{\partial^2}{\partial\,z^2} - \frac{3}{4\rho^2} + \left(\frac{\alpha^2}{\rho^2+(z\pm L)^2} - \frac{\alpha^2}{L\sqrt{\rho^2+(z\pm L)^2}}\right)\Big]\phi_0(\rho,z) = 0.$$

The solutions are

$$\phi^{\pm}_{0>}(\rho,z) = \frac{\rho^{\frac{3}{2}}}{\left(\rho^2+(z-L)^2\right)^{3/4}} I_{\pm 2\nu}\left(\frac{2\alpha}{\sqrt{L}}\sqrt{\rho^2+(z-L)^2}\right)$$

near $\rho \approx 0$ and $z \approx L$, and

$$\phi^{\pm}_{0<}(\rho,z) = \frac{\rho^{\frac{3}{2}}}{\left(\rho^2+(z+L)^2\right)^{3/4}} I_{\pm 2\nu}\left(\frac{2\alpha}{\sqrt{L}}\sqrt{\rho^2+(z+L)^2}\right)$$

near $\rho \approx 0$ and $z \approx -L$, with $\nu = \sqrt{\frac{9}{4}-\alpha^2}$.
i) For $\alpha^2 \leq \frac{5}{4}$ the solutions $\phi^{-}_{0>}$ and $\phi^{-}_{0<}$ are not normalizable near the singularities. The operator is essentially self adjoint with boundary conditions

$$\begin{aligned}
&\lim_{\rho\to 0,\, z\to L}\left(\hat{\mathbf{n}}\cdot\boldsymbol{\nabla}\phi(\rho,z)\;\phi_{>}(\rho,z) - \phi(\rho,z)\;\hat{\mathbf{n}}\cdot\boldsymbol{\nabla}\phi_{>}(\rho,z)\right) = 0,\\
&\lim_{\rho\to 0,\, z\to -L}\left(\hat{\mathbf{n}}\cdot\boldsymbol{\nabla}\phi(\rho,z)\;\phi_{<}(\rho,z) - \phi(\rho,z)\;\hat{\mathbf{n}}\cdot\boldsymbol{\nabla}\phi_{<}(\rho,z)\right) = 0,
\end{aligned} \tag{5.6}$$

where $\hat{\mathbf{n}}\cdot\boldsymbol{\nabla}$ is the normal derivative on a cylindric cut-off around the singularities and

$$\begin{aligned}
\phi_{>}(\rho,z) &= \left(\frac{\rho}{\sqrt{\rho^2+(z-L)^2}}\right)^{\frac{3}{2}}\left(\sqrt{\rho^2+(z-L)^2}\right)^{\nu},\\
\phi_{<}(\rho,z) &= \left(\frac{\rho}{\sqrt{\rho^2+(z-L)^2}}\right)^{\frac{3}{2}}\left(\sqrt{\rho^2+(z+L)^2}\right)^{\nu}.
\end{aligned} \tag{5.7}$$

For $\alpha^2 > \frac{5}{4}$ both behaviors of the zero modes are normalizable. There is a family of self adjoint extension parametrized by a parameter Λ with dimensions of $[\mathrm{L}]^{-1}$, defined by the following boundary conditions

$$\begin{aligned}\lim_{\rho\to 0,\, z\to L} \left(\hat{\mathbf{n}}\cdot\boldsymbol{\nabla}\phi(\rho,z)\ \phi_{\Lambda>}(\rho,z) - \phi(\rho,z)\ \hat{\mathbf{n}}\cdot\boldsymbol{\nabla}\phi_{\Lambda>}(\rho,z)\right) = 0,\\ \lim_{\rho\to 0,\, z\to -L} \left(\hat{\mathbf{n}}\cdot\boldsymbol{\nabla}\phi(\rho,z)\ \phi_{\Lambda<}(\rho,z) - \phi(\rho,z)\ \hat{\mathbf{n}}\cdot\boldsymbol{\nabla}\phi_{\Lambda<}(\rho,z)\right) = 0.\end{aligned} \tag{5.8}$$

The explicit form of $\phi_{\Lambda>}(\rho,z)$ and $\phi_{\Lambda<}(\rho,z)$ depends on the value of the coupling constant. **ii)** For $\frac{5}{4} < \alpha^2 \leq \frac{9}{4}$, $\alpha^2 \neq 2$:

$$\begin{aligned}\phi_{\Lambda>}(\rho,z) &= \left(\frac{\rho}{w_>}\right)^{\frac{3}{2}}\left((\Lambda w_>)^{\nu} - (\Lambda w_>)^{-\nu}\left(1+\frac{\alpha^2 w_>}{L(1-2\nu)}\right)\right),\\ \phi_{\Lambda<}(\rho,z) &= \left(\frac{\rho}{w_<}\right)^{\frac{3}{2}}\left((\Lambda w_<)^{\nu} - (\Lambda w_<)^{-\nu}\left(1+\frac{\alpha^2 w_<}{L(1-2\nu)}\right)\right),\end{aligned} \tag{5.9}$$

where $w_> = \sqrt{\rho^2+(z-L)^2}$ and $w_< = \sqrt{\rho^2+(z+L)^2}$. In this case also the terms $w^{1-\nu}$ inside the parenthesis must be taken into account because its derivative diverges at zero.
iii) For $\alpha^2 = 2$:

$$\begin{aligned}\phi_{\Lambda>}(\rho,z) &= \left(\frac{\rho}{w_>}\right)^{\frac{3}{2}}\left((\Lambda w_>)^{\frac{1}{2}} - (\Lambda w_>)^{-\frac{1}{2}}\left(1+\left(C+\log\left(\frac{2w_>}{L}\right)\right)\frac{2w_>}{L}\right)\right),\\ \phi_{\Lambda<}(\rho,z) &= \left(\frac{\rho}{w_<}\right)^{\frac{3}{2}}\left((\Lambda w_<)^{\frac{1}{2}} - (\Lambda w_<)^{-\frac{1}{2}}\left(1+\left(C+\log\left(\frac{2w_<}{L}\right)\right)\frac{2w_<}{L}\right)\right).\end{aligned} \tag{5.10}$$

with $C = -1 + 2\gamma$.

iv) For $\alpha^2 = \frac{9}{4}$:

$$\begin{aligned} \phi_{\Lambda>}(\rho,z) &= \left(\frac{\rho}{w_>}\right)^{\frac{3}{2}} (1-\log(\Lambda w_>))\,, \\ \phi_{\Lambda<}(\rho,z) &= \left(\frac{\rho}{w_<}\right)^{\frac{3}{2}} (1-\log(\Lambda w_<))\,. \end{aligned} \tag{5.11}$$

v) For $\alpha^2 > \frac{9}{4}$:

$$\begin{aligned} \phi_{\Lambda>}(\rho,z) &= \left(\frac{\rho}{w_>}\right)^{\frac{3}{2}} \left((\Lambda w_>)^{\nu} - (\Lambda w_>)^{-\nu}\right), \\ \phi_{\Lambda<}(\rho,z) &= \left(\frac{\rho}{w_<}\right)^{\frac{3}{2}} \left((\Lambda w_<)^{\nu} - (\Lambda w_<)^{-\nu}\right). \end{aligned} \tag{5.12}$$

Let us recall the one quark case now in cylindrical coordinates, where the Coulomb potential generated by a quark at the origin reads

$$V(\rho,z) = \frac{\alpha^2}{\rho^2+z^2}.$$

The bound states solutions in cylindric coordinates are

$$\phi(\rho,z) = \frac{\rho^{3/2}}{(\rho^2+z^2)^{3/4}} K_\nu\left(\lambda\sqrt{\rho^2+z^2}\right).$$

with $\nu = \sqrt{\frac{9}{4}-\alpha^2}$. It is easy to show that this solution correspond to the solution (3.31) with $\hat{\mathbf{n}} = \hat{\mathbf{e}}_z$ and that the general solution (B.9) is proportional to $\boldsymbol{Y}_{jj0}$ with $j=1$. The ansatz (5.4) preserves the cylindrical symmetry around the z axis, and any other possible solution is proportional to $\mathbf{Y}_{jj0}$, with $j>1$. For example the solution

$$\phi(\rho,z) = \frac{z\,\rho^{3/2}}{(\rho^2+z^2)^{5/4}} K_\nu\left(\lambda\sqrt{\rho^2+z^2}\right),$$

with $\nu = \sqrt{\frac{25}{4} - \alpha^2}$, correspond to $j = 2$.

This check is important because it allow to verify the consistency with the limit when the two quarks are far away. In that case the eigenvalues should converge to the values of one quark case. Finally, even if the cases corresponding to $j > 1$ of the one quark case will be not developed any further, as they have larger critical charge respect to the $j = 1$ case, they shows us also how to construct the boundary conditions corresponding to more general external conditions.

Unfortunately the equation (5.5) can not be solved analytically: as in the one dimensional system, numeric methods must be used. In this case, the situation is more complicated, because the system is really a two dimensional. We use the package "pdetool" of MathLab. To bound the domain of the computation we enclose the system in a large semicircle of radius r_∞ on the half plane (ρ, z) with $\rho > 0$, where we consider Dirichlet boundary conditions. Then we use the reflection on the plane $z = 0$ to restrict the domain to a quadrant with $z < 0$. On the boundary $z = 0$ we consider Neumann boundary conditions for symmetric states and Dirichlet boundary conditions for antisymmetric states. Besides that we have to introduce a semicircular cut-off around each quark to impose the boundary conditions (5.6) and (5.8) on the cut off. Figure 5.1 shows the implementation of the operational domain.

5.1.1. Subcritical regime

As in the case of one quark, there are different regimes according the values of the coupling constant. For $\alpha \leq \frac{5}{4}$, the operator associated to (5.5) is essentially self adjoint and has positive spectrum. There are not unstable negative modes. In the regime $\frac{5}{4} < \alpha^2 \leq \frac{9}{4}$, at each distance there are two solutions of (5.5) matching the boundary conditions (5.6) for $\Lambda \neq \pm\infty$, one symmetric and one antisymmetric under z reflection. For $\Lambda = \pm\infty$ again there are not solutions.

Let us focus first on the interval $2 < \alpha^2 < \frac{9}{4}$. The negative eigenvalues of the two unstable modes for large distances L become degenerate and

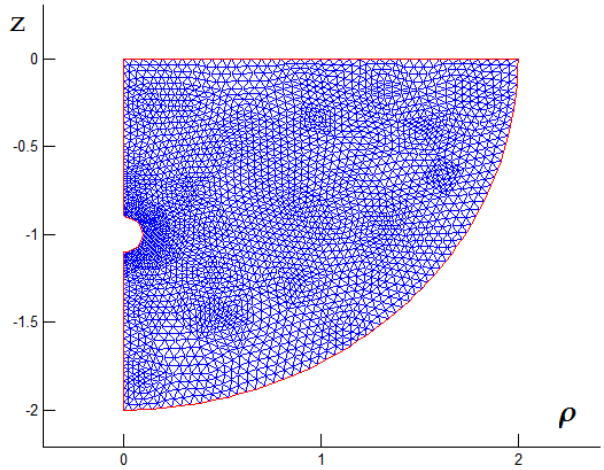

Figure 5.1: Domain for the two quarks problem.

coincide with the one quarks unstable modes. They start to increase when the distance between the quarks decreases, until the reach the zero at a critical distance. The antisymmetric mode disappeara at larger distance than the symmetric one, exactly like in the one dimensional model. The critical distance grows when we decrease the coupling constant α till it becomes ∞ for $\alpha^2 = 2$.

Let us consider the case $\alpha = 1.495$ in the subcritical regime and fix the parameter of the boundary conditions the parameter $\Lambda = 10$. In this case the eigenvalue of one quark is $-\lambda^2 = -124.58$. The radius of the cut off must be small enough and the grid of the domain must be thin enough to guarantee respectively that the eigenvalue has practically reached is asymptotic value and is stable. The parameters choice affect the time of computation that can become enormous. A good compromise between precision of the eigenvalue (2% error) and time of computation (around 10 minutes each point) is reached choosing the radius of the cut off $r_0 = 0.001$, the radius of the domain $r_\infty = 2$ and six refinement of the grid.

In figure 5.2 we display the symmetric (red disks) and the antisymmetric

(blue circles) eigenvalues founded numerically changing the separation distance between the quarks. The symmetric eigenvalue is always lower than

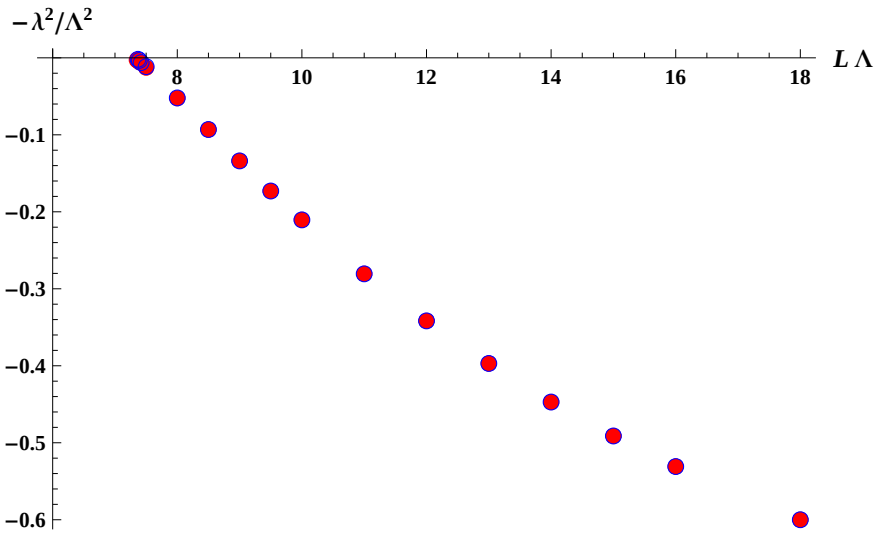

Figure 5.2: Symmetric (red disks) and antisymmetric (blue disks) eigenvalues for the subcritical case $\alpha = 1.495$

the antisymmetric one. In both cases there is a critical distance, where the eigenvalues vanish, the symmetric mode disappears at shorter distances that the antisymmetric mode. The splitting between symmetric and the antisymmetric is very small, and converges to zero for large distances. In fact it is only appreciable when one is very close to the critical distance, as it is shown in the Figure 5.3. The symmetric and the antisymmetric numerical eigenvalues can be fitted with the curve

$$-\lambda^2(L) = -\lambda_1^2\Lambda^2\big(1 + c_2 \arctan(c_3\Lambda\, L)\big),$$

where $-\lambda_1^2\Lambda^2 = -124.58$ is the eigenvalue of the one quark case, $c_2 = -1.14$ and $c_3 = 0.11$ for the symmetric mode, while $c_2 = 1.15$ and $c_3 = -0.11$ for the antisymmetric mode (see figure 5.4 and 5.5). The fit gives the criti-

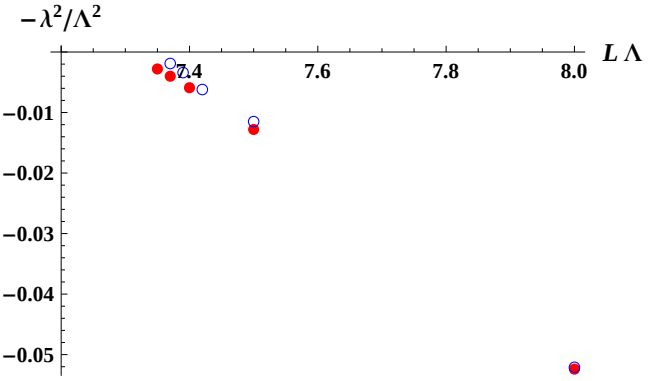

Figure 5.3: Splitting of the symmetric and antisymmetric eigenvalues near the critical distance

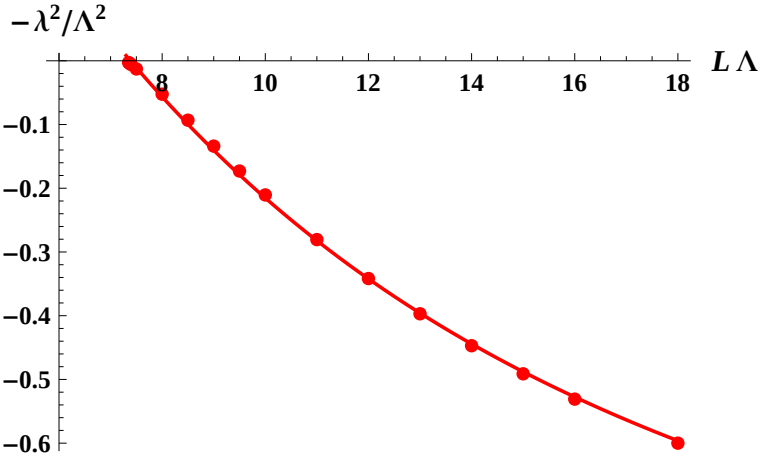

Figure 5.4: Fit of the antisymmetric mode by the curve $-\lambda^2(L) = -\lambda_1^2\Lambda^2\big(1 + c_2 \arctan(c_3\Lambda\, L)\big)$with $c_2 = -1.14$ and $c_3 = 0.11$ for $\alpha = 1.495$

cal distance $L_s^c\Lambda = 7.38$ ($L_a^c\Lambda = 7.40$) for the symmetric (antisymmetric) unstable modes, respectively. In Figures 5.6, 5.7, 5.8 and 5.9 the shape of

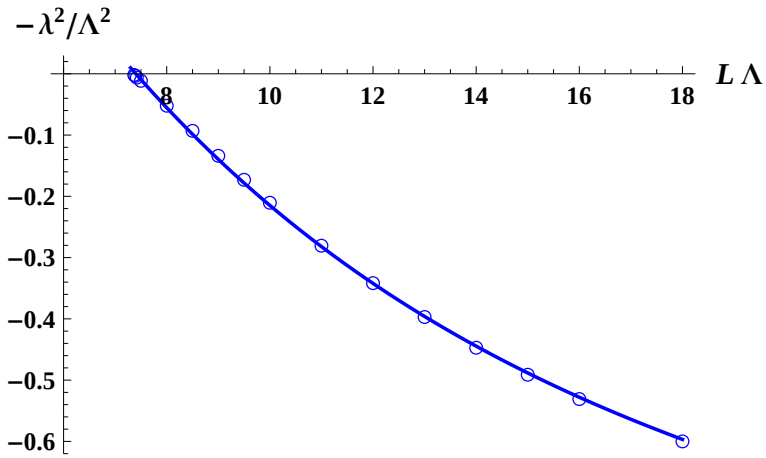

Figure 5.5: Fit of the antisymmetric mode by the curve $-\lambda^2(L) = -\lambda_1^2\Lambda^2\big(1 + c_2 \arctan(c_3\Lambda\, L)\big)$ with $c_2 = 1.15$ and $c_3 = -0.11$ for $\alpha = 1.495$

the symmetric and the antisymmetric unstable modes are shown. The configuration of the symmetric mode, the one that drive the instability, has a shape of a thick string connecting the two quarks.
As example of coupling constant near $\alpha = \sqrt{2}$ the result obtained for the estimated critical distances for $\alpha = 1.42$ are $L_s^c\Lambda = 67.687$ and $L_a^c\Lambda = 67.689$, respectively, showing the increasing of the critical distance with the coupling constant.

In the regime $\frac{5}{4} < \alpha^2 \leq \sqrt{2}$ for all Λ except for $\Lambda \neq \pm\infty$, by reducing the $q - \bar{q}$ distance, the two negative eigenvalues start to decrease, and they become more and more negative. For these boundary conditions there is not a critical distance, because for each separation, both symmetric and antisymmetric bound states are negative modes.

In summary, in the regime $\alpha^2 \leq \frac{5}{4}$, as a consequence of the essentially self-adjointness and the conformal symmetry of the second order variation operator, there are not negative modes. For $\sqrt{2} < \alpha^2 \leq \frac{9}{4}$, breaking the conformal symmetry, a critical distance exists that tends to infinity for

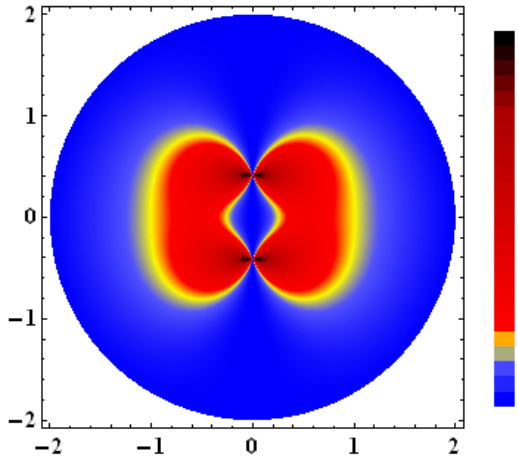

Figure 5.6: Density plot for symmetric unstable mode at $\alpha = 1.495$

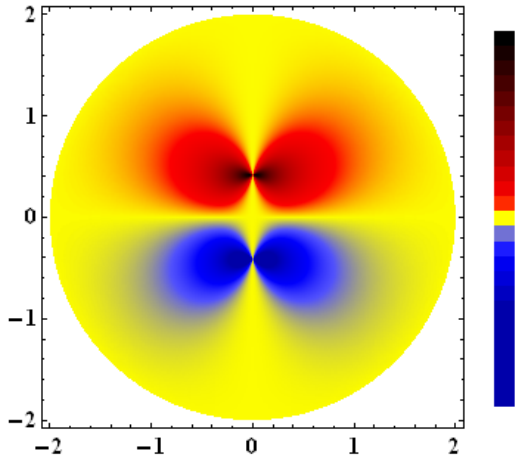

Figure 5.7: Density plot for antisymmetric unstable mode at $\alpha = 1.495$

$\alpha^2 = 2$. For sizes smaller than a critical distance there are not unstable

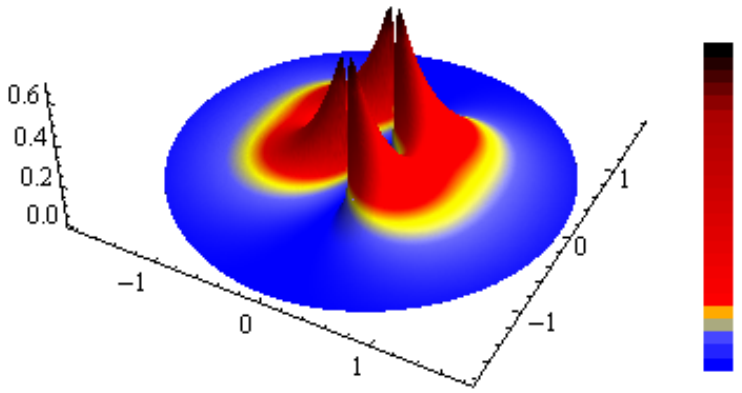

Figure 5.8: 3D plot for symmetric unstable mode at $\alpha = 1.495$

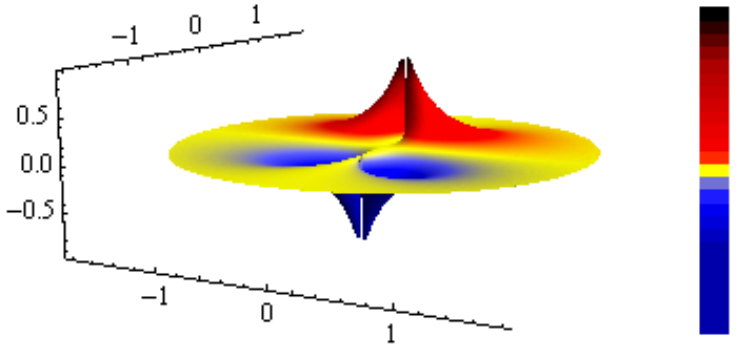

Figure 5.9: 3D plot for antisymmetric unstable mode at $\alpha = 1.495$

modes, while for distances larger than the critical distance a symmetric and an antisymmetric unstable modes appear. In order to match in a continue way these two regimes of the coupling constant, in the regime $\frac{5}{4} < \alpha^2 \leq \sqrt{2}$ the parameter $\Lambda = +\infty$ is chosen. This is equivalent to do not break

the conformal symmetry also in this regime and as consequence there are not negative modes at any distance. The infinity of the critical distance approaching to $\alpha^2 = 2$ from the right matches perfectly this condition. The full dependence of the critical distance on the coupling constant will considered later.

The picture emerging is that for $\alpha^2 \leq 2$ there are not negative modes, while for $\alpha^2 > 2$ it exist a critical distance which marks the existence of unstable mode. If the conformal symmetry had been broken also in the regime $\frac{5}{4} < \alpha^2 \leq 2$, it would be a non natural match between the different regimes: for $\alpha^2 \leq \frac{5}{4}$ no negative modes, crossing the critical coupling $\alpha^2 = \frac{5}{4}$ there are negative modes at all the distance for $\frac{5}{4} < \alpha^2 \leq 2$, while for $\sqrt{2} < \alpha^2 \leq \frac{9}{4}$ there are negative modes only if the separation between the quarks is bigger than a critical distance that becomes infinite for $\alpha^2 = 2$.

5.1.2. Supercritical regime

In the strong coupling regime $\alpha^2 > \frac{9}{4}$, for each distance there is an infinite number of unstable modes, half of them symmetric while the other half are antisymmetric. From this viewpoint they can be organized by symmetric-antismmetric pairs. In each pear the symmetric state is s always more negative. The modes of each pair become degenerate for large distances, converging to the unstable modes of the case of one quark in the supercritical regime. They value increases with decreasing the distances, until they become null at the critical distance. Even if each unstable mode disappears by reducing the distance between the quarks, there is always an infinite number of negative modes, marking the strong instability of the Coulomb potential in this regime.

Let us consider a particular case with coupling constant $\alpha = 2.5$ and boundary condition with $\Lambda = 12$. In this case, two consecutive eigenvalues of one quark are $-\lambda^2 = -28.337$ and $-\lambda^2 = -655.733$. In the supercritical case the simulation converge faster that in the subcritical case. The reason of this stability is due to the fact that for subcritical α the solution tends to infinity at the singularity, while for supercritical α the solution even if oscillates it goes to zero. In this case the simulation are performed by

setting the cut off at $r_0 = 0.001$, the radius of the domain at $r_\infty = 2$ and six refinement of the grid. The precision of the eigenvalue (0.1% error) is reached in computation time of 1 minute per point.

In figures 5.10 and 5.11 we display the numerical values found for two consecutive pairs of symmetric and antisymmetric eigenvalues. Again, the

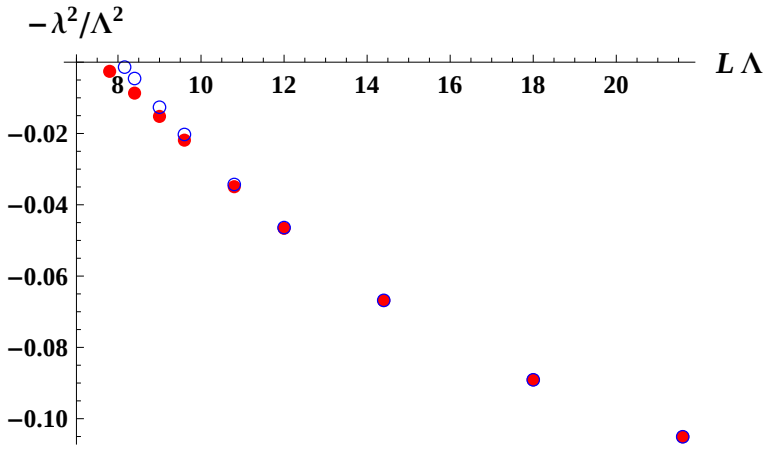

Figure 5.10: Symmetric (red disks) and antisymmetric (blue disks) pair eigenvalues for the supercritical case $\alpha = 2.5$

points can be fitted with the curves

$$-\lambda^2(L) = -\lambda_1^2\Lambda^2\big(1 + c_2 \arctan(c_3\Lambda\, L)\big),$$

where, for the first pair of eigenvalues, $-\lambda_1^2\Lambda^2 = -28.337$, is fitted by $c_2 = -1.115$ ($c_2 = -1.215$), $c_3 = 0.103$ ($d_3 = 0.115$) for the symmetric (antisymmetric) modes, while for the second pair plotted in figure 5.12 and 5.13, $-\lambda_1^2\Lambda^2 = -655.733$ the parameters of the fit are $c_2 = -1.1017$ ($s_2 = -1.198$), $c_3 = 0.489, 0.541$ respectively for the symmetric and antisymmetric modes. From the fits we can extract the values of the critical distances. They are given by $L^c_{s,1}\Lambda = 7.76$ and $L^c_{a,1}\Lambda = 8.09$ for the symmetric and antisymmetric modes of the first pair and by $L^c_{s,2}\Lambda = 1.59$ and $L^c_{a,2}\Lambda = 1.67$ for the symmetric and antisymmetric modes of the second

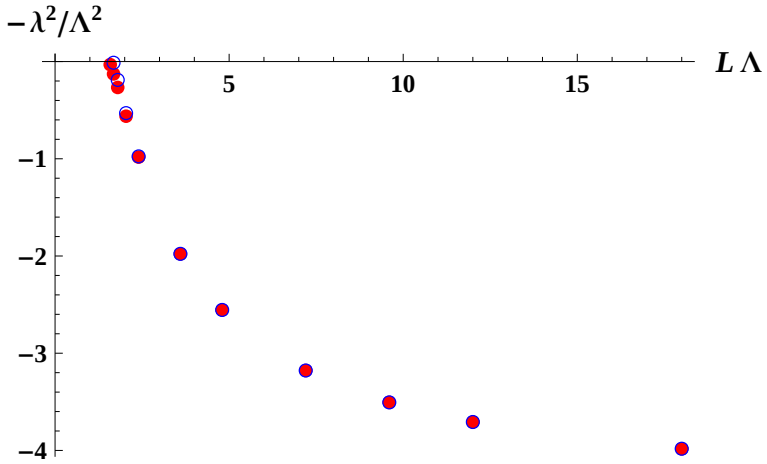

Figure 5.11: Symmetric (red disks) and antisymmetric (blue disks) pair eigenvalues for the subcritical case $\alpha = 2.5$

pair of eigenvalues. It is possible to see that the symmetric mode always reaches the zero level at larger distances. It is also interesting to check the relation obtained analytically in the toy model. The ratio between two successive eigenvalues of the one quark case, that are the limit value for infinite separation of two quarks, in the supercritical case is

$$\frac{\lambda^2_{n+1}}{\lambda^2_n} = \exp\left[\frac{2\pi\, i}{\nu}\right].$$

For the critical distance we find from the numerical stimations

$$\frac{L^c_{s,1}}{L^c_{s,2}} = 4.88 \quad \text{and} \quad \frac{L^c_{a,1}}{L^c_{a,2}} = 4.84,$$

that practically coincide with the value $\exp\left[\frac{2\pi\, i}{\nu}\right] \simeq 4.81$.
In figures 5.14, 5.15, 5.16 and 5.17 the symmetric and the antisymmetric unstable modes are shown. It is possible to notice the oscillations near the singularities.

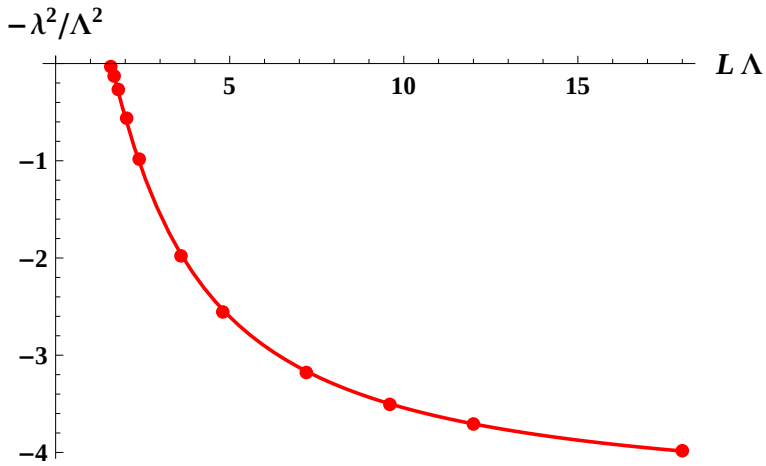

Figure 5.12: Fit of the symmetric mode by the curve $-\lambda^2(L) = -\lambda_1^2\Lambda^2\big(1 + c_2 \arctan(c_3\Lambda\, L)\big)$ with $c_2 = -1.115$ and $c_3 = 0.103$ for $\alpha = 2.5$

5.2. Analytic appoximation

Since the results of numerical simulations are very relevant for understanding the mechanism of confinement we would like to have an analytic understanding of the main effects. The behavior of the eigenvalues of the relevant operator are determined by two conditions, the exponential decay at infinity and the boundary conditions at the quark singularities. Once assumed that a normalizable solution at infinity exists, the possible eigenvalues will depend uniquely on the behavior of the solution near the singularities. As the boundary conditions are the same at both quarks, one can reduce to investigate the behavior of the solution near one of them. In the proximity of one quark the effect of the other can be approximated by a

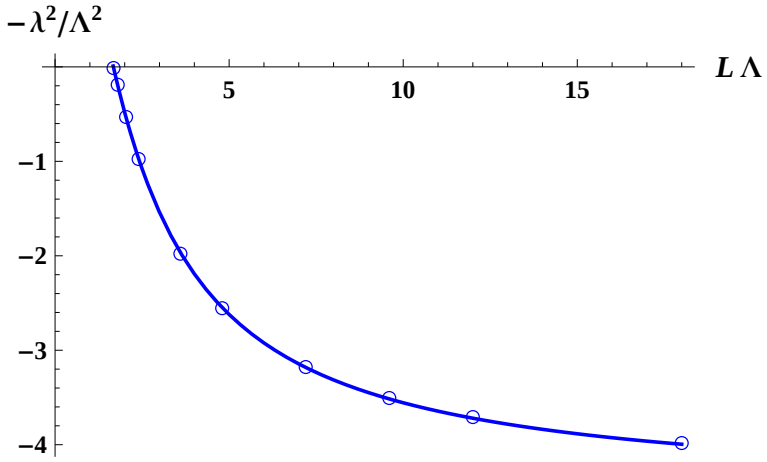

Figure 5.13: Fit of the anti-symmetric mode by the curve $-\lambda^2(L) = -\lambda_1^2\Lambda^2\big(1 + c_2 \arctan(c_3\Lambda\, L)\big)$ with $c_2 = -1.215$ and $c_3 = 0.115$ for $\alpha = 2.5$

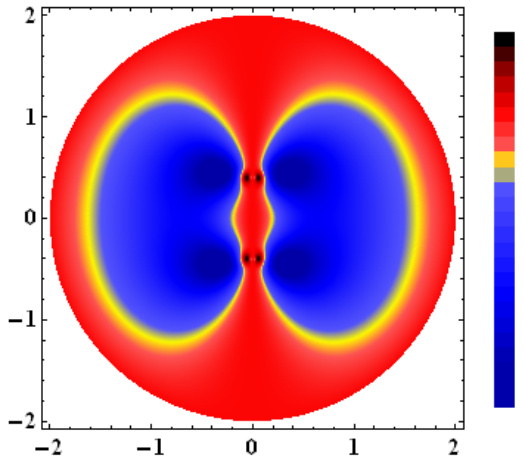

Figure 5.14: Density plot for the symmetric unstable mode at $\alpha = 2.5$

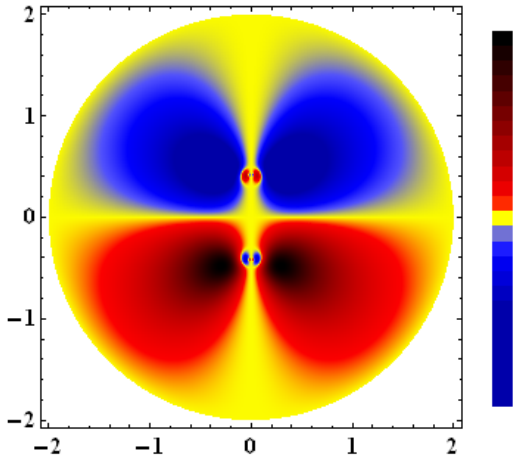

Figure 5.15: Density plot for the antisymmetric unstable mode at $\alpha = 2.5$

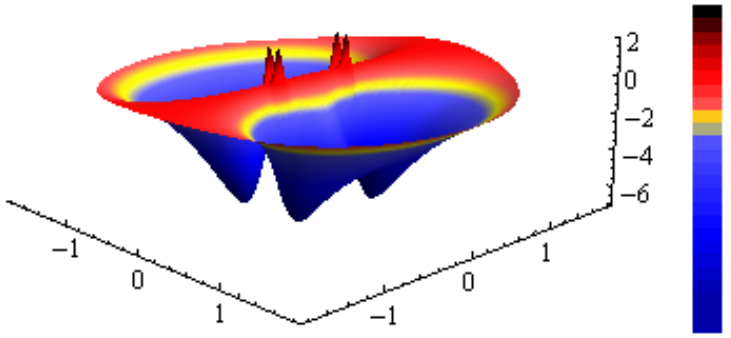

Figure 5.16: 3D plot for symmetric unstable mode at $\alpha = 2.5$

constant, so that the equation (5.5) reduce to

$$\left[-\frac{\partial^2}{\partial\,\rho^2} - \frac{\partial^2}{\partial\,w^2} + \frac{3}{4\rho^2} - \left(\frac{\alpha}{\sqrt{\rho^2+w^2}} - \frac{\alpha}{2L}\right)^2\right]\phi(\rho,z) = -\lambda^2\phi(\rho,z), \tag{5.13}$$

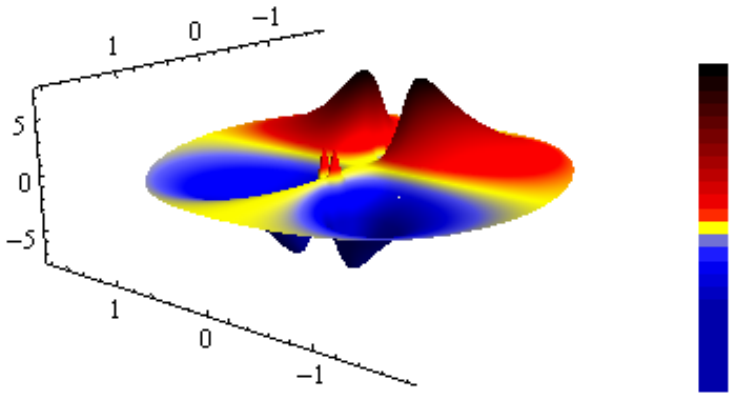

Figure 5.17: 3D plot for antisymmetric unstable mode at $\alpha = 2.5$

where $w = z \pm L$. This introduces a new via to analytically address the spectral problem. It is possible to understand the approximation also from another viewpoint: the standard procedure to find the eigenvalues is to find the a normalizable solution and then to expand it near the singularity in order to match the boundary condition. The strategy is to interchange these two steps, making first the expansion of the equation near the singularity, and taking the limit $\rho \to 0$ and $z \to \pm L$ without discarding any term, and then to find a solution of this simplified equation. In general it is possible to find an analytic solution of this simplified equation, on which the boundary condition can be imposed. In the intermediate regime $\frac{5}{4} < \alpha^2 \leq \frac{9}{4}$ and for $\alpha < 2L\lambda$ there is one real solution decaying at infinity, given in terms of Whittaker function:

$$\phi(\rho, w) = \frac{\rho^{\frac{3}{2}}}{\rho^2 + z^2} W\left(-\frac{\alpha}{\sqrt{4L^2\lambda^2 - \alpha^2}}, \nu, \frac{\sqrt{4L^2\lambda^2 - \alpha^2}}{L}\sqrt{\rho^2 + w^2}\right). \tag{5.14}$$

When the the real solution is concentrated near the quark, more this approximation is more reliable. The approximation is more accurate then for large eigenvalues. But even if when the eigenvalue start to increase and the

wave function spreads out of the quarks, near the quarks the exact solution and the approximate solution are very close. Using the expansion of the Whittaker near $\rho \simeq 0$ and $w \simeq 0$,

$$W \simeq \left(\left(\frac{\left(\frac{\sqrt{4L^2\lambda^2-\alpha^2}}{L}\right)^{\frac{1}{2}+\nu} \Gamma[-2\nu]}{\Gamma[\frac{1}{2}-\nu+\frac{\alpha^2}{\sqrt{4L^2\lambda^2-\alpha^2}}]} \right) r^{\nu} + \left(\frac{\left(\frac{\sqrt{4L^2\lambda^2-\alpha^2}}{L}\right)^{\frac{1}{2}-\nu} \Gamma[2\nu]}{\Gamma[\frac{1}{2}+\nu+\frac{\alpha^2}{\sqrt{4L^2\lambda^2-\alpha^2}}]} \right) r^{-\nu} \right)$$

where $r = \sqrt{\rho^2 + w^2}$, the boundary conditions reduce to:

$$\frac{\Gamma[1-2\nu]}{\Gamma[\frac{1}{2}-\nu+\frac{\alpha^2}{\sqrt{4L^2\lambda^2-\alpha^2}}]} - \frac{\Gamma[1+2\nu]}{\Gamma[\frac{1}{2}+\nu+\frac{\alpha^2}{\sqrt{4L^2\lambda^2-\alpha^2}}]} \left(\frac{L\Lambda}{\sqrt{4L^2\lambda^2-\alpha^2}} \right)^{2\nu} = 0 \tag{5.15}$$

The relation (5.15) define an implicit function for the eigenvalue in function of the separation. With this method there is just one solution, there is no difference between symmetric and antisymmetric eigenvalue for $\alpha < 2L\lambda$. This is in agreement with the fact that the split tends to zero for large separation. In figure 5.18 it is shown the perfect agreement between the numerical eigenvalues and the analytic curve obtained with the approximation, for $\alpha = 1.495$, in the subcritical regime, and in figure 5.19 the same for one couple of eigenvalues for $\alpha = 2.5$, in the supercritical regime.

From the implicit equation it is possible to see also that for $\frac{5}{4} < \alpha^2 < 2$ and $\Lambda \neq 0, \infty$, decreasing the separation, the eigenvalue becomes more and more negative.

To find out the critical distance L_c where the unstable modes disappear it is necessary to go beyond $\alpha = 2L\lambda$. For $\alpha > 2L\lambda$ the solution 5.14 becomes complex and there are two independent real solutions matching the physical boundary conditions. This is in agreement with the exact solution of the negative eigenvalue problem, where there are two different solutions: one which is parity symmetric and the other which is antisymmetric. The corresponding eigenvalues are slightly different, being the lowest the symmetric mode which is leading the instability. For $\frac{5}{4} < \alpha^2 \leq \frac{9}{4}$, the

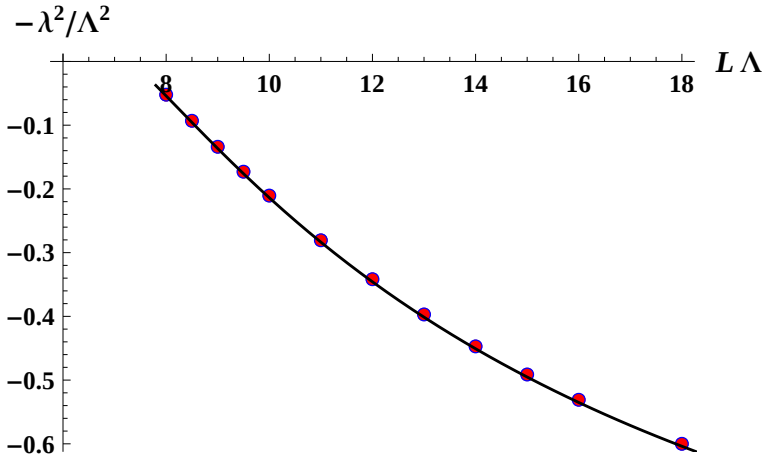

Figure 5.18: Blue disk: symmetric mode, red circle: antisymmetric mode, black line: approximated curve, for $\alpha = 1.495$

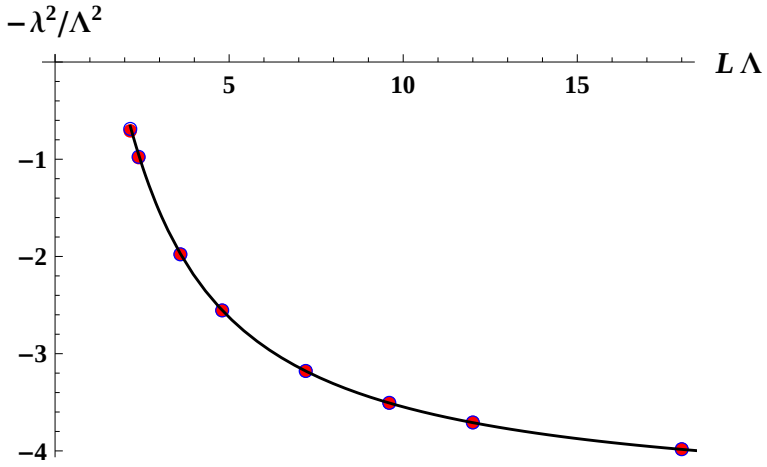

Figure 5.19: Blue disk: symmetric mode, red circle: antisymmetric mode, black line: approximated curve, for $\alpha = 2.5$

approximate real solution corresponding to the exact symmetric solution is

$$\phi(\rho,w)=\frac{\rho^{\frac{3}{2}}}{\rho^2+z^2}Im\left[W\left(-\frac{\alpha}{\sqrt{4L^2\lambda^2-\alpha^2}},\nu,\frac{\sqrt{4L^2\lambda^2-\alpha^2}}{L}\sqrt{\rho^2+w^2}\right)\right], \tag{5.16}$$

and the other one corresponding to the antisymmetric solutions is

$$\phi(\rho,w)=\frac{\rho^{\frac{3}{2}}}{\rho^2+z^2}Re\left[W\left(-\frac{\alpha}{\sqrt{4L^2\lambda^2-\alpha^2}},\nu,\frac{\sqrt{4L^2\lambda^2-\alpha^2}}{L}\sqrt{\rho^2+w^2}\right)\right]. \tag{5.17}$$

The approximate critical distance can be obtained setting $\lambda=0$ in the previous formula (5.16) and (5.17):

$$\phi(\rho,w)=\frac{\rho^{\frac{3}{2}}}{\rho^2+z^2}Im\left[W\left(i\alpha,\nu,\frac{i\alpha}{L}\sqrt{\rho^2+w^2}\right)\right], \tag{5.18}$$

and

$$\phi(\rho,w)=\frac{\rho^{\frac{3}{2}}}{\rho^2+z^2}Re\left[W\left(i\alpha,\nu,\frac{i\alpha}{L}\sqrt{\rho^2+w^2}\right)\right]. \tag{5.19}$$

We find the symmetric and antisymmetric zero mode of (5.13) and imposing the boundary conditions on (5.18) and (5.19). The boundary conditions are satisfied for

$$\tilde{L}_s^c=\frac{\alpha}{\Lambda}\left(\frac{\Gamma(1-2\nu)Im\left[\frac{i^{\frac{1}{2}+\nu}}{\Gamma\left(-i\alpha-\nu+\frac{1}{2}\right)}\right]}{\Gamma(1+2\nu)Im\left[\frac{i^{\frac{1}{2}}(-i)^{\nu}}{\Gamma\left(-i\alpha+\nu+\frac{1}{2}\right)}\right]}\right)^{\frac{1}{2\nu}} \tag{5.20}$$

and

$$\tilde{L}_a^c=\frac{\alpha}{\Lambda}\left(\frac{\Gamma(1-2\nu)Re\left[\frac{i^{\frac{1}{2}+\nu}}{\Gamma\left(-i\alpha-\nu+\frac{1}{2}\right)}\right]}{\Gamma(1+2\nu)Re\left[\frac{i^{\frac{1}{2}}(-i)^{\nu}}{\Gamma\left(-i\alpha+\nu+\frac{1}{2}\right)}\right]}\right)^{\frac{1}{2\nu}} \tag{5.21}$$

In particular, for $\alpha=1.495$ we get $\Lambda\tilde{L}_s^c=7.28$ and $\Lambda\tilde{L}_a^c=7.31$, while for $\alpha=1.42$, it is $\Lambda\tilde{L}_s^c=67.550$ and $\Lambda\tilde{L}_a^c=67.555$ in perfect agreement with

the numerical critical distance founded before (respectively $\Lambda L_s^c = 7.38$, $\Lambda L_a^c = 7.40$ and $L_s^c\Lambda = 67.687$ $L_a^c\Lambda = 67.689$)

Notice that $\tilde{L}_s^c < \tilde{L}_a^c$ but the difference can not be appreciated: in Figure 5.20 it we display the dependence of the approximated symmetric critical distance on the coupling constant in the interval $2 < \alpha^2 \leq \frac{9}{4}$. We

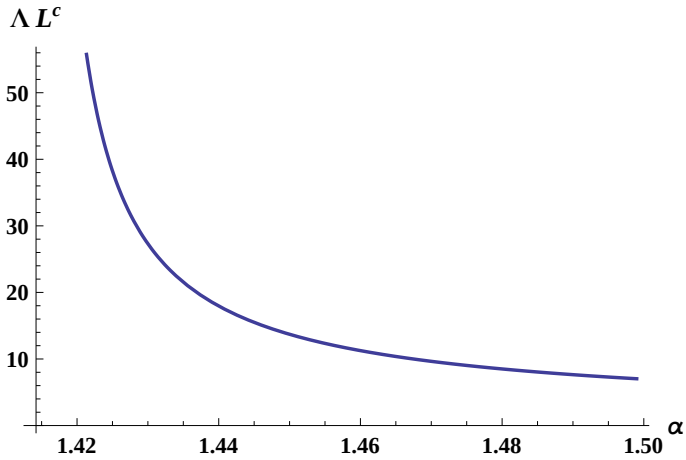

Figure 5.20: α-dependence of the approximated symmetric critical distance in the subcritical regime

can see that the critical distance can reach very large values as $\alpha \to \sqrt{2}$, in agreement with the absence of negative modes for $\alpha \leq \sqrt{2}$.

Coulomb regime instability

In summary, the study of gluonic instabilities in the case of a heavy quark-antiquark pair background, lead us to a remarkable effects in a very interesting intermediate regime for the coupling constant, $2 < \alpha^2 \leq \frac{9}{4}$. In this regime, due to the breaking of the conformal invariance by the renormalization of the singularities of the potential, there exists a critical distance L_c between the $q - \bar{q}$ pairs. For larger distances there are two unstable modes, one parity symmetric and one parity antisymmetric respect

the z axis. Each of these modes are double degenerated. In fact, as in the one quark case, because of the reality condition of gauge fields, there is one real unstable mode proportional to T^1 and another one proportional to T^2. For large distances the symmetric and antisymmetric eigenvalues become degenerate and converge to the value of the single negative eigenvalue of the single quark case. By reducing the distance between the quarks, the eigenvalues start to grow, until they cross the zero value at a critical distance and then they become positive. The symmetric eigenvalue is always more negative than the antisymmetric one and than it becomes zero to a shorter distance, so it is the one which marks the instability.

The situation is better understood from the opposite point of view: one can think to start with a very small $q - \bar{q}$ pair where the quarks are so close that there are not unstable modes. In this case the Coulomb regime is consistent and stable. Moving away the quarks, at a very particular distance, the symmetric double degenerate unstable mode appears. In this case, due to the change of the integration path according the saddle point evaluation, the partition function acquires a factor of $i^2 = -1$, that give rise to a complex free energy. This is a signal of the instability of the Coulomb solution. In fact at short distances the Coulomb phase is stable, the quarks interact via Coulomb interaction which leads to asymptotic freedom, but trying to separate the pair, crossing the critical distance, the expansion around the Coulomb background is no more valid. The interaction between the quarks will be different, opening the possibility of a confining behavior: the system is leaving the domain of asymptotic freedom and enter into the realm of confinement.

The critical distance for $\alpha = \sqrt{2}$ is infinite, while starting from $\alpha = \frac{3}{2}$ is zero, as for every separation, there are infinite negative unstable modes, which means that the Coulomb phase is unstable for any separation of the pair. This is compatible with the fact that the theory is confining in the strong coupling expansion. The dependence of the critical distance is then in agreement with the interpretation of the intermediate regime as interpolating between the asymptotic freedom of small coupling constant and the confinement of large coupling constant.

The transition from the asymptotic regime to a presumable confining

regime for intermediate values of the strong coupling constant is a strong indication that QCD smoothly interpolates from an asymptotic freedom regime to a confinement regime. The mere existence of a finite region of couplings $\alpha \in (\sqrt{2}, \frac{3}{2}]$, where the transition occurs for a given value of the α coupling, just by changing the separation between the two quarks, implies that the transition between the two regimes does not involves a critical phase transition. There is not a sharp separation at a given a coupling between two different regimes. There is a simple crossover. This is the first indication derived from first principles that QCD does not undergo a phase transition at intermediate energy scales.

A very interesting property of the symmetric mode, which is the lowest unstable mode, the one that it marks the change between stability and instability, is that it exhibits a thick string connecting the two quarks, supporting a picture of QCD where confinement is induced by thick strings rather than by fundamental strings.

The instabilities dues to negative modes of gluon fluctuations on a heavy meson background just means that the expansion around a Coulomb background is not consistent for intermediate values of the coupling constant at large distances. However, the functional integral is well defined. The pathology only means that the Coulomb saddle point is not relevant. The real physical problem is that the unstable modes do not point out to gauge field backgrounds where to find relevant saddle point configurations. Usually, in fact, the unstable modes get stabilized by higher order fluctuation self-interactions. In that case the non-perturbative contribution of these modes would give rise to a linearly growing effective potential which would provide an evidence for confinement. But in this case the peculiar form of the unstable modes (5.4) implies that

$$[\tau_\nu, \tau\mu] = 0,$$

which means that the quadratic approximation is exact, and stability cannot be restored by higher order terms in the usual way. For these reasons, whether or not the instability means that at larger distances the theory is confining is unclear and remains as an open problem.

6

Light quark instabilities

The critical value of coupling constant, $\alpha_c = \sqrt{2}$ where the gluon instabilities arise is larger than Gribov's critical value, $\alpha_c = 3\pi(1 - \sqrt{2/3})/4 \simeq 0.43$. In the Gribov scenario of confinement a fundamental role is played by light quarks in destabilization of the Coulomb phase. In simple terms, the Coulomb phase instability would imply a vacuum decay into light quark-antiquark pairs. In order to derive this picture from first principles one has to consider dynamical quarks with small masses. In this chapter we analyze the source of possible instabilities coming from the fermionic sector of the action. The contribution of dynamical quarks to vacuum energy is given by the determinant of Dirac operator $i\not{D} + m$:

$$Z = \int DA \, \exp[-S_E^{YM}(A) - S_E^Y(A)] \det\left(i\not{D} + m\right).$$

The operator $i\not{D} + m$ is not selfadjoint because it is the sum of an anti-selfadjoint operator $i\not{D}$ and a selfadjoint one m. Thus, all eigenvalues are of the of the form $i\lambda + m$ with λ real. Now, since $i\not{D}$ anticommutes with

γ_5, i.e. $\{\gamma^\mu, \gamma^5\} = 0$, for any eigenvalue $i\lambda$ of $i\not{D}$ there is another one of the form $-i\lambda$. Therefore, the fermionic determinant can be expressed as

$$\det(i\not{D} + m) = \prod_\lambda (i\lambda + m)(-i\lambda + m) = \prod_\lambda (\lambda^2 + m^2) > 0,$$

which is strictly positive. In the saddle point approximation, including one loop corrections, the partition function is given by

$$Z^{(1)} = \exp[-S_0] \det\left(\delta^{(2)} S_E^{YM}\right)^{-\frac{1}{2}} \det\left(i\not{D}_c + m\right),$$

where $A_\mu^c = i\Phi(\mathbf{x})\delta_{\mu 0} T^3$, $\Phi(\mathbf{x})$ being the Coulomb potential generated by the external heavy quarks, and $\not{D}_c$ denotes the covariant derivative in a Coulomb background

$$\not{D}_c = \gamma_\mu(\partial_\mu + iA_\mu^0). \tag{6.1}$$

The imaginary Coulomb background might break the stability properties. In fact some eigenvalues $i\lambda$ can become real, implying that the Coulomb phase would become unstable when $i\lambda = -m$. This would introduce a new source of vacuum instability generated by the fluctuations of the dynamical quarks. The root of possible instabilities are the singularities of Coulomb potentials which require the introduction of consistent boundary conditions, similar to those introduced in chapter 2 for graphene.

6.1. Quarks instabilities in a Coulomb heavy quark background

Let us multiply the Dirac operator in Coulomb background by$i\gamma_0$ on the left, i.e.

$$i\gamma_0(i\not{D}_c + m) \tag{6.2}$$

Notice that the only color dependent term of the operator $\not{D}_c$ is the Coulomb potential term. Stationary spinor eigenvalues of the operator (6.2) are of the form

$$\Psi = (\Psi_+(\mathbf{x}), \Psi_-(\mathbf{x}))e^{iEx_0},$$

where the two $SU(2)$ color components of $\Psi_{\pm}(\mathbf{x})$ satisfy the following equations

$$iE\Psi_{\pm}(\mathbf{x}) + \left(\pm\frac{\Phi(r)}{2} - \gamma^0\gamma^i\partial_i + m\, i\gamma_0\right)\Psi_{\pm}(\mathbf{x}) = 0.$$

Since the operator within the brackets is hermitian with real eigenvalues η, considering both positive and negative energies we get

$$\det\left(i\gamma_0(i\not{D}_c + m)\right) = \prod_{\eta}(iE+\eta)(-iE+\eta) = (E^2+\eta^2) > 0,$$

unless $E = \eta = 0$. Due to the identity

$$\det(i\gamma_0)\det(i\not{D}_c + m) = \det\left(i\gamma_0(i\not{D}_c + m)\right),$$

it follows that $\det(i\not{D}_c + m)$ is well defined (not imaginary nor negative). The only possible pathologies can occur when $E = \eta = 0$, i.e. when there is a zero mode of the Dirac operator $\left(i\gamma_0(i\not{D}_c + m)\right)$. Let us consider only the second color $\Psi_{-}(\mathbf{x})$ component of the spinor Ψ and omit the color subindex to simplify the notation. A parallel analysis of the other component will give similar results. The zero modes are then solutions of the

$$\left(-i\gamma^0_M\gamma^i\partial_i - \frac{\Phi(r)}{2} + m\gamma^0\right)\Psi = H_c\Psi = 0, \tag{6.3}$$

where we reintroduce the Minkowski $\gamma^0_M = -i\gamma^0$ matrix, to show that the zero mode problem is reduced to find out the zero-modes of the Dirac Hamiltonian H_c with Coulomb potential in Minkowski space-time. Then, the techniques used to find the Dirac spectrum in the graphene can reintroduced. However, we know that the Hydrogen spectrum does not have zero energy bound states, but in the strong coupling regime when we need to introduce extra the boundary condition around the Coulomb singularities it can be possible.

Let us consider the case of a single heavy quark. Then, $\Phi(r) = \frac{\alpha}{r}$. Because to the spherical symmetry the total angular momentum and the parity operators commute with the Hamiltonian. To built such a eigenstates

of definite energy we can use the appropriate combinations of states with definite angular momentum and spin. A stationary Dirac spinor can be defined in terms of spherical spinors $\Omega^j_{l\,m_j}$ from the following ansatz

$$\Psi_{jm} = \begin{pmatrix} G_j(r)\Omega^j_{l\,m_j} \\ iF_j(r)\Omega^j_{l'\,m_j}, \end{pmatrix} \tag{6.4}$$

with $l' = 2j - l$: $l' = l + 1$ for $j = l + \frac{1}{2}$ and $l' = l - 1$ for $j = l - \frac{1}{2}$. Explicitly:

$$\Omega^{l+\frac{1}{2}}_{l\,m_j} = \frac{1}{\sqrt{2j}} \begin{pmatrix} \sqrt{j+m_j}\; Y^l_{m_j-\frac{1}{2}} \\ \sqrt{j-m_j}\; Y^l_{m_j+\frac{1}{2}} \end{pmatrix}, \tag{6.5}$$

for $j = l + \frac{1}{2}$ and

$$\Omega^{l-\frac{1}{2}}_{l\,m_j} = \frac{1}{\sqrt{2j+2}} \begin{pmatrix} -\sqrt{j+1-m_j}\; Y^l_{m_j-\frac{1}{2}} \\ \sqrt{j+1+m_j}\; Y^l_{m_j+\frac{1}{2}} \end{pmatrix}, \tag{6.6}$$

for $j = l - \frac{1}{2}$. Let us introduce the orbital angular momentum $\mathbf{L} = -i\hat{\mathbf{r}} \times \boldsymbol{\nabla}$ and spin-orbit $\mathbf{K} = \mathbb{I} + \boldsymbol{\sigma} \cdot \mathbf{L}$ operators. Now using the following relations

$$\boldsymbol{\sigma} \cdot \hat{\mathbf{r}}\, \Omega^j_{j\pm\frac{1}{2}\,m_j} = -\Omega^j_{j\mp\frac{1}{2}\,m_j}, \tag{6.7}$$

and

$$(2 + \mathbf{L}\cdot\boldsymbol{\sigma})\Omega^j_{l\,m_j} = (1-k)\Omega^j_{l\,m_j} \qquad (2 + \mathbf{L}\cdot\boldsymbol{\sigma})\Omega^j_{l'\,m_j} = (1+k)\Omega^j_{l'\,m_j} \tag{6.8}$$

where $k = \mp(j + \frac{1}{2})$ for $j = l \pm \frac{1}{2}$ it is possible to show that

$$\sigma^i \partial_i \left(G(r)\Omega^j_{l\,m_j} \right) = -\Omega^j_{l'\,m_j} \left(\frac{d}{dr} + \frac{k+1}{r} \right) G(r), \tag{6.9}$$

and

$$\sigma^i \partial_i \left(F(r)\Omega^j_{l'\,m_j} \right) = -\Omega^j_{l\,m_j} \left(\frac{d}{dr} - \frac{k-1}{r} \right) F(r). \tag{6.10}$$

From (6.3) we find a relation between $G(r)$ and $F(r)$

$$G'(r) + \frac{1+k}{r}G(r) - \Big(\frac{\alpha}{2r} + m\Big)F(r) = 0 \tag{6.11}$$

$$F'(r) + \frac{1-k}{r}F(r) + \Big(\frac{\alpha}{2r} - m\Big)F(r) = 0, \tag{6.12}$$

where we omitted the index j for simplicity.

Self adjoint Boundary conditions

Because the UV singularities introduced by the external quarks in the Dirac Hamiltonian H_c operator defined in (6.3), we have to introduce boundary conditions that the dynamical quark fields have to satisfy at the singularities. To obtain a well defined self adjoint operator Dirac operator we have to follow the steps carried out in the two dimensional case of chapter 2. First we introduce an spherical cut-off of radius r_0 around each singularity. Let us assume that the quark is located at the origin. The most general boundary condition is given by a unitary operator $U(\mathbf{r_0})$ defined on the S^2 cut-off sphere of radius r_0

$$(1 + \hat{\not{n}})\Psi(r_0) = U(\mathbf{r_0})\gamma_0(1 - \hat{\not{n}})\Psi(r_0),$$

where $\hat{\not{n}} = \mathbf{r_0}/r_0$ is the unit normal vector to the cut-off boundary S^2 sphere. If the boundary condition has to preserve rotation invariance $U(\mathbf{r_0})$ has to be an infinite diagonal matrix of $U(1)$ phases in the angular momentum decomposition of the boundary spinor space, i.e.

$$(1 + \hat{\not{n}})\Psi_j(r_0) = \mathrm{e}^{i\beta_j^0}\gamma_0(1 - \hat{\not{n}})\Psi(r_0). \tag{6.13}$$

Now, to define the ultraviolet limit by removal of the cut-off r_0 we follow the the same prescription as in chapter 2. First we analyze the asymptotic zero modes of Dirac Hamiltonian H_c. Depending on the strength of the coupling constant α we have three different regimes.

Case I) $\alpha^2 < 2(j+\frac{1}{2})^2 - 1$

For $\alpha^2 < 4(j+\frac{1}{2})^2 - 1$ there is just one asymptotic zero mode given by

$$\begin{aligned} G_0(r) &= C_+\, r^{-1+\nu} \\ F_0(r) &= r^{-1+\nu} \end{aligned} \tag{6.14}$$

with $C_+ = \frac{2(k-\nu)}{\alpha}$ and $\nu = \sqrt{k^2 - \frac{\alpha^2}{4}}$.

Case II) $\alpha^2 > 4(j+\frac{1}{2})^2 - 1$, $\alpha^2 \neq 4(j+\frac{1}{2})^2$

In this case there is a family of asymptotic zero modes parameterized by Λ with the dimension of the inverse of the distance [1]

$$\begin{aligned} G_0(r) &= C_+\,(\Lambda r)^{-1+\nu} \pm C_+\,(\Lambda r)^{-1-\nu} \\ F_0(r) &= (\Lambda r)^{-1+\nu} \pm (\Lambda r)^{-1-\nu} \end{aligned} \tag{6.15}$$

$C_\pm = \frac{2(k\mp\nu)}{\alpha}$ and $\nu = \sqrt{k^2 - \frac{\alpha^2}{4}}$.

Case III) $\alpha^2 = 4(j+\frac{1}{2})^2$

In that case

$$\begin{aligned} G_0(r) &= r^{-1}\frac{k}{|k|}\left(1 \pm \left(\log(\Lambda r) - \frac{1}{k}\right)\right) \\ F_0(r) &= r^{-1}\Big(1 \pm \log(\Lambda r)\Big). \end{aligned} \tag{6.16}$$

In the case I the existence of only one asymptotic zero-mode implies that the operator H_c is essentially selfadjoint and we do not need to impose an extra boundary condition. In fact, in this case the spectrum coincide

[1] In fact there are more posibilities if $\alpha^2 > 4(j+\frac{1}{2})^2 - 1$ because we can introduce a complex phase $e^{i\theta}$ instead of $\pm$ sign flip as we considered in the graphene case of chapter 2. Here we assume that $\theta = n\pi$ for simplicity and then we allows to merge the cases II and IV of chapter 2

with the Hydrogen one, where we already know that there are not solution with zero energy. Thus, the Coulomb phase is stable under light quark fluctuation in this regime.

In the other two case we need to remove the cut-off, sending r_0 to zero. We follow the RG flow shown by the asymptotic zero modes. We can associate a zero mode to the boundary condition defined by β_j^0 in (6.13) by means of the relation

$$e^{i\,\beta_j^0} = \frac{F_0^j(\,r_0) + iG_0^j(\,r_0)}{F_0^j(\,r_0) - iG_0^j(\,r_0)}. \tag{6.17}$$

If we consider a smaller cut-off $r_\epsilon < r_0$ we can use boundary condition which is given by a running phase β_ϵ^j defined following the flow of zero mode (F_0^j, G_0^j) associated to the initial phase β_0^j at r_0 by the relations (6.17),

$$e^{i\,\beta_\epsilon^j} = \frac{F_0^j(\,r_\epsilon) + iG_0^j(\,r_\epsilon)}{F_0^j(\,r_\epsilon) - iG_0^j(\,r_\epsilon)}. \tag{6.18}$$

More explicitly, we define the boundary condition by the following relation

$$\lim_{r\to 0}\Big(F^j(r)G_0^j(r) - G^j(r)F_0^j(r)\Big) = 0, \tag{6.19}$$

derived from (6.17) and (6.17).

Once that we have fixed the boundary conditions which ensure that H_c is a selfadjoint operator we can search for zero modes on its spectrum.

The existence of non trivial boundary conditions might make possible of normalizable zero modes in the regime $\alpha^2 > 4(j+\frac{1}{2})^2 - 1$ of (6.11) and (6.12), for very special values of the parameter Λ labeling the boundary condition. Let us introduce a new variable $x = 2mr$ and following ansatz

$$\begin{aligned} G(x) &= \frac{1}{r}\exp\Big[-\frac{x}{2}\Big]\Big(\phi_1(x) + \phi_2(x)\Big), \\ F(x) &= \frac{1}{r}\exp\Big[-\frac{x}{2}\Big]\Big(\phi_1(x) - \phi_2(x)\Big). \end{aligned} \tag{6.20}$$

This allows to decouple the two equations and give rise to a second order equation for $\phi_1(x)$

$$\phi_1''(x) + \left(\frac{1}{x} - 1\right)\phi_1'(x) + \left(\frac{\alpha^2 - 4k^2}{4x^2} - \frac{1}{x}\right)\phi_1(x) = 0$$

and a constrain for $\phi_2(x)$ in terms of $\phi_1(x)$:

$$\phi_2(x) = \frac{2x}{\alpha + 2k}\big(\phi_1(x) - \phi_1'(x)\big).$$

Let us fix the total angular momentum to its lower value $j = \frac{1}{2}$, so that $k = \pm 1$ There localize solutions in terms of the Hypergeometric function U:

$$\begin{aligned} \phi_1(x) &= x^\nu\, U(1+\nu, 1+2\nu, x), \\ \phi_2(x) &= \frac{2}{\alpha + 2k}\, x^\nu\, U(\nu, 1+2\nu, x), \end{aligned}$$

Using the asymptotic expansion of the Hypergeometric function for $x \simeq 0$:

$$x^\nu\, U(1+\nu, 1+2\nu, x) \simeq \frac{\Gamma[-2\nu]}{\Gamma[1-\nu]}x^\nu + \frac{\Gamma[2\nu]}{\Gamma[1+\nu]}x^\nu$$

$$x^\nu\, U(\nu, 1+2\nu, x) \simeq \frac{\Gamma[-2\nu]}{\Gamma[-\nu]}x^\nu + \frac{\Gamma[2\nu]}{\Gamma[\nu]}x^{-\nu},$$

it is easy to show that in the regime II for $3 < \alpha^2 < 4$ the solution matches the boundary conditions only for one value of Λ

$$\Lambda_c = \frac{m}{2}\left(\pm\frac{(\alpha + 2\nu + k)\Gamma[\frac{1}{2} - \nu]}{(\alpha - 2\nu + k)\Gamma[\frac{1}{2} + \nu]}\right)^{\frac{1}{2\nu}},$$

for $k = \pm 1$, respectively. In n the regime III ($\alpha^2 = 4$) there is only on solution for $k = 1$ and

$$\Lambda_c = 2m\, e^{-\frac{1}{2} + \gamma}.$$

Finally, for $\alpha^2 > 4$ in the regime II there is an infinity discrete series of values of Λ

$$\Lambda_c^n = \frac{m}{2}\left(\pm\frac{(\alpha+2\nu+k)\Gamma[\frac{1}{2}-\nu]}{(\alpha-2\nu+k)\Gamma[\frac{1}{2}+\nu]}\right)^{\frac{1}{2\nu}} \exp\left[\frac{\pi i}{\nu}n\right],$$

with $n = 0, \pm1, \pm2, \ldots$ and both signs of $k = \pm1$.

The light quark fluctuations only make Coulomb regime is only unstable on this cases and for those particular boundary conditions. For any types of the boundary conditions parameter the Coulomb background of one heavy quark is stable under dynamical quark fluctuations. However, as pointed out above, one quark background does not correspond to a physical quantum state because global gauge invariance is not preserved in such a background. For this reason we shall consider next a more realistic background of a pair of heavy quark antiquark.

6.2. Quarks instabilities in heavy quark-antiquark background

In the Coulomb background generated by a quark and antiquark, the potential in the operator (6.3) becomes, according (3.2):

$$\Phi = \alpha\left(\frac{1}{|\mathbf{x}+\mathbf{L}|} - \frac{1}{|\mathbf{x}-\mathbf{L}|}\right),$$

with $\mathbf{L} = (0, 0, L)$. The search of instabilities is reduced to find solutions zero modes of the Dirac Hamiltonian (6.3) in such a background. Even if they cannot be found analytically there is an analytic argument which shows the existence of these zero-modes. As in the case of gluon fluctuations a good approximation of the spectral problem is to reduce, in a neighborhood of one quark ($\rho \simeq 0, z \simeq \pm L$), the effect of the other to a constant, so the background potential becomes:

$$\Phi = \alpha\left(\frac{1}{\sqrt{\rho^2+w^2}} - \frac{1}{2L}\right), \tag{6.21}$$

where $w = z \pm L$. Equation (6.3) than becomes:

$$\left(-i\gamma^0\gamma^i\partial_i - \frac{\alpha}{2r} + \frac{\alpha}{4L} + m\gamma^0\right)\Psi = 0,$$

which is equivalent to the problem of finding a bound state with energy $E = -\frac{\alpha}{4L}$ of the Dirac equation in a Coulomb potential with $\alpha' = \frac{\alpha}{2}$. Again, we know that such a negative energy solutions do not exist in the hydrogen atom spectrum, but the existence of new types of boundary conditions opens new posibilities.

Using the same techniques as in the one quark backgrounds we can start with the same ansatz for the spinors (6.4). A similar analysis, leads to the following equations for $G(r)$ and $F(r)$

$$G'(r) + \frac{1+k}{r}G(r) - \left(\frac{\alpha}{2r} - \frac{\alpha}{4L} + m\right)F(r) = 0 \tag{6.22}$$

$$F'(r) + \frac{1-k}{r}F(r) + \left(\frac{\alpha}{2r} - \frac{\alpha}{4L} - m\right)F(r) = 0. \tag{6.23}$$

The singularity at $r = 0$ is renormalized with the self adjoint boundary condition (**??**), where $G_0(r)$ and $F_0(r)$ are the asymptotic zero modes obtained by neglecting the non diverging terms of (6.22) and (6.23). In fact, they are the same as those of one quark background (6.14), (6.15) and (6.16). This is nice because the structure of the quarks should not be dependent on how many other quarks are in the space.

The interesting observation is that since now we have a new scale given by the distance between the quarks $2L$ it might be possible that for any boundary condition one can find a critical distance where the Dirac Hamiltonian present a zero mode. In the regime I ($\alpha^2 \leq 2(j+\frac{1}{2})^2 - 1$) this is impossible, as the problem is equivalent to find bound states with negative energies of the hydrogen spectrum. The search of bound states with negative energies must be then focused to the regimes II and III for $\alpha^2 > 2(j+\frac{1}{2})^2 - 1$. Again we introduce the change of variable $x = 2\epsilon r$, $\epsilon = \sqrt{m^2 - \frac{\alpha^2}{16L^2}}$ and

the following ansatz

$$\begin{aligned} G(x) &= \sqrt{m-\frac{\alpha}{4L}}\,\frac{e^{-\frac{x}{2}}}{r}\Big(\phi_1(x)+\phi_2(x)\Big), \\ F(x) &= \sqrt{m+\frac{\alpha}{4L}}\,\frac{e^{-\frac{x}{2}}}{r}\Big(\phi_1(x)-\phi_2(x)\Big). \end{aligned} \tag{6.24}$$

Again $\phi_1(x)$ has to be a solution of a second order differential equation

$$\phi_1''(x)+\left(\frac{1}{x}-1\right)\phi_1'(x)+\left(\frac{\alpha^2}{4x^2}-\frac{\alpha^2}{8L\epsilon x}-\frac{k^2}{x^2}-\frac{1}{x}\right)\phi_1(x)=0,$$

and $\phi_2(x)$ can be given in terms of $\phi_(x)$ by

$$\phi_2(x)=\frac{(\alpha^2+8L\epsilon x)\phi_1(x)-8L\epsilon x\phi_1'(x)}{4\alpha Lm+8kL\epsilon}.$$

Normalizable solutions are given in terms of the Hypergeometric function U:

$$\phi_1(x)=\left(k+\frac{m\alpha}{2\epsilon}\right)x^\nu\,U\left(\frac{\alpha^2}{4L\epsilon}+1+\nu,1+2\nu,x\right)$$

and

$$\phi_2(x)=x^\nu\,U\left(\frac{\alpha^2}{4L\epsilon}+\nu,1+2\nu,x\right)$$

with $\nu=\sqrt{k^2-\alpha^2}$, and were we have fixed the total angular momentum $j=\frac{1}{2}$ and the parity $k=-1$. Using the asymptotic expansion of the Hypergeometric function for $x\simeq 0$:

$$x^\nu\,U(1+\nu,1+2\nu,x)\simeq\frac{\Gamma[-2\nu]}{\Gamma[1+\frac{\alpha^2}{4\epsilon L}-\nu]}x^\nu+\frac{\Gamma[2\nu]}{\Gamma[1+\frac{\alpha^2}{4\epsilon L}+\nu]}x^\nu$$

$$x^\nu\,U(\nu,1+2\nu,x)\simeq\frac{\Gamma[\frac{\alpha^2}{4\epsilon L}-2\nu]}{\Gamma[-\nu]}x^\nu+\frac{\Gamma[\frac{\alpha^2}{4\epsilon L}+2\nu]}{\Gamma[\nu]}x^{-\nu},$$

it is possible to see that the boundary conditions for the regime II ($\alpha^2 > 2(j+\frac{1}{2})^2 - 1$) reducee to

$$\frac{\left(\alpha^2 - 4\alpha L m + 2\varsigma(1-\nu)\right)\Gamma[-2\nu]\Gamma[1+\frac{\alpha^2}{2\varsigma}+\nu]}{\left(\alpha^2 - 4\alpha L m + 2\varsigma(1+\nu)\right)\Gamma[2\nu]\Gamma[1+\frac{\alpha^2}{2\varsigma}-\nu]} = -\left(\frac{2\epsilon L^c}{\varsigma}\right)^{2\nu}$$

with $\varsigma = \sqrt{16m^2L_c^2 - \alpha^2}$. Indeed, for each value of the parameter the boundary condition Λ there is a critical distance that satisfies the boundary condition (see Fig. 6.1 for the charge $\alpha = 1.8$). For that particular

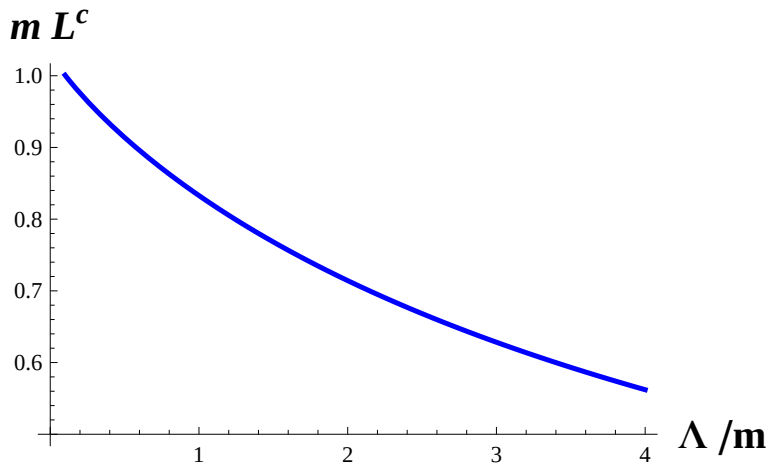

Figure 6.1: Dependence of the critical distance L^c on the boundary conditions scale Λ for $\alpha = 1.8$

separation L_c of the two quarks the fermionic determinant vanishes. The vanishing of the fermionic determinant is induced by the spectral flow of eingenvalues of the Dirac operator. It occurs when one eigenvalue with negative energy crosses the zero level at the critical distance. This phenomenon reflects the vacuum instability associated to a quark-antiquark pair creation induced by a zero energy level crossing which generates both a hole in the Dirac see and a positive energy quark state.

The value of the critical distance L_c where the phenomenon occurs decreases with Λ. Notice that for very short distances the approximation (6.21) is not longer valid because $m^2 - \frac{\alpha^2}{16L^2}$ must be positive. The critical distance also depends on the value of the coupling constant a (Fig. 6.2). When the coupling increases the critical distance decreases, which is consistent with the fact in that in the strong regime the theory is confining for all distances.

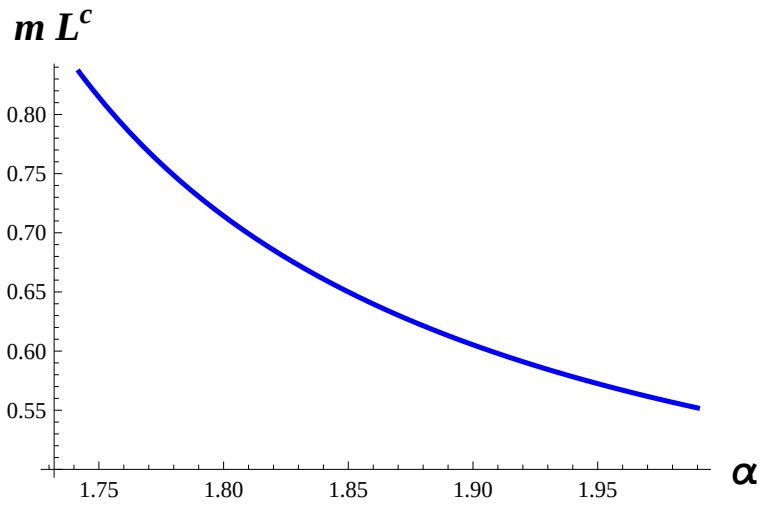

Figure 6.2: Dependence of the critical distance L^c on the coupling constant α for $\Lambda = 2$

6.3. Alternative approach to search instabilities

In this section we analyze an alternative method to find zero modes of the Dirac operator

$$(i\not{D}_c + m)\Psi = 0.$$

Let us consider first the case of one static quark, with $\not{D}_c$ defined by (6.1). Again the color we concentrate on the lower color component Ψ_- and omit

the subindex to simplify the notation

$$[i\gamma_\mu(\partial_\mu + iA_\mu) + m]\,\Psi = 0, \tag{6.25}$$

where $A_\mu = i\frac{\Phi(r)}{2}\delta_{\mu 0}$, $\Phi(r) = \frac{\alpha}{r}$. Let us introduce the chiral projection operator

$$P_1 = \frac{1}{2}(1-\gamma_5), \quad P_1 = \frac{1}{2}(1+\gamma_5),$$

with $\gamma_5 = \gamma_0\gamma_1\gamma_2\gamma_3$ and the corresponding chiral spinors $\Psi_1 \equiv P_1\Psi$, $\Psi_2 \equiv P_2\Psi$. Due to the structure of the projector, the zero modes of the spectrum of Dirac operator in a static heavy quark background can be derived from the following ansatz

$$\Psi_1 = \begin{pmatrix} \Psi^+ \\ \Psi^+ \end{pmatrix} e^{-iEx_0}, \quad \Psi_2 = \begin{pmatrix} \Psi^- \\ -\Psi^- \end{pmatrix} e^{-iEx_0}.$$

It is easy to show, using the relation $P_1\gamma_\mu = \gamma_\mu P_2$ that

$$-m\Psi_2 = i\gamma_\mu\left(\partial_\mu + iA_\mu\right)\Psi_1. \tag{6.26}$$

This means knowing the chiral component Ψ_1 we know the complete solution Ψ. Using the previous relation we get

$$m\,[i\gamma_\mu(\partial_\mu + iA_\mu) + m]\,[i\gamma_\nu(\partial_\nu + iA_\nu) - m]\,\Psi^+ = 0.$$

and

$$\left(-\Delta + E^2 - \frac{\Phi^2}{4} - iE\Phi + \frac{i}{2}\boldsymbol{\sigma}\cdot\boldsymbol{\nabla}\Phi + m^2\right)\Psi^+ = 0.$$

Searching the zero modes for static quark fluctuations implies that $E = 0$ and in that case

$$\left(-\Delta - \frac{\alpha^2 + 2i\alpha\boldsymbol{\sigma}\cdot\hat{\mathbf{r}}}{4r^2} + m^2\right)\Psi^+ = 0. \tag{6.27}$$

In order to diagonalize the spin dependent term, we expand the bispinor in terms of spinorial spherical harmonics (6.5) and (6.6):

$$\Psi^+ = A\phi^+(r)\left(\Omega^j_{j-\frac{1}{2}\,m_j} - \frac{2i}{\alpha}c_+\Omega^j_{j+\frac{1}{2}\,m_j}\right) + B\phi^-(r)\left(\Omega^j_{j-\frac{1}{2}\,m_j} - \frac{2i}{\alpha}c_-\Omega^j_{j+\frac{1}{2}\,m_j}\right), \tag{6.28}$$

with $c_\pm = (j + \frac{1}{2} \pm \nu)$ and $\nu = \sqrt{(j+\frac{1}{2})^2 - \frac{\alpha^2}{4}}$. Using the property (6.7) it is possible to show that the functions $\phi^\pm$ satisfy the equation

$$\left(\frac{d^2}{dr^2} + \frac{2}{r}\frac{d}{dr} - m^2 - \frac{\nu^2 \pm \nu}{r^2} \right) \phi^\pm(r) = 0.$$

For $\alpha^2 > 3$ we have normalizable solutions of the form

$$\phi^\pm(r) = \frac{K_{\frac{1}{2}\pm\nu}}{\sqrt{mr}}.$$

Once we have found Ψ_1, it is possible to derive Ψ_2 from (6.26). Let us write Ψ^+ in a slightly different way

$$\Psi^+ = O_1(r)\Omega^j_{j-\frac{1}{2}\,m_j} - i\,O_2(r)\Omega^j_{j+\frac{1}{2}\,m_j}, \tag{6.29}$$

where

$$O_1(r) = A\,\phi^+(r) + B\,\phi^-(r)$$

and

$$O_2(r) = \frac{2}{\alpha}\left(A\,c_+\,\phi^+(r) + B\,c_-\,\phi^-(r) \right).$$

Using that (6.9) and (6.10) we obtain

$$\Psi^- = \widetilde{O_1}(r)\Omega^j_{j-\frac{1}{2}\,m_j} - i\,\widetilde{O_2}(r)\Omega^j_{j+\frac{1}{2}\,m_j}, \tag{6.30}$$

with

$$\widetilde{O_1}(r) = \frac{1}{m}\left(\frac{\alpha}{2r}\,O_1(r) - \left(\frac{d}{dr} + \frac{(j+\frac{1}{2})+1}{r} \right) O_2(r) \right),$$

and

$$\widetilde{O_2}(r) = \frac{1}{m}\left(\frac{\alpha}{2r}\,O_2(r) + \left(\frac{d}{dr} + \frac{-(j+\frac{1}{2})+1}{r} \right) O_1(r) \right),$$

Due to the spherical symmetry of the system, the state must have a definite parity. This is achieved if the upper two spinor $\Psi^+ + \Psi^-$ is proportional to $\Omega^j_{j-\frac{1}{2}\,m_j}$ and the lower two spinor $\Psi^+ - \Psi^-$ is proportional to $\Omega^j_{j+\frac{1}{2}\,m_j}$:

$$O_1(r) = \widetilde{O_1}(r), \text{ and } O_2(r) = -\widetilde{O_2}(r).$$

or if the upper two spinor $\Psi^+ + \Psi^-$ is proportional to $\Omega^j_{j+\frac{1}{2}\,m_j}$ and the lower two spinor $\Psi^+ - \Psi^-$ is proportional to $\Omega^j_{j-\frac{1}{2}\,m_j}$:

$$O_1(r) = -\widetilde{O_1}(r), \text{ and } O_2(r) = \widetilde{O_2}(r).$$

This fixes the ratio between the coefficients A and B (6.28),

$$\frac{B}{A} = \mp\frac{2(j+\frac{1}{2}) - \alpha + 2\nu}{2(j+\frac{1}{2}) - \alpha - 2\nu}.$$

It's easy to verify that with this combination, the solution does coincide with (6.20). In the first case the connection is,

$$G(r) = C\,O_1(r), \quad \text{and} \quad F(r) = -C\,O_2(r),$$

with $k = -(j+\frac{1}{2})$, whereas in the second one it is given by

$$F(r) = C'\,O_1(r), \quad \text{and} \quad G(r) = C'\,O_2(r),$$

with $k = (j+\frac{1}{2})$, with C and C' constant.

In the case of a background generated by a quark and an antiquark pair, using the well know approximation near one quark, the potential A_μ (6.25) reduces to

$$A_\mu(\overrightarrow{x}) = i\frac{\Phi(r)}{2}\delta_{\mu 0}, \quad \Phi = \alpha\left(\frac{1}{r} - \frac{1}{2L}\right),$$

The equation (6.27) then becomes:

$$\left(-\Delta - \frac{\alpha^2}{16L^2} + \frac{\alpha^2}{4L\,r} - \frac{\alpha^2 + 2i\alpha\boldsymbol{\sigma}\cdot\hat{\mathbf{r}}}{4r^2} + m^2\right)\Psi^+ = 0.$$

Using the same ansatz (6.28) we get the equations

$$\left(\frac{d^2}{dr^2} + \frac{2}{r}\frac{d}{dr} - \frac{\alpha^2}{4rL} + \frac{\alpha^2}{16L^2} - m^2 - \frac{\nu^2 \pm \nu}{r^2}\right)\phi^{\pm}(r) = 0.$$

In the regime II $\alpha^2 > 3$ the normalizable solutions are given in terms of Hypergeometric functions:

$$\phi^{\pm}(r) = e^{-\epsilon\, r} r^{\pm\nu} U\left(\frac{\alpha^2}{8L\epsilon} + 1 \pm \nu, 2 \pm 2\nu, 2\epsilon r\right), \tag{6.31}$$

where $\epsilon = \sqrt{16m^2L^2 - \alpha^2}/4L$. Once Ψ_+ is found, Ψ_- can be calculated following the same steps from (6.29) to (6.30). We can write Ψ^+ in a different way

$$\Psi^+ = O_1(r)\Omega^j_{j-\frac{1}{2}\, m_j} - i\, O_2(r)\Omega^j_{j+\frac{1}{2}\, m_j},$$

where

$$O_1(r) = A\,\phi^+(r) + B\,\phi^-(r), \quad O_2(r) = \frac{2}{\alpha}\left(A\, c_+\,\phi^+(r) + B\, c_-\,\phi^-(r)\right),$$

with $\phi^{\pm}$ now given by (6.31). Finally, we get

$$\Psi^- = \widetilde{O_1}(r)\Omega^j_{j-\frac{1}{2}\, m_j} - i\,\widetilde{O_2}(r)\Omega^j_{j+\frac{1}{2}\, m_j},$$

where now

$$\widetilde{O_1}(r) = \frac{1}{m}\left(\left(-\frac{\alpha}{4L} + \frac{\alpha}{2r}\right) O_1(r) - \left(\frac{d}{dr} + \frac{(j+\frac{1}{2})+1}{r}\right) O_2(r)\right),$$

and

$$\widetilde{O_2}(r) = \frac{1}{m}\left(\left(-\frac{\alpha}{4L} + \frac{\alpha}{2r}\right) O_2(r) + \left(\frac{d}{dr} + \frac{-(j+\frac{1}{2})+1}{r}\right) O_1(r)\right),$$

Requiring again that the solution has definite parity $O_1(r) = \pm\widetilde{O_1}(r)$ and $O_2(r) = \mp\widetilde{O_2}(r)$, leads fixes the ratio

$$\frac{B}{A} = -\left(\frac{16m^2L^2 - \alpha^2}{4L^2}\right)^{-\nu} \frac{\alpha^2 \pm 4\alpha Lm - (1 + 2j + 2\nu)\sqrt{16m^2L^2 - \alpha^2}}{\alpha^2 \pm 4\alpha Lm - (1 + 2j - \nu)\sqrt{16m^2L^2 - \alpha^2}}$$

and implies that

$$G(r) = C\, O_1(r), \quad \text{and} \quad F(r) = -C\, O_2(r),$$

with $k = -(j + \frac{1}{2})$, while in the second one

$$F(r) = C'\, O_1(r), \quad \text{and} \quad G(r) = C'\, O_2(r),$$

with $k = (j + \frac{1}{2})$ (C and C' are constant). Thus, the solution found by this method does coincide with (6.24) founded with the other approach, and there are no extra solutions. The derivation also shows that both methods are completely equivalent.

6.4. The role of light quark fluctuations

The Gribov approach to confinement is based on the instability in heavy quarks Coulomb backgrounds for values of the effective coupling constant larger than $\alpha_s \simeq 0.43$. The instability would imply a vacuum decay into light quark-antiquark pairs. In the previous chapters, from first principles, it has been shown the existence of an instability of the Coulomb phase in pure gauge theories for $\alpha > \sqrt{2}$, much beyond the Gribov critical value. However, Gribov assigned a leading role to lighter dynamical quarks in the confinement mechanism. For this reason, the last chapter has been dedicated to analyze the effects of dynamical quarks in the instability of the Coulomb phase.

The results show the appearance of new instabilities in the fermionic sector beyond a new value of the critical coupling constant $\alpha = \sqrt{3}$. The mechanism driving the instability is the spectral flow of the eigenvalues induced by the introduction of a dimensional parameter Λ in the self adjoint boundary conditions. Considering first one heavy quark Coulomb background, for each $\alpha > 3$. We have been shown the existence of a discrete number of parameters at which zero modes of the light quarks determinant appear. In the presence of zero modes, the partition function becomes zero and this implies an infinite amount of energy in the system, the signal of the creation of a quark antiquark pair, inducing the instability of Coulomb

phase.

In the heavy quark antiquark Coulomb background it has been shown that for each $\alpha \in (\sqrt{3}, 2]$ and for each value of the parameter of the boundary conditions, there exists a critical distance between the pair where the zero modes appear. The situation is different respect the instabilities due to gluonic fluctuation, where the instabilities hold for an interval of distances. In the case of fermionic fluctuations only at particular values of the separation between the pair. In particular, the critical distance decreases at large coupling constant, in agreement with the idea of permanent confinement for all distances for large value of the coupling constant. For $\alpha > 2$ also there is an infinite discrete values of distances at which the zero modes appear.

However, the value of the coupling constant where the fermionic instabilities begin to arise $\alpha = \sqrt{3}$ is larger than the critical value $\alpha = \sqrt{2}$ where the pure gauge fluctuations start to develop negative modes. This means that the fundamental instability is due to the boson sector instead of light quark as it was advocated by Gribov. These results provides further consistency to the picture where quark confinement is mainly driven by gluon fluctuation instabilities.

A

Boundary conditions for singular potentials

Let us consider the differential operator

$$H = -\frac{d^2}{dx^2} - \frac{a}{x^2}. \tag{A.1}$$

H is a very special Hamiltonian with a conformal invariant singular potential. Let us analyze the theory of boundary conditions which induce self adjoint extension of (A.1) over the whole half line $(0, \infty)$. Due to the singularity, the self adjoint extensions have to be given in terms of asymptotic boundary conditions.

A.1. Regularization by a space cut off x_0

Let us consider a space cut-off $x_0 > 0$ is introduced near the singularity. On the half line $(x_0, +\infty)$ any self adjoint extension of H_β is defined by the restriction of $H^\dagger$ to a domain of functions ψ satisfying the following boundary conditions

$$e^{i\beta_0} = \frac{\psi(x_0) - i\psi'(x_0)}{\psi(x_0) + i\psi'(x_0)}, \tag{A.2}$$

where $\beta_0 \in [0, \pi)$ is an arbitrary angle. Notice that even if the wave functions ψ are complex the value $\frac{\psi'}{\psi}(x_0) = tan\beta/2$ is always real. This is a requirement due to hermiticity. To define an asymptotic selfadjoint Hamiltonian in the whole half line we have to renormalize the initial phase β_0 in the process of removing the UV cut-off x_0.
An convenient ingredient in that limit is given by the asymptotic zero modes that encode the divergent behavior of the operator H. They are defined by

$$\left(-\frac{d^2}{dx^2} - \frac{a}{x^2}\right)\psi_0(x) = 0. \tag{A.3}$$

The key observation is that as the cut-off goes to zero, the function belonging to the domain of the self adjoint extension behaves as zero mode near the singularity. In the limit, the boundary condition (A.2) must be then satisfied by the zero modes.
The solutions of (A.3) are

$$\psi_0(x) = x^{\frac{1}{2}\pm\nu}$$

for $a \neq \frac{1}{4}$, and

$$\psi_0(x) = x^{\frac{1}{2}} \quad \text{and} \quad \psi(x) = x^{\frac{1}{2}}\log(\Lambda x)$$

for $a = \frac{1}{4}$, with $\nu = \sqrt{\frac{1}{4} - a}$ and Λ a fixed scale parameter with dimension $[L]^{-1}$.
There are different regime depending on the value of the parameter a. Notice that ν is real for $a \leq \frac{1}{4}$ and imaginary for $a > \frac{1}{4}$.

i) For $a \leq -\frac{3}{4}$ the solution $\psi_0(x) = x^{\frac{1}{2}-\nu}$ is not normalizable at $x = 0$ and must be excluded. The most general zero mode is simply given by

$$\psi_0(x) = N x^{\frac{1}{2}+\nu} \tag{A.4}$$

with N arbitrary constant.
For $a > -\frac{3}{4}$ both solutions are normalizable and the zero mode is in general a linear combination of the two behaviors. The general zero mode, such that $\frac{\psi_0'(x)}{\psi_0(x)}$ is real, is given by:
ii) for $-\frac{3}{4} < a < \frac{1}{4}$

$$\psi_0(x) = N\, x^{\frac{1}{2}} \left(\cos\theta(\Lambda x)^{\nu} - \sin\theta(\Lambda x)^{-\nu}\right), \tag{A.5}$$

iii) for $a = \frac{1}{4}$

$$\psi_0(x) = N\, x^{\frac{1}{2}} \left(\cos\theta - \sin\theta \log(\Lambda x)\right), \tag{A.6}$$

iv) for $a > \frac{1}{4}$

$$\psi_0(x) = N\, x^{\frac{1}{2}} \left(\exp(-i\theta)(\Lambda x)^{\nu} + \exp(i\theta)(\Lambda x)^{-\nu}\right), \tag{A.7}$$

where N is an arbitrary constant, Λ fixed parameter with dimension $[L]^{-1}$ and $t \in [0, 1)$.

A.2. Renormalization of the phase

The idea is, once fixed the cut-off x_0, to associate to the phase β_0 a zero mode defined by (A.4), (A.5), (A.6) and (A.7)

$$(\beta_0, x_0) \to \psi_0,$$

through the definition

$$\frac{\psi_0(x_0) - i\psi_0'(x_0)}{\psi_0(x_0) + i\psi_0'(x_0)} := e^{i\beta_0}, \tag{A.8}$$

It is easy to see that the left term is a well defined phase. More precisely, the relation (A.8) defines a class of equivalence of zero mode, as the normalization constant is factorized. The explicit relation depends on the constant a.

i) For $a \leq -\frac{3}{4}$ there is just one family of zero mode. This means that at each cut-off there is not the freedom to choose the phase. The phase and the cut off are connected by the following formula.

$$x_0 = -\frac{1+2\nu}{2\Lambda y}$$

This is telling us that there is a unique self adjoint extension for $a \leq -\frac{3}{4}$. For $a > -\frac{3}{4}$ as a family of zero modes exists, there is the freedom to choose β_0 fixed x_0. For simplicity we define $\zeta = \tan\theta$, the parameter characterizing the zero mode. Fixed x_0, to each $\beta_0 \in [0, 2\pi)$ is assigned a zero mode through the following relations:

ii) for $-\frac{3}{4} < a < \frac{1}{4}$

$$\zeta = \frac{1+2\nu+2\,\tan\left(\frac{\beta_0}{2}\right)\,\Lambda x_0}{1-2\nu+2\,\tan\left(\frac{\beta_0}{2}\right)\,\Lambda x_0}(\Lambda x_0)^{2\nu},$$

iii) for $a = \frac{1}{4}$

$$\zeta = \frac{1+2\,\tan\left(\frac{\beta_0}{2}\right)\,\Lambda x_0}{2+(1+2\,\tan\left(\frac{\beta_0}{2}\right)\,\Lambda x_0)\log(\Lambda x_0)},$$

iv) for $a > \frac{1}{4}$

$$\zeta = \frac{-|\nu|\,\tan(|\nu|\log(\Lambda x_0)) + \Lambda x_0(1+\tan\left(\frac{\beta_0}{2}\right))}{|\nu| + \,\Lambda x_0(1+\tan\left(\frac{\beta_0}{2}\right))\tan(|\nu|\log(\Lambda x_0))}.$$

After having defined the boundary condition in a cut-off domain through a phase at which we have assigned a zero mode, the next step is to remove

the cut-off. At a different cut-off the boundary conditions are determined by a new phase β: it must be given a procedure how to change the phase reducing the cut-off in terms of the initial phase. Being ψ_0 the zero mode, defined by t, associated to the initial phase β_0 at x_0, the phase β at different ϵ is renormalized according

$$e^{i\beta(\epsilon)} := \frac{\psi_0(\epsilon) - i\psi_0'(\epsilon)}{\psi_0(\epsilon) + i\psi_0'(\epsilon)}. \tag{A.9}$$

The idea is then that the initial phase define a zero mode and the phase run keeping fix the zero mode. Schematically:

$$(\beta_0, x_0) \to \psi_0 \to \beta(\epsilon).$$

The explicit form of the renormalization function for β depends by the value of the charge. We define $y = \tan\left(\frac{\beta}{2}\right)$, the parameter to be renormalized. The renormalization function are:
i) for $a \leq \frac{1}{4}$

$$y = -\frac{1+2\nu}{2\Lambda\epsilon}$$

ii) for $\frac{3}{4} < a < \frac{1}{4}$

$$y = -\frac{1+\nu}{2\Lambda\epsilon}\left(2 + \frac{4\tan\theta}{(\Lambda\epsilon)^{2\nu} - \tan\theta}\right)$$

iii) for $a = \frac{1}{4}$

$$y = -\frac{1}{2\Lambda\epsilon}\left(1 + \frac{2\tan\theta}{z\log(\Lambda\epsilon) - 1}\right)$$

iv) for $a > \frac{1}{4}$

$$y = -1 + 2|\nu|\tan\Big(\pi\, t + |\nu|\log(\Lambda\epsilon)\Big)$$

A.3. Boundary conditions and bound states

Let us define H as a self adjoint operator on all $(0,\infty)$. Once started with the boundary condition (A.2) on the cut-off x_0, decreasing ϵ it is imposed that it must be satisfied

$$e^{i\beta} = \frac{\psi(\epsilon) - i\psi'(\epsilon)}{\psi(\epsilon) + i\psi'(\epsilon)}, \tag{A.10}$$

with β running according (A.9). Explicitly, in the limit $\epsilon \to 0$, the boundary conditions (A.10) that define the domain of the self adjoint extensions are:

$$\lim_{x\to 0} \big(\psi(x)\psi_0'(x) - \psi'(x)\psi_0(x)\big) = 0. \tag{A.11}$$

Resuming, the self adjoint extensions on $(0,\infty)$ are defined by boundary conditions in terms of zero mode. For $a > -\frac{3}{4}$ the family of self adjoint extensions is parameterized by the parameter $t \in [0,\pi)$:

$$(\beta_0, x_0) \to \psi_0 \to \beta(\epsilon) \to \text{s.a. H.}$$

Explicitly:
i) for $a \le \frac{1}{4}$

$$\lim_{x\to 0} \left((\frac{1}{2} + \nu)\psi(x) - x\psi'(x) \right) = 0,$$

ii) for $\frac{3}{4} < a < \frac{1}{4}$

$$\lim_{x\to 0} \Big((\Lambda\epsilon)^{2\nu}(\mu_+\psi(x) - x\psi'(x)) + \tan(\pi\, t)(\mu_-\psi(x) + x\psi'(x)) \Big) = 0$$

where $\mu_\pm = \frac{1}{2} \pm \nu$,
iii) for $a = \frac{1}{4}$

$$\lim_{x\to 0} \left(\Big(1 - \tan\theta(2 + \log(\Lambda x))\Big)\psi(x) + 2x\Big(\tan\theta \log(\Lambda x) - 1\Big)\psi'(x) \right) = 0$$

iv) for $a > \frac{1}{4}$

$$\lim_{x\to 0}\left(2x\psi'(x) - \Big(1 - 2|\nu|\tan(\theta + |\nu|\log(\Lambda x))\Big)\psi(x)\right) = 0$$

Once defined (A.1) as self adjoint operator on all $(0,\infty)$, the objective is to find the bound states, the normalizable solutions of the equation

$$\left(-\frac{d^2}{dx^2} - \frac{a}{x^2}\right)\psi(x) = -\lambda^2\psi(x), \tag{A.12}$$

satisfying the boundary condition (A.11).
i) For $a \leq -\frac{3}{4}$ the are not normalizable solution of (A.12). Consequently there are not bound states. For $a > -\frac{3}{4}$ there is a normalizable solution in terms of the Bessel function K:

$$\psi(x) = \sqrt{x}K_\nu(\lambda x),$$

with $\nu = \sqrt{\frac{1}{2} - a}$. To match the boundary conditions, we need the asymptotic expansion of the solution near the singularity:

$$\psi(x) \cong \sqrt{x}\left(\Gamma[-\nu]\left(\frac{\lambda x}{2}\right)^{\nu} + \Gamma[\nu]\left(\frac{\lambda x}{2}\right)^{-\nu}\right)$$

for $a \neq \frac{1}{4}$ and

$$\psi(x) \cong \sqrt{x}\,(\gamma - \log 2 + \log(\lambda x))$$

for $a = \frac{1}{4}$. It easy to prove then that
ii) for $\frac{3}{4} < a < \frac{1}{4}$ there is one bound state for $t \in [0, \frac{1}{2})$

$$-\lambda^2 = -4\Lambda^2\left(\cot\theta\frac{\Gamma[1+\nu]}{\Gamma[1-\nu]}\right)^{\frac{1}{\nu}}$$

and no bound states for $t \in [\frac{1}{2}, 1)$,
iii) for $a = \frac{1}{4}$ there is one bound state for all $t \in [0, 1)$

$$-\lambda^2 = -4\Lambda^2 e^{-2\gamma - 2\cot\theta}$$

, **iv**) for $a > \frac{1}{4}$ there is a infinite number of bound states for all $t \in [0, 1)$

$$-\lambda^2 = -4\Lambda^2 \exp\left[\frac{2i\pi}{\nu}(t+n) + \frac{1}{\nu}\log\left(-\frac{\Gamma[1+\nu]}{\Gamma[1-\nu]}\right)\right],$$

with $n = 0, \pm 1, \pm 2 \ldots$

A.4. Scale parameter

For dimensional reason, a scale parameter Λ is introduced with dimension $[L]^{-1}$, and the self adjoint extensions, for $a > -\frac{3}{4}$, are classified with a dimensionless parameter t. From a physical point of view it is useful to convert this two parameters into a unique parameter Λ_θ with dimension $[L]^{-1}$, that make evident the breaking of scale symmetry.
i) For $a \leq -\frac{3}{4}$ the absence of the parameter is telling us that the scale symmetry is not broken.
ii) For $-\frac{3}{4} < a < \frac{1}{4}$ it is $\Lambda_\theta = |\tan\theta|^{-\frac{1}{2\nu}}\Lambda$. The scale transformation $x \to lx$ implies a change of the scale parameter $\Lambda_\theta \to l^{-1}\Lambda_\theta$. This change the domain of the self adjoint extension: the scale symmetry is broken. There are two particular cases, corresponding to $t = 0, \frac{1}{2}$ or, equivalently, $\Lambda_\theta = 0, \Lambda_\theta = \infty$. In these cases the boundary conditions are determined by only one of the two asymptotic behaviors $x^{\frac{1}{2}\pm\nu}$. The Hamiltonian are scale invariant. These are the only two cases respecting the symmetry scale in this regime.
iii) For $a = \frac{1}{4}$ it is $\Lambda_\theta = \exp[-\cot\theta]\Lambda$. Similar consideration of the case ii) are valid. Now the only case respecting scale symmetry is $\Lambda_\theta = 0, \Lambda_\theta = \infty$, where the boundary condition are defined by $x^{\frac{1}{2}}$.
iv) For $a > \frac{1}{4}$ it is $\Lambda_\theta = e^{\frac{t}{|\nu|}}\Lambda$. The parameter Λ_θ breaks the conformal invariance but not completely, since a discrete conformal symmetry is preserved. In fact the boundary conditions and the spectrum are invariant under for $l = e^{\frac{\pi n}{|\nu|}}$, that is under the rescaling $\Lambda_\theta \to \Lambda e^{\frac{\pi n}{|\nu|}}$, with $n = 0, \pm 1, \pm 2 \ldots$.

B

General solution for gluonic instabilities

For completeness we shall analyze the general solution for the unstable gluon fluctuations, and show that that considered in (3.31) is the one which gives the lowest critical charge and so it is the most relevant for the stability. Let us consider the spherical ansatz for gluonic fluctuations τ_μ:

$$\begin{aligned} \tau_0^\pm &= f^\pm(r) Y_{\tilde{j}\tilde{m}} \\ \boldsymbol{\tau}^\pm &= b_1^\pm(r)\boldsymbol{Y}_{jj+1m} + b_0^\pm(r)\boldsymbol{Y}_{jjm} + b_{-1}^\pm(r)\boldsymbol{Y}_{jj+1m}, \end{aligned} \tag{B.1}$$

where Y_{jm} are the spherical harmonics and $\boldsymbol{Y}_{jlm}$ are the vector spherical harmonics and they describe the coupling of the orbital angular momentum L with the spin $S = 1$of the gluons to give the total angular momentum $J(j, m)$. The definition of the vector spherical harmonics is

$$\boldsymbol{Y}_{jlm} = \Sigma_{mq} Y_{lm}(\theta, \phi)(lm1q|l1jm)\hat{e}_q, \tag{B.2}$$

where $(lm1q|l1jm)$ are the Clebsch-Gordan coefficients, $q = -1, 0, 1$, $\hat{e}_1$, $\hat{e}_0$ and $\hat{e}_{-1}$ are the unit vectors in the spherical basis that are related to the

unit vectors $\hat{e}_x$, $\hat{e}_y$ and $\hat{e}_z$ along the coordinate axes by

$$\hat{e}_x = -\frac{1}{\sqrt{2}}(\hat{e}_1 + \hat{e}_{-1}), \quad \hat{e}_y = \frac{i}{\sqrt{2}}(\hat{e}_1 - \hat{e}_{-1}), \quad \hat{e}_z = \hat{e}_0. \tag{B.3}$$

Let us recall some formulas which for $j > 0$ (the case $j = 0$ will be considered later):

$$\begin{aligned}
\frac{\mathbf{r}}{r}Y_{jm} &= -\sqrt{\frac{j+1}{2j+1}}\boldsymbol{Y}_{jj+1m} + \sqrt{\frac{j}{2j+1}}\boldsymbol{Y}_{jj-1m} \\
\boldsymbol{\nabla}(\phi(r)Y_{jm}) &= -\sqrt{\frac{j+1}{2j+1}}\Big[\frac{d}{dr} - \frac{j}{r}\Big]\phi(r)\boldsymbol{Y}_{jj+1m} \\
&\quad +\sqrt{\frac{j}{2j+1}}\Big[\frac{d}{dr} + \frac{j+1}{r}\Big]\phi(r)\boldsymbol{Y}_{jj-1m} \\
\boldsymbol{\nabla}\cdot(\phi(r)\boldsymbol{Y}_{jj+1m}) &= -\sqrt{\frac{j+1}{2j+1}}\Big[\frac{d}{dr} + \frac{j+2}{r}\Big]\phi(r)Y_{jm} \\
\boldsymbol{\nabla}\cdot(\phi(r)\boldsymbol{Y}_{jjm}) &= 0 \\
\boldsymbol{\nabla}\cdot(\phi(r)\boldsymbol{Y}_{jj-1m}) &= \sqrt{\frac{j}{2j+1}}\Big[\frac{d}{dr} - \frac{j-1}{r}\Big]\phi(r)Y_{jm}
\end{aligned}$$

$$\begin{aligned}
\boldsymbol{\nabla}\times(\phi(r)\boldsymbol{Y}_{jj+1m}) &= i\sqrt{\frac{j}{2j+1}}\Big[\frac{d}{dr} + \frac{j+2}{r}\Big]\phi(r)\boldsymbol{Y}_{jjm} \\
\boldsymbol{\nabla}\times(\phi(r)\boldsymbol{Y}_{jj-1m}) &= i\sqrt{\frac{j+1}{2j+1}}\Big[\frac{d}{dr} - \frac{j-1}{r}]\phi(r)\boldsymbol{Y}_{jjm} \\
\boldsymbol{\nabla}\times(\phi(r)\boldsymbol{Y}_{jjm}) &= i\sqrt{\frac{j}{2j+1}}\Big[\frac{d}{dr} - \frac{j}{r}\Big]\phi(r)\boldsymbol{Y}_{jj+1m} \\
&\quad +i\sqrt{\frac{j+1}{2j+1}}\Big[\frac{d}{dr} + \frac{j+1}{r}\Big]\phi(r)\boldsymbol{Y}_{jj-1m}
\end{aligned}$$

$$
\begin{aligned}
\boldsymbol{\nabla}\times(\boldsymbol{\nabla}\times(\phi(r)\boldsymbol{Y}_{jj+1m})) &= -\frac{j}{2j+1}\Big[\triangle_r-\frac{(j+1)(j+2)}{r^2}\Big]\phi(r)\boldsymbol{Y}_{jj+1m}\\
&\quad -\frac{\sqrt{j(j+1)}}{2j+1}\Big[\triangle_r+\frac{2j+1}{r}\frac{d}{dr}\\
&\quad +\frac{j(j+2)}{r^2}\Big]\phi(r)\boldsymbol{Y}_{jj-1m}\\
\boldsymbol{\nabla}\times(\boldsymbol{\nabla}\times(\phi(r)\boldsymbol{Y}_{jjm})) &= -\Big[\triangle_r-\frac{j(j+1)}{r^2}\Big]\phi(r)\boldsymbol{Y}_{jjm}\\
\boldsymbol{\nabla}\times(\boldsymbol{\nabla}\times(\phi(r)\boldsymbol{Y}_{jj-1m})) &= -\frac{\sqrt{j(j+1)}}{2j+1}\Big[\triangle_r-\frac{2j+1}{r}\frac{d}{dr}\\
&\quad +\frac{(j+1)(j-1)}{r^2}\Big]\phi(r)\boldsymbol{Y}_{jj+1m}\\
&\quad -\frac{j+1}{2j+1}\Big[\triangle_r-\frac{j(j-1)}{r^2}\Big]\phi(r)\boldsymbol{Y}_{jj-1m}
\end{aligned}
$$

$$
\frac{\mathbf{r}}{r}\cdot\boldsymbol{Y}_{jjm}=0,\quad \frac{\mathbf{r}}{r}\cdot\boldsymbol{Y}_{jj+1m}=-\sqrt{\frac{j+1}{2j+1}}Y_{jm},\quad \frac{\mathbf{r}}{r}\cdot\boldsymbol{Y}_{jj-1m}=\sqrt{\frac{j}{2j+1}}Y_{jm}
$$

$$
\frac{\mathbf{r}}{r}Y_{jm}=-\sqrt{\frac{j+1}{2j+1}}\boldsymbol{Y}_{jj+1m}+\sqrt{\frac{j}{2j+1}}\boldsymbol{Y}_{jj-1m}
$$

where $\triangle_r=\frac{d^2}{dr^2}+\frac{2}{r}\frac{d}{dr}$. Using the formulas above, recalling the vectorial identity $\boldsymbol{\nabla}\times(\boldsymbol{\nabla}\times\boldsymbol{\tau})=\boldsymbol{\nabla}(\boldsymbol{\nabla}\cdot\boldsymbol{\tau})-\triangle\boldsymbol{\tau}$. and fixing $\widetilde{j}=j$ and $\widetilde{m}=m$ in (B.1), from (3.30) we get the following four equations eigenvalue equations

$$
\begin{aligned}
&-\Big[\triangle_r-\frac{j(j+1)}{r^2}\Big]f^{\pm}\pm\frac{\alpha}{r}\Big(-\sqrt{\frac{j+1}{2j+1}}\Big[\frac{d}{dr}+\frac{j+3}{r}\Big]b^{\pm}_{+1}\\
&+\sqrt{\frac{j}{2j+1}}\Big[\frac{d}{dr}-\frac{j-2}{r}\Big]b^{\pm}_{-1}\Big)=-\lambda^2 f^{\pm}
\end{aligned}
\tag{B.4}
$$

$$-\frac{j}{2j+1}\Big[\triangle_r+\frac{\alpha^2-(j+1)(j+2)}{r^2}\Big]b^{\pm}_{+1}-\frac{\sqrt{j(j+1)}}{2j+1}\Big[\triangle_r-\frac{2j+1}{r}\frac{d}{dr}$$
$$+\frac{(j+1)(j-1)}{r^2}\Big]b^{\pm}_{-1}\mp\frac{\alpha}{r}\sqrt{\frac{j+1}{2j+1}}\Big[\frac{d}{dr}-\frac{j+2}{r}\Big]f^{\pm}=-\lambda^2 b^{\pm}_{+1} \qquad \text{(B.5)}$$

$$-\frac{\sqrt{j(j+1)}}{2j+1}\Big[\triangle_r+\frac{2j+1}{r}\frac{d}{dr}+\frac{j(j+2)}{r^2}\Big]b^{\pm}_{+1}-\frac{j+1}{2j+1}\Big[\triangle_r$$
$$+\frac{\alpha^2-j(j-1)}{r^2}\Big]b^{\pm}_{-1}\pm\frac{\alpha}{r}\sqrt{\frac{j}{2j+1}}\Big[\frac{d}{dr}+\frac{j-1}{r}\Big]f^{\pm}=-\lambda^2 b^{\pm}_{+1} \qquad \text{(B.6)}$$

$$\Big[-\triangle_r-\frac{\alpha^2-j(j+1)}{r^2}\Big]b^{\pm}_0=-\lambda^2 b^{\pm}_0. \qquad \text{(B.7)}$$

Looking at the last four equations, we have that possible unstable modes are of the form

$$\boldsymbol{\tau}^{\pm}=b^{\pm}_0\Sigma_m c^{\pm}_m \boldsymbol{Y}_{jjm}, \quad \tau_0=0, \qquad \text{(B.8)}$$

with j fixed, $b^{\pm}_0$ satisfying (B.7) and c_m constant chosen in order to satisfy the reality condition of the fields (3.25). The functions $b^{\pm}_0$ satisfy the same equation (A.12), with $a=\alpha^2-j(j+1)$. The critical coupling constant where unstable modes start to appear is $\alpha^2=-\frac{3}{4}+j(j+1)$ and its value is increasing with the total angular momentum.
If we call $b(r)=b^{\pm}_0$ the bound state of (B.7), for j fixed, we have $2(2j+1)$ unstable modes given by

$$\begin{aligned}
\tau^{+}_1 &= \tau^{-}_1 = i\,b(r)\boldsymbol{Y}_{jj0}\\
\tau^{+}_2 &= -\tau^{-}_2 = b(r)\boldsymbol{Y}_{jj0}\\
\tau^{+}_{4n-1} &= \tau^{-}_{4n-1} = b(r)\Big(\boldsymbol{Y}_{jjn}+(-1)^{n+1}\boldsymbol{Y}_{jj-n}\Big)\\
\tau^{+}_{4n} &= \tau^{-}_{4n} = i\,b(r)\Big(\boldsymbol{Y}_{jjn}+(-1)^{n}\boldsymbol{Y}_{jj-n}\Big)\\
\tau^{+}_{4n+1} &= -\tau^{-}_{4n+1} = b(r)\Big(\boldsymbol{Y}_{jjn}+(-1)^{n}\boldsymbol{Y}_{jj-n}\Big)\\
\tau^{+}_{4n+2} &= -\tau^{-}_{4n+2} = i\,b(r)\Big(\boldsymbol{Y}_{jjn}+(-1)^{n+1}\boldsymbol{Y}_{jj-n}\Big),
\end{aligned} \qquad \text{(B.9)}$$

with $n = 1, \dots j$. It iss easy to show that the previous unstable mode (3.31) correspond to $j = 1$. In fact in that case

$$\begin{aligned}
\tau_1^+ &= \tau_1^- = b(r)\big(\sin\theta\sin\varphi\,\hat{e}_x - \sin\theta\cos\varphi\,\hat{e}_y\big)\\
\tau_2^+ &= -\tau_2^- = i\,b(r)\big(\sin\theta\sin\varphi\,\hat{e}_x - \sin\theta\cos\varphi\,\hat{e}_y\big)\\
\tau_3^+ &= \tau_3^- = b(r)\big(\cos\theta\,\hat{e}_x - \sin\theta\cos\varphi\,\hat{e}_z\big)\\
\tau_4^+ &= \tau_4^- = i\,b(r)\big(\cos\theta\,\hat{e}_x - \sin\theta\cos\varphi\,\hat{e}_z\big)\\
\tau_5^+ &= -\tau_5^- = b(r)\big(-\cos\theta\,\hat{e}_y + \sin\theta\cos\varphi\,\hat{e}_z\big)\\
\tau_6^+ &= -\tau_6^- = i\,b(r)\big(-\cos\theta\,\hat{e}_y + \sin\theta\cos\varphi\,\hat{e}_z\big).
\end{aligned}$$

The modes proportional to $\boldsymbol{Y}_{220}$ are, in the approach (3.31),

$$\boldsymbol{\tau}^\pm = \frac{\mathbf{x}\times\mathbf{e}_z}{|\mathbf{x}|^2}\,\cos\theta\,\phi^\pm(|\mathbf{x}|), \quad \tau_0^\pm = 0,$$

Let us to show that, however, it is not possible to have unstable modes with lower angular momentum. For $j = 0$ the ansatz is instead

$$\begin{aligned}
\tau_0^\pm &= f^\pm(r)Y_{00}\\
\boldsymbol{\tau}^\pm &= b^\pm(r)\boldsymbol{Y}_{010}.
\end{aligned} \tag{B.10}$$

We arrive at the two following coupled equations:

$$\begin{aligned}
&\triangle f^\pm(r) \mp \frac{\alpha}{r}\left(b'^\pm(r) + \frac{3}{r}b(r)\right) = -\lambda^2 f(r)\\
&b(r) = \mp\frac{r^2}{\alpha^2 - r^2\lambda^2}\left(f'(r) + \frac{2}{r}f(r)\right).
\end{aligned}$$

These two equation are incompatible: notice the singularity of $b^\pm$ for $r = \frac{\alpha}{r}$ that make the function not normalizable. This shows the impossibility of having unstable modes with j=0.

B.1. Quark-antiquark Coulomb background

Let us understand the origin of the instability of the Coulomb regime in the case of a heavy $q-\bar{q}$ pair. The most general ansatz for the variations of the fields, compatible with the cylindrical symmetry of the problem is:

$$\tau_0^{\pm} = T_m^{\pm}(\rho, z)e^{im\phi}$$

$$\boldsymbol{\tau}^{\pm} = R_m^{\pm}(\rho, z)e^{im\phi}\hat{u}_\rho + F_m^{\pm}(\rho, z)e^{im\phi}\hat{u}_\phi + Z_m^{\pm}(\rho, z)e^{im\phi}\hat{u}_z$$

We insert the variations in the equations (5.3): using the identity $\boldsymbol{\nabla}\times(\boldsymbol{\nabla}\times\boldsymbol{\tau}) = \boldsymbol{\nabla}(\boldsymbol{\nabla}\cdot\boldsymbol{\tau}) - \triangle\,\boldsymbol{\tau}$, we get

$$\triangle\tau_0^{\pm} = \left(\frac{1}{\rho}\frac{\partial T_m^{\pm}}{\partial\rho} + \frac{\partial^2 T_m^{\pm}}{\partial\rho^2} - \frac{m^2}{\rho^2}T_m^{\pm} + \frac{\partial^2 T_m^{\pm}}{\partial z^2}\right)e^{im\phi},$$

$$\boldsymbol{\nabla}\tau_0^{\pm} = \frac{\partial T_m^{\pm}}{\partial\rho}e^{im\phi}\hat{u}_\rho + \frac{im}{\rho}T_m^{\pm}e^{im\phi}\hat{u}_\phi + \frac{\partial T_m^{\pm}}{\partial z}e^{im\phi}\hat{u}_z,$$

$$\boldsymbol{\nabla}\cdot\boldsymbol{\tau}^{\pm} = \left(\frac{\partial R_m^{\pm}}{\partial\rho} + \frac{R_m^{\pm}}{\rho} + \frac{im}{\rho}F_m^{\pm} + \frac{\partial Z_m^{\pm}}{\partial z}\right)e^{im\phi},$$

$$\boldsymbol{\nabla}\times(\boldsymbol{\nabla}\times\boldsymbol{\tau}^{\pm}) =$$

$$\left[\frac{im}{\rho^2}\left(\frac{\partial(\rho F_m^{\pm})}{\partial\rho} - imR_m^{\pm}\right) - \frac{\partial}{\partial z}\left(\frac{\partial R_m^{\pm}}{\partial z} - \frac{\partial Z_m^{\pm}}{\partial\rho}\right)\right]e^{im\phi}\hat{u}_\rho +$$

$$\left[\frac{\partial}{\partial z}\left(\frac{im}{\rho}Z_m^{\pm} - \frac{\partial F_m^{\pm}}{\partial z}\right) - \frac{\partial}{\partial\rho}\left(\frac{1}{\rho}\left(\frac{\partial(\rho F_m^{\pm})}{\partial\rho} - imR_m^{\pm}\right)\right)\right]e^{im\phi}\hat{u}_\phi +$$

$$\frac{1}{\rho}\left[\frac{\partial}{\partial\rho}\left(\rho\left(\frac{\partial R_m^{\pm}}{\partial z} - \frac{\partial Z_m^{\pm}}{\partial\rho}\right)\right) - im\left(\frac{1}{\rho}imZ_m^{\pm} - \frac{\partial F_m^{\pm}}{\partial z}\right)\right]e^{im\phi}\hat{u}_z,$$

The eigenvalues of these gluonic fluctuations are solutions of the four equations

1. $$\left(\frac{1}{\rho}\frac{\partial T_m^{\pm}}{\partial\rho} + \frac{\partial^2 T_m^{\pm}}{\partial\rho^2} - \frac{m^2}{\rho^2}T_m^{\pm} + \frac{\partial^2 T_m^{\pm}}{\partial z^2}\right) \pm \left[\phi\left(\frac{\partial R_m^{\pm}}{\partial\rho} + \frac{R_m^{\pm}}{\rho} + \right.\right.$$
$$\left.\left. + \frac{im}{\rho}F_m^{\pm} + \frac{\partial Z_m^{\pm}}{\partial z}\right) - R_m^{\pm}\phi'_\rho - Z_m^{\pm}\phi'_z\right] = -\lambda^2 T_m^{\pm}$$

2. $$\frac{im}{\rho^2}\left(\frac{\partial(\rho F_m^{\pm})}{\partial\rho} - imR_m^{\pm}\right) - \frac{\partial}{\partial z}\left(\frac{\partial R_m^{\pm}}{\partial z} - \frac{\partial Z_m^{\pm}}{\partial\rho}\right) - \phi^2 R_m^{\pm} \pm \left[2T_m^{\pm}\phi'_{\rho} + \phi\frac{\partial T_m^{\pm}}{\partial\rho}\right] = -\lambda^2 R_m^{\pm}$$

3. $$\frac{\partial}{\partial z}\left(\frac{im}{\rho}Z_m^{\pm} - \frac{\partial F_m^{\pm}}{\partial z}\right) - \frac{\partial}{\partial\rho}\left(\frac{1}{\rho}\left(\frac{\partial(\rho F_m^{\pm})}{\partial\rho} - imR_m^{\pm}\right)\right) - \phi^2 F_m^{\pm} \pm \left[\phi\frac{im}{\rho}T_m^{\pm}\right] = -\lambda^2 F_m^{\pm}$$

4. $$\frac{1}{\rho}\left[\frac{\partial}{\partial\rho}\left(\rho\left(\frac{\partial R_m^{\pm}}{\partial z} - \frac{\partial Z_m^{\pm}}{\partial\rho}\right)\right) - im\left(\frac{1}{\rho}imZ_m^{\pm} - \frac{\partial F_m^{\pm}}{\partial z}\right)\right] - \phi^2 Z_m^{\pm} \pm \left[2T_m^{\pm}\phi'_z + \phi\frac{\partial T_m^{\pm}}{\partial z}\right] = -\lambda^2 Z_m^{\pm}$$

Setting $T^{\pm} = R^{\pm} = Z^{\pm} = 0$, $m = 0$ and $F^{\pm} = \rho^{-1/2}\phi^{\pm}(\rho, z)$ we obtain the unstable modes (5.4) and from 3) we obtain a decoupled equation which is exactly (5.5). This is the only possible decoupled equation. Any attempt to to obtain an equation for the other component always fails. Thus all unstable moes in the $q - \bar{q}$ background are generalizations of the magnetic field perturbation (5.4).

Conclusions

In the search of an analytic proof of confinement in QCD, based on Gribov conjecture, we have found:

1. The original Gribov motivation based on the unitarity loss of QED in a Coulomb supercritical regime is not completely correct. The Coulomb phase is stable even in the supercritical regime. The Dirac Hamiltonian is selfadjoint. The only remarkable feature is that for large values of the Coulomb charge ($Z > 118$) one needs to select a boundary condition near the Coulomb singularity. The choice of boundary condition is labeled by a dimensionful parameter Λ_θ, which introduces an anomalous breaking of conformal symmetry.

2. The same physical phenomena occurs in 2-dimensional condensed matter systems with lower values of the critical charge. In particular, in the analysis of graphene impurities the critical charge can attain as low values as $Z = 1$. A detailed analysis of the supercritical regime including many body interactions gives rise to a screening phenomenon of the charge impurity. The theoretical predictions are in agreement with recent experimental data concerning this phenomenon.

3. In the saddle point approximation to Yang-Mills theory in the presence of external quarks, we found that the Coulomb solutions become unstable for values of the strong coupling constant α_s larger than $\sqrt{5}/2$. The instability is due to the appearance of negative modes in the gluon fluctu-

ations around the Coulomb gauge field configuration.

4. The same analysis shows that the Coulomb regime is also unstable in a background of heavy $q-\bar{q}$ quarks. In that case for coupling constants $\alpha_s > \sqrt{2}$ the same phenomenon occurs, but it becomes strongly dependent on the distance between the quarks of the $q-\bar{q}$ pair. For any choice of boundary condition there is a critical distance L_c such that, the Coulomb background is stable for $q-\bar{q}$ pairs with size lower than $2L_c$ and become unstable for larger sizes $L > L_c$ of the $q-\bar{q}$ pair.

5. In the intermediate regime $\sqrt{2} < \alpha_s < 3/2$ the compatibility of asymptotic freedom and confinement is explicit. The critical distance approaches at infinite for $\alpha_s = \sqrt{2}$. At small couplings $\alpha < \sqrt{2}$ the Coulomb phase is always stable and at large couplings $\alpha > \frac{3}{2}$ it is always unstable, no matter what the size of $q-\bar{q}$ pair is. In the intermediate regime the stability properties depend on the distance between the $q-\bar{q}$ pair, pointing out the existence of a smooth interpolation from an asymptotic freedom regime to a confinement regime. These are the first analytic indications derived from first principles that QCD does not undergo a phase transition at intermediate energy scales.

6. It is remarkable that the fluctuations leading to the instability of the Coulomb regime exhibit a prominent thick string connecting the two quarks which points out to a picture of QCD where confinement would be driven by thick strings rather than by fundamental strings.

7. In Gribov's confinement picture a prominent role is assigned to dynamical light quarks in the confinement mechanism. Our analysis of the contribution of light quarks fluctuations in a Coulomb background pointed our the existence of new type of fermionic instabilities. They only appear for couplings larger than $\alpha_s = \sqrt{3}$. For each coupling bigger than this new critical value ($\sqrt{3} < \alpha_s \leq 2$) there exists a distance where the vacuum energy of the system becomes infinite. This is the signal of quark antiquark pair creation, that breaks the chromoelectric string and induces the insta-

bility of Coulomb phase.

8. However, the fact that fermionic instabilities appear at larger values of the coupling constant than in the bosonic case. points out that the confinement mechanism is mostly driven by gluons rather than light quarks, unlike in the scenario advocated by Gribov.

9. The new results confirm most of the features of the Gribov scenario and our derivation from first principles opens a new avenue to the analytic proof of quark confinement.

Conclusiones

En la búsqueda de una demostración analítica del confinamiento en QCD basada en la conjetura de Gribov hemos encontrado:

1. La motivación original de Gribov basada en la pérdida de unitariedad de QED en un régimen de Coulomb supercrítico no es del todo correcta. La fase de Coulomb es estable incluso en el régimen supercrítico. El hamiltoniano de Dirac es autoadjunto. El único detalle relevante es que para valores grandes de la carga de Coulomb ($Z > 118$) es necesario seleccionar una condición de contorno cerca de la singularidad de Coulomb. La elección de la condición de contorno se puede etiquetar por un parámetro con dimensiones λ que introduce una ruptura anómala de la simetría conforme.

2. El mismo fenómeno físico se produce en sistemas bidimensionales de materia condensada, pero con valores más bajos de la carga crítica. En particular, en el análisis de impurezas en el grafeno, la carga crítica puede alcanzar valores tan bajos como $Z = 1$. Un análisis detallado del régimen supercrítico teniendo en cuenta interacciones de muchos cuerpos da lugar a un fenómero de apantallamiento de la carga de la impureza. Las predicciones teóricas sobre este fenómeno coinciden con datos experimentales recientes.

3. En la aproximación del punto de silla a la teoría de Yang-Mills en presencia de quarks externos, encontramos que las soluciones de Coulomb se vuelven inestables para valores constantes del acoplamiento fuerte α_s may-

ores que $\sqrt{5}/2$. La inestabilidad se debe a la aparición de modos negativos en las fluctuaciones del gluón alrededor de la configuración de Coulomb del campo gauge.

4. El mismo análisis muestra que el régimen de Coulomb también es inestable en un fondo de quarks $q-\bar{q}$ pesados. En ese caso, para constantes de acoplamiento $\alpha_s > \sqrt{2}$ ocurre el mismo fenómeno, pero se vuelve fuertemente dependiente de la distancia entre los quarks del par $q - \bar{q}$. Para cualquier elección de la condición de contorno hay una distancia crítica L_c tal que el trasfondo de Coulomb es estable para pares $q - \bar{q}$ con tamaño más pequeño que $2L_c$ y se vuelve inestable para tamaños mayores $L > L_c$.

5 . En el régimen intermedio $\sqrt{2} < \alpha_s < 3/2$, la compatibilidad entre libertad asintótica y confinamiento es explícita. La distancia crítica se aproxima al infinito para $\alpha_s = \sqrt{2}$. Para acoplamiento más pequeño $\alpha_s < \sqrt{2}$ y acoplamiento más grande $\alpha_s > \frac{3}{2}$, la fase de Coulomb es respectivamente estable e inestable para todas las separaciones. Así, el régimen intermedio interpola suavemente desde un régimen de libertad asintótica a un régimen de confinamiento. Éstos son los primeros indicios analíticos derivados de primeros principios de que QCD no atraviesa una transición de fase a escalas de energía intermedias.

6. Resulta sorprendente que las fluctuaciones que conducen al régimen de inestabilidad de Coulomb exhiban una cuerda gruesa prominente que conecta los dos quarks, lo que apunta a una imagen de QCD en la que el confinamiento sería debido a cuerdas gruesas en lugar de a cuerdas fundamentales.

7. En la imagen de confinamiento de Gribov, se asigna un papel destacado a los quarks ligeros en el mecanismo de confinamiento. Nuestro análisis de la contribución de las fluctuaciones de los quarks ligeros al trasfondo de Coulomb señala la existencia de un nuevo tipo de inestabilidades fermiónicas. Éstas aparecen sólo para acoplamiento mayor que $\alpha_s = \sqrt{3}$. Para cada acoplamiento mayor que este nuevo valor crítico ($\sqrt{3} < \alpha_s \leq 2$)

existe una distancia donde la energía de vacío del sistema se vuelve infinita. Esto señala la formación de un par quark-antiquark que rompe la cuerda cromoeléctrica e induce la inestabilidad de la fase de Coulomb.

8. No obstante, el hecho de que las inestabilidades fermiónicas aparezcan a valores de la constante de acoplamiento más grandes que en el caso bosónico señala que el mecanismo de confinamiento está¡ dirigido principalmente por gluones en lugar de quarks ligeros, como defendía Gribov.

9. Los nuevos resultados confirman la mayoría de las ventajas del escenario de Gribov y nuestra derivación desde primeros principios abre una nueva vía a la demostración analítica del confinamiento de los quarks.

Bibliography

[1] I.J.R. Aitchison and A.J.G. Hey, *Gauge Theories in Particle Physics*, Adam Hilger Ltd, 1982.

[2] M. Asorey and A. Santagata, *Instability of Coulomb phase in QCD*, PoS ConfinementX (2012) 057.

[3] M. Asorey and A. Santagata, *Singular potentials: Confinement and Riemann hypothesis*, Nuovo Cimento C 36 (2013) 03.

[4] M. Asorey and A. Santagata, *Coulomb phase stability and quark confinement*, PoS QCD-TNT-III (2014) 004

[5] M. Asorey and A. Santagata, *Instabilities of Coulomb phases and quark confinement in QCD*

[6] M. Asorey and A. Santagata, *Critical Coulomb impurities in graphene*, In preparation (2014)

[7] M. Asorey, A. Ibort, G. Marmo, *Global theory of quantum boundary conditions and topology change*, Int.J.Mod.Phys. A20 (2005) 1001-1026, hep-th/0403048.

[8] M. Asorey, A. Ibort, G. Marmo, *Path integrals and boundary conditions*, arxiv:quant-ph/0609023.

[9] M. C. Baldiotti, D. M. Gitman, I. V. Tyutin, B. L. Voronov, *Self-adjoint extensions and spectral analysis in the generalized Kratzer problem*, Phys. Scr. 83 065007 (2011), arXiv:1009.4903

[10] G. S. Bali, *QCD forces and heavy quark bound states*, Phys.Rept. 343 (2001) 1-136, hep-ph/0001312.

[11] G. S. Bali, *QCD forces and heavy quark bound states*, Phys.Rept. 343 (2001) 1-136, arXiv:hep-ph/0001312.

[12] N. Brambilla and A. Vairo, *Quark confinement and hadron spectrum*, arXiv:hep-ph/9904330v1, 1999.

[13] K. E. Cahill, *Does Color Screening Confine Quarks?*, Phys.Rev.Lett. 41 (1978) 599

[14] F. Calogero, *Solution of the one-dimensional N body problems with quadratic and/or inversely quadratic pair potentials*, J.Math.Phys. 12 (1971) 419-436

[15] L. J. Carson, R. Goldflamand and L. Wilets *Partial Screening of Classical Color*, Phys.Rev. D28 (1983) 385.

[16] L. J. Carson, *Screening of Classical Color* , Phys.Rev. D29 (1984) 2355.

[17] K.M. Case, *Singular potentials*, Phys.Rev. 80 (1950) 797-806.

[18] A.H. Castro Neto, F. Guinea, N.M.R. Peres, K.S. Novoselov and A.K. Geim, *The electronic properties of graphene* , Rev.Mod.Phys. 81 (2009) 109-162.

[19] B. Chakraborty, K. S. Gupta and S. Sen, *Effect of topological defects and Coulomb charge on the low energy quantum dynamics of gapped graphene* , J.Phys. A 46 (2013) 055303.

[20] M. Creutz, *Monte Carlo Study of Quantized SU(2) Gauge Theory*, Phys.Rev. D21 (1980) 2308-2315.

[21] Y. L. Dokshitzer and D. E. Kharzeev, *The Gribov Conception of Quantum Chromodynamics*, Ann. Rev. Nucl. Part. Sci. 54 (2004) 487, arXiv:hep-ph/0404216.

[22] V. Efimov, *Energy levels arising form the resonant two-body forces in a three-body system*, Phys.Lett. B33 (1970) 563-564.

[23] J.G. Esteve, *Origin of the anomalies: The Modified Heisenberg equation*, Phys.Rev. D66 (2002) 125013, arXiv:hep-th/0207164.

[24] J.G. Esteve, *Anomalies in Conservation Laws in the Hamiltonian Formalism*, Phys.Rev. D34 (1986) 674-677.

[25] C. Ewerz, *Gribov's Confinement Scenario*, Nucl.Phys.Proc.Suppl. 90 (2000) 130-132 , arXiv:hep-ph/0008229.

[26] C. Ewerz, *Gribov's Confinement Scenario*, Nucl.Phys.Proc.Suppl. 90 (2000) 130-132 , arXiv:hep-ph/0008229.

[27] C. Ewerz, *Gribov's equation for the Green function of light quarks*, Eur.Phys.J. C13 (2000) 503-518, arXiv:hep-ph/0001038.

[28] C. Ewerz, *Gribov's picture of confinement and chiral symmetry breaking*, Prepared for Conference: C05-05-22.3, p.366-378, arXiv:hep-ph/0601271.

[29] L. D. Faddeev and A. A. Slavnov, Gauge Fields: Introduction to Quantum Theory, Benjamin/Cummings (1980)

[30] E. Ferreira and J. Sesma, *Regge trajectories for the inverse square potential*, J.Math.Phys. 11 (1970) 3245-3250

[31] E. Ferreira, J. Sesma and P.L. Torres *On scattering and bound states for a singular potential*, Prog.Theor.Phys. 43 (1970) 1-9

[32] W. Frank, D.J. Land and R.M. Spector, *Singular potentials*, Rev. Mod. Phys. 43 (1971) 36-98.

[33] R. A. Freedman, L. Wilets, S. D. Ellis, E. M. Henley, *Classical Chromodynamics of Two Sources: Charges and Magnetic Moments*, Phys.Rev. D22 (1980) 3128.

[34] O.V. Gamayun, E.V. Gorbar and V.P. Gusynin, *Supercritical Coulomb center and excitonic instability in graphene*, Phys. Rev. B 80, 165429 (2009), arXiv:0907.5409.

[35] O.V. Gamayun, E.V. Gorbar and V.P. Gusynin, *Gap generation and semimetal-insulator phase transition in graphene*, Phys.Rev. B81 (2010) 075429, arXiv:0911.4878.

[36] D.M. Gitman, I.V. Tyutin and B.L. Voronov, *Self-adjoint extensions and spectral analysis in Calogero problem*, arXiv:0903.5277.

[37] D. M. Gitman, A. D. Levin, I. V. Tyutin and B. L. Voronov, *Electronic Structure of Superheavy Atoms. Revisited*, arXiv:1112.2648.

[38] V. N. Gribov, *QCD at large and short distances (annotated version)*, Eur. Phys. J. C 10 (1999) 71, arXiv:hep-ph/9807224.

[39] V. N. Gribov, *The theory of quark confinement*, Eur. Phys. J. C 10 (1999) 91, arXiv:hep-ph/9902279.

[40] V. N. Gribov, *Orsay Lectures on confinement I*, LPT Orsay 92-60 (1993), arXiv:hep-ph/9403218.

[41] V. N. Gribov, *Orsay Lectures on confinement II*, LPT Orsay 94 -20 (1994), arXiv:hep-ph/9404332.

[42] V. N. Gribov, *Orsay Lectures on confinement III*, LPT Orsay (1999) 99-37 , arXiv:hep-ph/9905285.

[43] V.N. Gribov, *Talk at Perturbative QCD Workshop*, Lund, Sweden, May 21D24, 1991. Preprint LU-TP- 91-7 (unpublished).

[44] V.N. Gribov, *Gauge Theories and Quark Confinement. Collection of works*, Phasis Publishing House, Moscow (2002), 357

[45] D. Griffiths, *Introduction to Elementaey Particles*, John Wiley & Sons, 1987.

[46] D. J. Gross and F. Wilczek, *Asymptotically Free Gauge Theories. 1*, Phys. Rev. D8 (1973) 3633-3652.

[47] D. J. Gross and F. Wilczek, *Asymptotically Free Gauge Theories. 2*, Phys. Rev. D9 (1974) 980-993 .

[48] R. Gupta, *Introduction to Lattice QCD*, arXiv:hep-lat/9807028.

[49] K. S. Gupta, S. Sen, *Bound states in gapped graphene with impurities: Effective low-energy description of short-range interactions*, Phys. Rev. B 78 (2008) 205429.

[50] K. S. Gupta, S. Sen, *Bound States in Graphene*, Mod.Phys.Lett. A24 (2009) 99-107.

[51] K.S. Gupta and S.G. Rajeev, *Renormalization in quantum mechanics*, Phys.Rev. D48 (1993) 5940-5945, arxiv:hep-th/9305052

[52] K. S. Gupta, E. Harikumar, A. R. de Queiroz, *A Dirac type xp-Model and the Riemann Zeros*, EPL, 102 (2013) 10006, arXiv:1205.6755

[53] A. J. G. Hey and J. E. Mandula, *Charge Confinement By Classical Instabilities*, Phys.Rev. D19 (1979) 1856

[54] V.R. Khalilov, C.-L. Ho , *Dirac electron in a Coulomb field in (2+1)-dimensions*, Mod.Phys.Lett. A13 (1998) 615-622, hep-th/9801012

[55] I.B. Khriplovich, *Interaction of Classical Yang-Mills Charges and the Problem of Quark Confinement*, Sov.Phys.JETP 47 (1978) 18, Zh.Eksp.Teor.Fiz. 74 (1978) 37-42

[56] D. Kloepfer, A. De Martino, R. Egger, *Bound States and Supercriticality in Graphene-Based Topological Insulators*, Crystals 2013, 3(1), 14-27, arXiv:1301.2833

[57] V. N. Kotov, B. Uchoa, V. M. Pereira, A. H. Castro Neto, F. Guinea, *Electron-Electron Interactions in Graphene: Current Status and Perspectives* , Rev.Mod.Phys. 84 (2012) 1067

[58] M. Magg, *Simple Proof for Yang-Mills Instability*, Phys.Lett. B74 (1978) 246.

[59] M. Magg, *The Classical Yang-Mills Field of a Quark Source*, Phys.Lett. B77 (1978) 199.

[60] M. Magg, *Stability in the Yang-Mills System With an External Source*, Phys.Lett. B78 (1978) 481.

[61] M. Magg, *Stable Yang-Mills Fields for an Overcritical Point Source*, Nucl.Phys. B158 (1979) 154.

[62] J. M. Maldacena, *The Large N limit of superconformal field theories and supergravity*, Adv.Theor.Math.Phys. 2 (1998) 231-252, hep-th/9711200.

[63] S. Mandelstam, *Vortices and quark confinement in non-Abelian gauge theories*, Phys.Rept. 23 (1976) 245.

[64] S. Mandelstam, *General Introduction To Confinement* , Phys. Rep. 67 (1980) 109.

[65] J. E. Mandula, *Classical Yang-Mills potential*, Phys.Rev. D14 (1976) 3497.

[66] J. E. Mandula,*Color Screening by a Yang-Mills Instability*, Phys.Lett. B67 (1977) 175.

[67] J. E. Mandula, *Total Charge Screening* , Phys.Lett. B69 (1977) 495.

[68] J. E. Mandula and L. D. McLerran *Massless Scalar QED as a Model of Color Confinement*, Phys.Lett. B73 (1978) 193.

[69] J. Moser, *Three integrable Hamiltonian systems connnected with isospectral deformations*, Adv.Math. 16 (1975) 197-220

[70] B. Muller, H. Peitz, J. Rafelski, W. Greiner, *Solution of the Dirac equation for strong external fields*, Phys.Rev.Lett. 28 (1972) 1235

[71] B. Muller, J. Rafelski, W. Greiner, *Solution of the Dirac equation with two Coulomb centers*, Phys.Lett. B47 (1973) 5-7

[72] T. Muta, *Foundations of Quantum Chromodynamics*, World Scientific, 1987.

[73] D. S. Novikov, *Elastic scattering theory and transport in graphene*, Phys. Rev. B 76 (2007) 245435, arXiv:0706.1391

[74] K. S. Novoselov, A. K. Geim, S. V. Morozov, D. Jiang, Y. Zhang, S. V. Dubonos, I. V. Gregorieva, and A. A. Firsov, *Electric Field Effect in Atomically Thin Carbon Films*, Science 306, 666 (2004)

[75] C.H. Oh, R. Teh, W.K. Koo, *Low-energy Static Yang-mills Configurations*, Phys.Lett. B101 (1981) 337

[76] V. M. Pereira, V. N. Kotov, and A. H. Castro Neto *Supercritical Coulomb impurities in gapped graphene*, Phys. Rev. B 78 (2008) 085101, arXiv:0803.4195

[77] V. M. Pereira, J. Nilsson and A. H. Castro Neto, *Coulomb Impurity Problem in Graphene*, Phys. Rev. Lett. 99, 166802

[78] A. M. Perelomov, V. S. Popov, *Fall to the center in quantum mechanics*, Theor. Mat. Phys., 4 (1970) 664.

[79] M.E. Peskin and D.V. Schroeder, *An introduction to Quantum Field Theory*, Perseus Book, 1995.

[80] J. Polchinski and L. Susskind, *String theory and the size of hadrons*, arXiv:hep-th/0112204

[81] H. D. Politzer, *Reliable Perturbative Results for Strong Interactions?*, Phys. Rev. Lett. 30 (1973) 1346.

[82] J. Reinhardt and W. Greiner, *Quantum electrodynamics of strong fields*, Rep. Prog. Phys. 40-3, 219

[83] A.V. Shytov, M. I. Katsnelson and L. S. Levitov *Atomic Collapse and Quasi - Rydberg States in Graphene*, Phys. Rev. Lett. 99, 246802 (2007), arXiv:0708.0837

[84] A.V. Shytov, M. I. Katsnelson and L. S. Levitov *Vacuum Polarization and Screening of Supercritical Impurities in Graphene*, Phys. Rev. Lett. 99, 236801 (2007), arXiv:0705.4663

[85] A. Shytov, M. Rudner, N. Gu, M. Katsnelson, L. Levitov, *Atomic collapse, Lorentz boosts, Klein scattering, and other quantum-relativistic phenomena in graphene*, Phys. Rev. Lett. 99, 236801 (2007), arXiv:0812.1412

[86] G. Sierra, *$H = xp$ with interaction and the Riemann zeros*, Nucl.Phys. B776 (2007) 327-364, math-ph/0702034.

[87] G. Sierra, *A quantum mechanical model of the Riemann zeros*, New J.Phys. 10 (2008) 033016, arXiv:0712.0705.

[88] G. Sierra, *General covariant xp models and the Riemann zeros*, J.Phys. A45 (2012) 055209, arXiv:1110.3203.

[89] J. Molina-Vilaplana, G. Sierra, *An xp model on AdS_2 spacetime*, Nucl.Phys. B877 (2013) 107-123, arXiv:1212.2436.

[90] P. Sikivie and N. Weiss, *Screening Solutions To Classical Yang-mills Theory*, Phys.Rev.Lett. 40 (1978) 1411

[91] P. Sikivie and N. Weiss, *Classical Yang-Mills Theory in the Presence of External Sources*, Phys.Rev. D18 (1978) 3809

[92] P. Sikivie and N. Weiss, *Static Sources in Classical Yang-Mills Theory*, Phys.Rev. D20 (1979) 487

[93] P. Sikivie, *Instability of Abelian Field Configurations in Yang-Mills Theory* , Phys.Rev. D20 (1979) 877

[94] G. 't Hooft, *Topology of the Gauge Condition and New Confinement Phases in Nonabelian Gauge Theories*, Nucl.Phys. B190 (1981) 455.

[95] B.L. Voronov, D.M. Gitman and I.V. Tyutin, *Dirac Hamiltonian with superstrong Coulomb field*, Theor.Math.Phys. 150 (2007) 34-72, arXiv:quant-ph/0608221.

[96] V. Vyas, *Intrinsic Thickness of QCD Flux-Tubes*, arXiv:1004.2679.

[97] Y. Wang and at. *Observing Atomic Collapse Resonances in Artificial Nuclei on Graphene*, Science Vol. 340 no. 6133 (2013), 734-737

[98] J. Zinn-Justin, *Quantum Field Theory and Critical Phenomena*, Oxford Univ. Press (1989)